SCHOOL OF CIVIL ENGINE

NSF/CEE-81022

PB81-235921

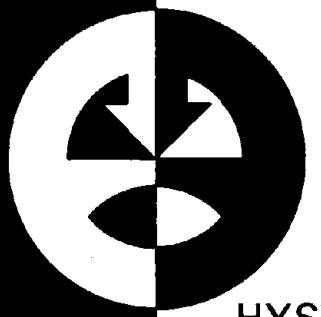

Structural Engineering

CE-STR-81-15

HYSTERESIS IDENTIFICATION OF MULTI-STORY BUILDINGS

Sassan Toussi
and
James T. P. Yao

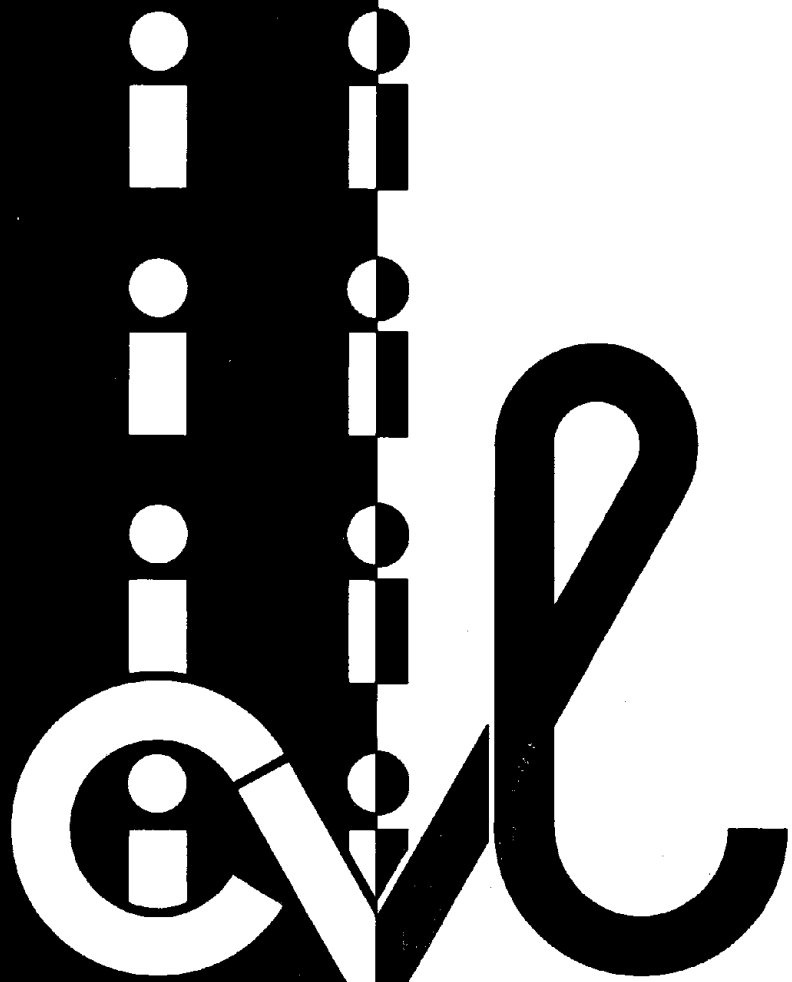

PURDUE UNIVERSITY

CE-STR-81-15

HYSTERESIS IDENTIFICATION OF MULTI-STORY BUILDINGS

by

Sassan Toussi and James T. P. Yao

Supported by

The National Science Foundation

Through

Grant No. PFR 7906296

May 1981

School of Civil Engineering

Purdue University

West Lafayette, IN 47907

TABLE OF CONTENTS

1. INTRODUCTION

1.1 Object and Scope

In an earlier report [14]; two simple techniques of system identification were presented for the estimation of the behavior of single-degree-of-freedom (SDOF) structural systems subjected to earthquake excitation. It was concluded that these methods can be further improved by using the applicable eror functions in the analysis of noise-corrupted test data. Moreover, these techniques can be extended to estimate the inter-story hysteretic behavior of multi-story structures.

In this report, results of the estimation of the behavior of multi-degree-of-freedom (MDOF) structural systems are presented. First, the hysteresis identification method and the corresponding error criterion are reviewed and described. The error criterion is a least-squares estimation procedure which is applied to both an unconstrained and a constrained problem. Then, a lumped-mass model which is used to form "M" different independent responses from the response of an "M" degrees of freedom structure is described. This model enables us to consider each one of the "M" responses as the output of a SDOF structural system which is, in fact, the relative response of a certain floor with respect to the next lower floor. Finally, the identification technique is applied to estimate the inter-story behavior of a laboratory tested, reinforced-concrete frame [3]. The frame was constructed and dynamically tested to failure at the University of Illinois by Healey and Sozen [3]. However, their data contained trends which needed to be filtered. The filtering techniques as used herein are also discussed.

In addition, we tried to investigate the effect of damping in the response of high-rise buildings. This investigation was focused on whether or not damping force plays a significant role in the nature of the structural response and, if so, what mathematical form for damping force would better represent this effect.

1.2 Acknowledgment

The authors are grateful to Professor M. A. Sozen and his fellow research assistants Mr. B. Algan and Mr. M. Kreger for their invaluable advice and test data. Useful comments of Professor E. C. Ting of Purdue University are also acknowledged. Appreciation is given to Molly Harrington for typing this report. This investigation is supported in part by the National Science Foundation.

2. HYSTERESIS IDENTIFICATION METHOD

The hysteresis identification method is briefly discussed in the first two sections herein. A detailed discussion of this technique is given in an earlier report [14]. In Section 2.4, the mathematical form for the damping force is described. The mathematical function was chosen in such a fashion that it would help to simplify the identification procedure. A literature review was also conducted to support the selected form. The remaining sections deal with the treatment of noise-corrupted data. The least-squares technique is used for the estimation of constrained and non-constrained coefficients.

2.1 System Model

Figure 1-a indicates the system model whose mass is assumed to be time-invariant. For this model, the relative acceleration (with respect to the base), $\ddot{x}(t)$, and the base acceleration, $\ddot{z}(t)$ are known and available. The restoring force, $f_R(t)$, is assumed to depend upon the relative displacement and the relative velocity between the floor and the base. Thus, we have

$$f_R(t) = f_R(x(t),\dot{x}(t)) \tag{1}$$

Traditionally we may consider $f_R(t)$ to consist of two separable parts, namely damping and spring forces which are functions of the relative velocity and the relative displacement, respectively. The non-linear damping and

spring properties of the system are shown in Figure 1-b, while the system's response to an arbitrary load is illustrated in Figure 1-c. Because the velocity and displacement change monotonically, forces should also change monotonically within intervals $t_i - t_{i-1}$, $i = 1,2,3,...$ Therefore, restoring force can be written in terms of two polynomials, one of which corresponds to the spring force and the other to the damping force, i.e.,

$$f_R(t) = f_D(\dot{x}) + f_S(x) \tag{2}$$

where

$$f_D(\dot{x}) = b_0 + b_1\dot{x} + b_2\dot{x}^2 + \ldots + b_p\dot{x}^p \tag{3}$$

$$f_S(x) = a_0 + a_1x + a_2x^2 + \ldots + a_qx^q \tag{4}$$

and

$$p + q \leq n_i - 1 \tag{5}$$

Substituting Equations 3 and 4 into Equation 2, we obtain,

$$f_R(x,\dot{x}) = c + a_1 + a_2x + \ldots + a_qx^q + b_1\dot{x} + b_2\dot{x}^2 + \ldots + b_p\dot{x}^p \tag{6}$$

where,

$$c = a_0 + b_0 \tag{7}$$

2.2 Identification Procedure

The relative velocity and displacement time-histories are obtained by integrating the relative acceleration response once and twice, respectively. Suppose n_i is the number of points within interval i. Repeating Equation 6 for the components of response at each n_i points gives n_i equations with n_i unknowns which in a matrix form is symbolized as follows:

$$F_R = XA \tag{8}$$

In this equation, F_R is the vector of applied force; X is the response matrix, and A represents the parameter vector to be estimated. The elements of F_R are determined from the system equilibrium equation.

$$f_R(t) = -m\ddot{z}(t) - m\ddot{x}(t) \tag{9}$$

where $m\ddot{x}(t)$ and $m\ddot{z}(t)$ are, respectively, the inertia and the base excitation forces. Since X and F_R are known quantities in Equation 8, The A vector is simply derived by obtaining the inverse of matrix X and substituting X^{-1} and F_R into Equation 10.

$$A = X^{-1} F_R \tag{10}$$

Having the parameter vector calculated, the damping and spring forces are obtained using the following equation

$$\begin{Bmatrix} f_S(t) \\ f_D(t) \end{Bmatrix} = \begin{bmatrix} 1 & x_t & x_t^2 & \cdots & x_t^q & 0 & 0 & 0 & \cdots & 0 \\ 0 & 0 & 0 & \cdots & 0 & 1 & \dot{x}_t & \dot{x}_t^2 & \cdots & \dot{x}_t^p \end{bmatrix} \begin{bmatrix} a_0 \\ a_1 \\ a_2 \\ \vdots \\ a_q \\ b_0 \\ b_1 \\ b_2 \\ \vdots \\ b_p \end{bmatrix} \tag{11}$$

2.3 System's Damping-Force

At present, there is a poor understanding of the damping mechanism in structures. In many cases, the structure is assumed to possess no damping. However, under dynamic load with a broad frequency spectrum, it is unreasonable to ignore damping effect since it prevents the structure from the excessive vibration.

The most important mathematical models representing damping in structures are linear viscous, Coulomb, and structural dampings. For viscous damping models, the damping takes the form of a force proportional to velocity and acting in a direction opposite to the velocity direction. Coulomb damping also opposes the motion, but it has a constant magnitude. Finally, the structural damping is associated with the internal energy dissipation due to the hysteresis effect in cyclic stress.

In recent years, the viscous damping models for representing the energy dissipation characteristics of actual structures are widely used. They are used with simple transient or random excitation. On the other hand, structural damping has shown good agreement with the measured response of large structures for typical low-frequency ranges. In using the structural damping models, the basic assumption is that the energy dissipated in one cycle of harmonic motion is proportional to the square of the amplitude and independent of the frequency of motion. Some materials, however, do not conform with this assumption. Moreover, Jerry and Ellis [4] from their experimental investigation concluded that the building at various amplitudes had shown nonlinearity. And this nonlinearity should be found in the frequency and damping characteristics of any mode.

In spite of the fact that the damping is not really proportional to the velocity in any kind of material or systems, these models have been successfully applied in analyzing vibration problems. The viscous and structural damping models have also given reasonable qualitative results for simple nonlinear systems.

The mathematical form of the viscous damping force used in our identification technique was reversible, non-linear, and symmetrical with respect to the origin, i.e.:

$$f_D(t) = \sum_{i=1}^{q} b_i \dot{x} |\dot{x}|^{i-1} \tag{12}$$

Although viscoelastic models are frequency dependent, it should be noticed that our system identification technique is applied to a SDOF system subjected to earthquake excitation. Therefore, because the system's response is dominated with its natural frequency we, indeed, always deal with only one fixed frequency (i.e., system's natural frequency). In other words, whatever is chosen for the damping force, it is related to the system's natural frequency only and is independent of any other frequency.

The reversibility property of the damping force is due to a physical interpretation. Since the damping force depends upon the velocity and the velocity value must return to zero at the end of the motion (i.e. not any permanent velocity), the damping force, therefore, has to pass through the origin. Finally, the non-linearity of the damping force is due to the experimental observations of Lazan [7]. He stated that nonlinear effects in damping are beneficial since the effective damping usually increases with increasing stress.

Finally, it should be mentioned that Coulomb damping model was intentionally neglected. Because it is represented by a constant value which is very difficult to distinguish it from the constant parameter of the spring-force function. However, as Lazan [7] pointed out, the Coulomb friction damping was the only practical case where the non-linear effects in damping was not beneficial. Moreover, Den Hartog [2] showed that for a SDOF system with constant force frictioned damping, the effective damping decreased with increasing vibration amplitude up to the point where the damping no longer could control the amplitude. It means that the effectiveness of the friction force is doubtful as the friction force is exceeded with the effective excitation force.

A detailed look at damping methods, measurements, and analysis is contained in Reference 13.

2.4 Error Criterion

So far in the discussion of the present method, the importance of the noise either resulted from the inaccurately measured input and/or output, the imperfect mathematical representation of the system behavior, or the combination of both was generally underestimated. Although, in many identification techniques the data are assumed to be noise-free, in our method because of performing the identification in rather short time-intervals, the effect of noise can not be ignored. The difficulties associated with the inversion of the matrix X of Equation 8 represent an example of the sensitivity of this method to measurement noise. The matrix is established with the assumption that the data are error-free and the assumed mathematical functions resemble the actual behavior. Because these are hypothetical considerations; we should expect to experience singularity problem in the matrix inversion process.

The presence of noise, therefore, compels us to refer to the mathematical statistics which makes full and rather accurate utilization of the information derived from the observations. At present, the method of Least Squares is widely applied in the treatment of the quantitative results obtained from experimental works. There are many textbooks which discuss the mathematical and statistical aspects of this technique. Among them, O. M. Leland, who has taught the least-squares method to civil engineering students over many years, has prepared a practical book for engineers [8].

In the following, however, the necessary formulae are derived by simplyfing the problem as the inversion of a matrix whose numbers of columns and rows are not equal. Then, a very simple solution to the problem of restricted parameters is presented.

2.4.1 Least Squares Approximate Solution

According to the assumptions made for damping force, Equations 4 and 5 which, respectively, define the damping and restoring forces should be redefined, i.e.,

$$f_D(t) = \sum_{i=1}^{q} b_i \dot{x} \, |\dot{x}|^{i-1} \tag{13-1}$$

and

$$f_R(t) = \sum_{j=0}^{p} a_j x^j + \sum_{i=1}^{q} b_i \dot{x} |\dot{x}|^{i-1} \tag{13-2}$$

Now we try to choose such values for p and q whose summation, m_i, is less than the numbers of points within interval i (i.e. $m_i < n_i$). Therefore, the substitution of the restoring force of each point in the equilibrium equation (i.e. Equation 9) gives n_i equations with m_i unknowns where $m_i < n_i$ which means we have more equations than unknowns. Furthermore, since no point can satisfy the equilibrium equation, it is inappropriate to consider Equation 8 as an equality. Consequently, an n_i x 1 error vector, e, should be introduced.

$$e = F_R - XA \tag{14}$$

Now, the parameter vector, A, is estimated by minimizing

$$E = e^T e = (F_R - XA)^T (F_R - XA) \tag{15}$$

This minimization which is called the least-squares estimation gives that A which minimizes the norm of the error vector, e. If some equations are more reliable than others but all equations are to be retained, a weighted least-squares approximation can be used. That is we should minimize

$$E_Q = e^T Q e = (F_R - XA)^T Q (F_R - XA) \tag{16}$$

where Q is a symmetrical, $m_i x m_i$, non-singular, and generally diagonal matrix.

To perform the minimization, Equation 16 is multiplied out and its derivatives with respect to A are set equal to zero.

$$E_Q = F_R^T Q F_R - F_R^T Q XA - A^T X^T Q F_R + A^T X^T Q XA \tag{17}$$

and

$$\frac{\partial E_Q}{\partial A} = - F_R^T QX - F_R^T QX + A^T X^T QX + A^T X^T QX = 0 \tag{18}$$

This gives

$$A^T X^T QX = F_R^T QX \tag{19}$$

or

$$A^T = F_R^T QX (X^T QX)^{-1} \tag{20}$$

Therefore, an estimate of vector A is obtained as follows

$$\hat{A} = (X^T QX)^{-1} X^T QF_R \tag{21}$$

The hat, "$\hat{}$", on A indicates that the derived formula for A is an estimated of A, not its actual value. Error vector, e, can also be calculated as

$$||e||_Q^2 = (F_R - X\hat{A})^T Q (F_R - X\hat{A}) \tag{22}$$

If Q is a unit matrix, then $\hat{A}$ and the expression for e become

$$\hat{A} = (X^T X)^{-1} X^T F_R \tag{23}$$

$$||e||^2 = (F_R - X\hat{A})^T (F_R - X\hat{A}) \tag{24}$$

Matrix $H = (X^T X)^{-1} X^T$ is a particular example of the generalized or pseudo-inverse of A [12].

In any event, the mathematical models being used are always the result of simplifying assumptions (e.g., the twisting and rocking motions may not be considered in many cases). Whether the violation of such rules is an indication of the inadequacy of the form of such models is not clear.

2.4.2 Least-Squares Solution for Constrained Parameters

The previously discussed least-squares estimation was a general case where the parameters were not subjected to any equality and/or inequality conditions. There are, however, cases where some parameters should not exceed certain limits or differ from fixed values. For example, consider the sign of the damping force, $F_D = a_4\dot{x}$, which should always be identical to the sign of the velocity response. Therefore, it compels us to enforce an inequality condition to the estimation procedure, i.e.

$$a_4 \geq 0 \tag{25}$$

Those who have tried to find a solution to this kind of problem have always assumed that they have a clear idea about the error vector defined in Equation 14. Zelner [16], for example, has considered the case of one fixed variable when the error vector is assumed to have a multi-variate normal distribution. In our case, there doesn't exist any information about the probability distribution of vector e. Consequently, we should look for that solution which doesn't require any prior knowledge about the e vector. Judge and Takayama [5] specified a general framework for the cases where there were linear inequality restraints on the individual coefficients or combinations. What, however, we apply to the problem is a very simple procedure which consists of two steps.

In the first step, we fit by least-squares the regression relationship,

$$f_R(t) = \sum_{i=0}^{q} a_i x^i + a_{q+1}\dot{x} \tag{26}$$

If $a_{q+1} \geq 0$, the estimates of coefficients are used without any modification. But if $a_{q+1} < 0$, then the second step is used which is to fit the same regression model (by least squares) except we set a_{q+1} equal to zero. However, Lovel and Prescott [9] showed that this procedure causes bias and can lead to inefficient parameter estimates!

3. LUMPED-MASS SYSTEM

Figure 2 shows the typical model for high-rise buildings. This model is a lumped-mass system with masses M_i, $i = 1,2,\ldots,N$, where N is the number of masses. It is assumed that these masses are connected by the nonlinear dashpots c_i, and the non-linear springs, K_i. The mass distribution is assumed to be known from the drawings or can be obtained from impulse-momentum relationship [9].

The recorded motions consist of the acceleration of the rigid base, $\ddot{z}(t)$, and the absolute acceleration of the floors, $\ddot{y}_i$, $i = 1,\ldots,N$. These quantities should have been measured during the motion of structure at each level by means of previously-installed accelerameters. The absolute velocity and displacement of each floor is obtained by integrating the corresponding absolute acceleration. The forces created in the springs and the dashpots are assumed to depend upon the relative displacement and velocity between the neighboring masses, respectively, i.e.

$$[F_S(t)]_i = F_S[x_i(t)], \quad i = 1,2,\ldots,N \tag{27-1}$$

$$[F_D(t)]_i = F_D[\dot{x}_i(t)], \quad i = 1,2,\ldots,N \tag{27-2}$$

where

$$x_i(t) = y_i(t) - y_{i-1}(t) \tag{28-1}$$

$$\dot{x}_i(t) = \dot{y}_i(t) - \dot{y}_{i-1}(t) \tag{28-2}$$

Now the equation of motion governing the system can be formed as follows:

$$
\begin{aligned}
&M_N \ddot{Y}_N(t) + F_D[\dot{x}_N(t)] + F_S[x_N(t)] = 0 \\
&M_{N-1} \ddot{Y}_{N-1}(t) + F_D[\dot{x}_{N-1}(t)] + F_S[x_{N-1}(t)] = F_D[\dot{x}_N(t)] + F_S[x_N(t)] \\
&\vdots \\
&M_i \ddot{Y}_i(t) + F_D[\dot{x}_i(t)] + F_S[x_i(t)] = F_D[\dot{x}_{i+1}(t)] + F_S[x_{i+1}(t)] \\
&\vdots \\
&M_2 \ddot{Y}_2(t) + F_D[\dot{x}_2(t)] + F_S[x_2(t)] = F_D[\dot{x}_3(t)] + F_S[x_3(t)] \\
&M_1 \ddot{Y}_1(t) + F_D[\dot{x}_1(t)] + F_S[x_1(t)] = F_D[\dot{x}_2(t)] + F_S(x_2(t)]
\end{aligned}
\tag{29}
$$

Adding i equations from the top together at a time while i = 1,...,N, gives the following N equations

$$
F_D[\dot{x}_i(t)] + F_S[x_i(t)] = \sum_{k=i}^{N} M_k \ddot{y}_k, \quad i = 1,2,\ldots,N \tag{30}
$$

In this equation, since the right hand side is known, the summation forces are available at any instance of time. The next step is to apply the hystersis identification method to distinguish these forces from each other.

4. APPLICATIONS

The applications of the identification technique as described earlier is presented herein. To investigate its feasibility and practicality, the response of a ten-story concrete frame which was dynamically tested at the University of Illinois was analyzed. The dynamic test procedure included a series of strong base motions, simulating a scaled version of the north-south component of the El-Centro earthquake of 1940. Healey and Sozen in [3] described their experimental work and presented the acceleration and displacement data obtained in three earthquake-simulation tests. Changes in the dynamic properties of the structure, such as apparent frequencies and equivalent damping were also discussed. In addition, the structure was subjected to sinusoidal base motions and underwent several free-vibration tests. Our

work, however, was restricted to the analysis of the response of the frame due to the earthquake excitations. The details of their experimental work is described by Healey and Sozen [3]. Nevertheless, the test structure, testing equipment and experimental procedure are described in the following section.

4.1 Description of Test Structure, Test Set-Up and Test Procedure

The test structure consists of two parallel, small scale, ten-story frames carrying a total mass of 4540 kg distributed equally to each floor as shown in Figure 3. Figure 4 shows the overall nominal dimensions of the frames. The height of the first and the tenth levels, as seen in Figure 3 and 4, were almost twenty percent higher than those of the other floors. The structure was tested with the earthquake simulator at the University of Illinois as shown in Figure 5. The directions of the frames were parallel to the direction of the motion.

The input motion for the three earthquake simulation tests was the recorded north-south component of the earthquake motion as measured at El-Centro, California in 1940. The acceleration levels, however, were different for each test run. The maximum recorded base accelerations for the first through third test was 0.4g, 0.95g and 1.42g, respectively. The acceleration at each level was measured by one accelerometer which was fastened to the longitudinal connections of the weights along the centerlines of the beams at each level and at the top of the base girder. These accelerometers measured the horizontal accelerations parallel to the imposed direction of motion. In addition to the accelerometer, there were twenty-one linear-voltage-differential transformers to measure the relative displacements. However, as will be discussed, the recorded displacements are not used in this investigation.

4.2 Data-Filtering Process

The displacement responses were obtained by integrating the recorded acceleration responses instead of using the measured displacements for the following reasons. First, there was a gap between the instance of recording the acceleration magnitude and the instance of recording the displacement magnitude. Although this gap had been estimated to be a very small fraction of a second, we decided not to use the displacement data because our technique required the components of response to be measured at same moment in time. Second, we happened to find that in converting the Illinois data tapes into the system at Purdue University, some portions of the displacement data were folded onto the other side of the zero line.

Figure 6 indicates the acceleration, velocity, and displacement of the second floor (RUN1) where the last two components were created by integrating the recorded acceleration history. Figure 8 indicates the same components of the response of the fourth floor for test run 2. The integration was performed with the use of Simpson's rule together with Newton's 3/8-rule. From Figure 6, it is apparent that the velocity history contains a linear trend while the displacement contains a parabolic one. The existence of these two trends proved that the recorded accelerations are noise corrupted. It should be noticed that the term "noise" doesn't refer to the output noise, rather it is the evidence of the presence of some offset voltages in the electrical instruments.

A traditional method of dealing with data containing a trend, is to fit a simple polynomial curve to the data. This fitted function provides a measure of the trend. Then the untrended data are simply obtained by subtracting the magnitude of the trend at each point from the magnitude of the original data at that point. For example, in this case, a linear function can be fitted to the velocity time-history to find the existing trend.

A second procedure for dealing with a trend is to use a linear filter which converts one set of data $\{x_t\}$, into another, $\{y_t\}$, by the linear operation

$$y_t = \sum_{r=-q}^{s} a_r x_{t+r} \tag{31}$$

where $\{a_r\}$ are a set of weights. In order to estimate the local mean, we should clearly choose the weights so that $\sum a_r = 1$. This equation is often refered to as a "moving average" [6]. A simple moving average is when

$$a_r = \frac{1}{2q+1} \qquad r = -q,\ldots,q \tag{32}$$

and the smoothed value of x_t (i.e. y_t) is

$$y_t = \frac{1}{2q+1} \sum_{i=t-q}^{t+q} x_i \tag{33}$$

This filtering technique can be applied to our acceleration time history to find the value of the constant trend.

Finally, a useful way of removing a trend is simply to subtract the point values of a data from their successive point values until it becomes stationary [1]. However, we didn't try this technique since we were not sure if earthquake motion time-history is stationary or not.

Our trend-removing process, however, appeared to be a trial-and-error type of operation. Because, first, a moving average technique was used to the acceleration data to find the constant-valued trend. It was then followed by subtracting this extracted value from the whole acceleration record. Integrating the trend-removed acceleration, once and twice gave the velocity and displacement time histories, respectively. Unfortunately, the plots of the results, obtained by the successive operations mentioned above, showed that the filtering procedure had failed to remove the trends from the response. From these plots, however, a better understanding of the problem was realized. It

was found that the constant valued trend in the acceleration data varied from one interval to another. Therefore, the remaining question was how to find where each interval started and ended.

Because the filtering process was time consuming and required a lot of labor, it was decided to remove the trend from only a portion of the acceleration data and leave the search for a more efficient filtering technique to our future work.

It was then decided to do the filtering on a five-second length of data and if the process failed to remove the trend, thus, the length would be decreased. The approach resulted in three time intervals of 3, 4 and 5 second time duration for test runs 1, 2 and 3 respectively. The removal of the trend was accomplished through fitting a linear regression to each one of the velocity data obtained by integrating the corresponding acceleration data. The tangent of the slope of the estimated line gave us the trend's constant value hidden in that specific portion of acceleration data. The subtraction of the trend from the original acceleration response yielded the horizontal acceleration response.

Figures 8-10 present the absolute acceleration, velocity, and displacement histories of the test structure for the first test run. Figures 11-13 and 14-16 show the responses of the test structure for the second and third test runs, respecitvely.

4.3 Identification of Non-Linear Structural System

In this section, the application of the identification technique in analyzing the structural response to each test run is presented. As mentioned earlier the input motion for all the test runs was the recorded earthquake motion at El-Centro, California (1940). The only difference between these inputs was the use of different mulipliers which gave the test rune-3 input the highest intensity while the test run-1 input gained the lowest intensity.

Each response was evaluated through the use of four different mathematical forms for the restoring force. The spring force was restricted to a polynomial of degree three, while the viscous damping force was given zero, linear, restricted linear, and a third-degree reversal sysmetrical form. The selection of four different forms for damping force was aimed to investigate the effect of damping in high-rise buildings. To obtain the relative response between the floors, we assumed that all the floor masses are equal. This assumption, however, was not far from the actual situation since the total structure mass had been evenly distributed through the floors. In addition, the dimension of the different elements of the floors (beam, column, etc.) were identical except that the height of the first and the tenth floors were higher than those of others. Therefore, we prefered to factor out the mass from the equilibrium equation (i.e. Equation 30) and let the forces be expressed in acceleration unit.

The relative responses were utilized using the lumped-mass model described earlier. Figure 17-19 illustrate the results of using the lumped-mass system model to determine the inter-story responses of the test structure for three test runs, respectively. In these figures, it is seen that some displacement histories as well as a few velocity response histories become much thicker in some portions of their time durations. This problem was the best illustration of a highly-fluctuating time series. It also demonstrated why most of the identification techniques required the use of an error function.

4.3.1 Undamped System

It was assumed that the effect of the damping force is neglegible. A polynomials of degree three was chosen for the spring force.

$$f_S(x) = \sum_{i=0}^{3} a_i x^i \qquad (34)$$

Figures 20-22 present the estimated hysteretic behavior of floors for test run 1 through 3, respectively. As mentioned earlier, the forces are expressed in units of acceleration because the masses were factored out through the equilibrium equation.

4.3.2 Linear-Viscous-Damping System

The system was once again given the same form of spring force but it gained a linear-viscous-damping force as follows:

$$f_D(\dot{x}) = a_4\dot{x} \tag{35}$$

The estimated hysteretic behavior of floors are shown in Figures 23-25 while the estimates of a_4 and their standard deviation, σ, are presented in Table 1. The most apparent feature of the table is that the standard deviations of a_4 are rather large values in comparison with the mean value of a_4. On the other hand, there is no visible discontinuity between the segments of the corresponding spring force-displacement diagrams. Therefore, it is concluded that structural damping, can neither be modeled with a constant-valued force nor a product of a constant coefficient and the velocity quantity.

4.3.3 (Restricted) Linear-Viscous-Damping System

There is a school of thought which describes structural damping as a phenomenon to be in phase with the velocity. This consideration leads to a less degree of frequency-dependence on damping forces which provides a better agreement with the experimental results showing that the damping forces are nearly independent of the test frequency.

Therefore, by preserving the spring force form as before, the following linear-restricted function was used for modeling the damping force:

$$f_D(\dot{x}) = a_4\dot{x} \tag{36}$$

where

Table 1: Estimates of Linear-Viscous Damping Force Coefficient and Its Standard-Deviation

	Test Run 1		Test Run 2		Test Run 3	
	$\hat{a}$	σ	$\hat{a}$	σ	$\hat{a}$	σ
1st Floor	67.56	119.74	25.50	101.19	59.06	53.79
2nd Floor	56.49	93.32	26.66	153.96	71.32	117.65
3rd Floor	168.88	240.18	34.65	88.74	14.25	79.51
4th Floor	57.81	231.97	16.92	117.72	21.55	92.75
5th Floor	108.55	148.06	14.72	128.86	31.94	71.53
6th Floor	52.26	235.54	26.28	93.78	12.88	127.03
7th Floor	130.75	298.72	-.95	132.69	51.61	64.98
8th Floor	95.63	291.95	8.80	103.58	53.13	87.49
9th Floor	-17.09	154.94	9.77	104.53	24.90	112.07
10 Floor	41.57	66.95	7.85	58.44	15.28	25.46

$$a_4 \geq 0 \tag{37}$$

The results are shown in Figure 27-29 for each test run, respectively.

4.3.4 Non-Linear-Viscous-Damping System

Finally, a cubic function which was symetrical with respect to the origin was assumed for damping force

$$F_D(\dot{x}) = a_4\dot{x} + a_5\,\dot{x}|\dot{x}| + a_6\dot{x}^3 \tag{38}$$

Figures 29-31 show the hysteretic behavior of floors for each one of the test runs, respectively.

5. SUMMARY AND DISCUSSION

The response of a ten-story reinforced-concrete test structure, constructed and subjected to several simulated earthquake excitations at the University of Illinois was used as a means to study the feasibility and practicality of a hysteresis identification technique as presented herein. The main features and significant findings of this investigation are listed in the following:

(1) The lumped-mass system was in most cases successful in utilization of the inter-story response dominated by one apparent frequency. However, in a few number of cases the results were not the representation of SDOF system responses. Indeed, the apparent frequency decreased as nonlinearity started to dominate the behavior of structure.

(2) Although damping doesn't seem to have a significant effect on the nature of the response of structures subjected to earthquake excitation, its consideration is beneficial in the sense that there won't be a problem such as one shown in Figure 20-b. Moreover, the loops of spring force-displacement curves estimated for the system when the damping was considered are more meaningful from the energy dissipation point of view than the case when the damping

effect was neglected. Figures 32-35 are used to illustrate a comparison of the several cases where the system damping form was chosen to be zero, linear, restricted linear, and symmetrical cubic. It is apparent from these figures that a restricted linear-damping force can not be a good model to represent structural damping. However, the technique used in the restricted linear case was not a powerful estimation method in producing the minimum error, in the least squares sense. As a concluding remark, damping should be considered and a linear-viscous-damping force suffices this purpose.

(3) One of the interesting results of this study is the similarity between the conclusions made from the observed crack patterns as shown in Figure 46 and those results as obtained from our identification technique as shown in Figures 36-45. They both indicated that the structure had behaved linearly for the first test run and had experienced nonlinearity for the test runs 2 and 3.

(4) A unique feature of the present method which doesn't exist in other similar system identification technique is that time-variant properties for the structure are considered herein. Udwadia and Kuo [15], for example presented a nonparametric identification technique which describes the structural characteristic with the use of two polynomial series. However, unlike the present method, the coefficients of the series remain constant throughout the whole duration. Consequently, any permanent deformation can not be identified. Similarly, the technique presented by Masri et. al. [11] did not include the consideration of any hysteretic-type spring force. Therefore, if permanent deformation is used to assess the damage occured to structure neither of the above-mentioned techniques is applicable.

REFERENCES

[1] Box, G.E.P., and Jenkins, G.M., Time Series Analysis, Forcasting and Control, San Francisco, Holden-Day, 1970.

[2] Hartog, J.P.D., Mechanical Vibrations, McGraw-Hill, New York, 1968, Chapter 8.

[3] Healey, T.J., and Sozen, M.T., Experimental Study of the Dynamic Response of a Ten-Story Reinforced Concrete Frame with a Tall First Story, Civil Engineering Studies, Structural Research Series No. 450, University of Illinois, August 1978.

[4] Jeary, A.P., and Ellis, B.R., "Vibration Test of Structure at Varied Amplitudes," Proceedings of the Second Speciality Conference on Dynamic Response of Structures, ASCE, January 15-16, 1981, pp. 281-94.

[5] Judge, G.C., and Takayama, T., "Inequality Restrictions in Reqression Analysis," Journal of American Statistical Association, March 1965, Volume 61, No. 313, pp. 166-79.

[6] Kendal, M.G., Time Series, London, Griffin, 1973.

[7] Lazan, B.J., Damping of Materials and Members in Structural Mechanics, Pergomon Press, New York, 1968.

[8] Leland, O.M., Practical Least Squares, McGraw-Hill, 1921.

[9] Lovell, M.C., and Prescot, E., "Multiple Regression with Inequality Constraints: Pretesting Bias, Hypothesis Testing and Efficiency," Journal of the American Statistical Association, June 1970, Volume 65, No. 330, pp. 913-25.

[10] Marsi, S.F., and Anderson, J.C., "Identification/Modeling Studies of Non-Linear Multidegree Systems", Vol. 3, Analytical and Experimental Studies of Non-Linear System Modeling, - A Progress Report A_T(49-24-0262), U.S. Nuclear Regulatory Commission, April, 1980.

[11] Masri, S. F., Bekey, G. A., Sassi, H., and Caughey, T.K., "Non-Parametric Identification of a Class of Nonlinear Multidegree Dynamic Systems," University of Southern California, Los Angeles, California, 90007.

[12] Papoulis, A., Probability, Random Variables and Stochastic Process, McGraw-Hill, New York, 1965.

[13] Plunkett, R., "Vibration Damping," Applied Mechanics Surveys, Spartan Books, Washington, D.C., 1966.

[14] Toussi, S., and Yao, J.T.P., Identification of Hysteretic Behavior For Existing Structures, Report No. CE-STR-80-19, School of Civil Engineering, Purdue University, West Lafayette, IN, December, 1980.

[15] Udawadia, F.E., and Kuo, C.P., "Nonparameteric Identification of a Class of Nonlinear Close-Coupled Dynamic Systems", University of Southern California, Los Angeles, California.

[16] Zellner, A., Linear Regression with Inequality Constraints on the Coefficient, Muneographed Report 6109 of the International Center for Management Science, 1961.

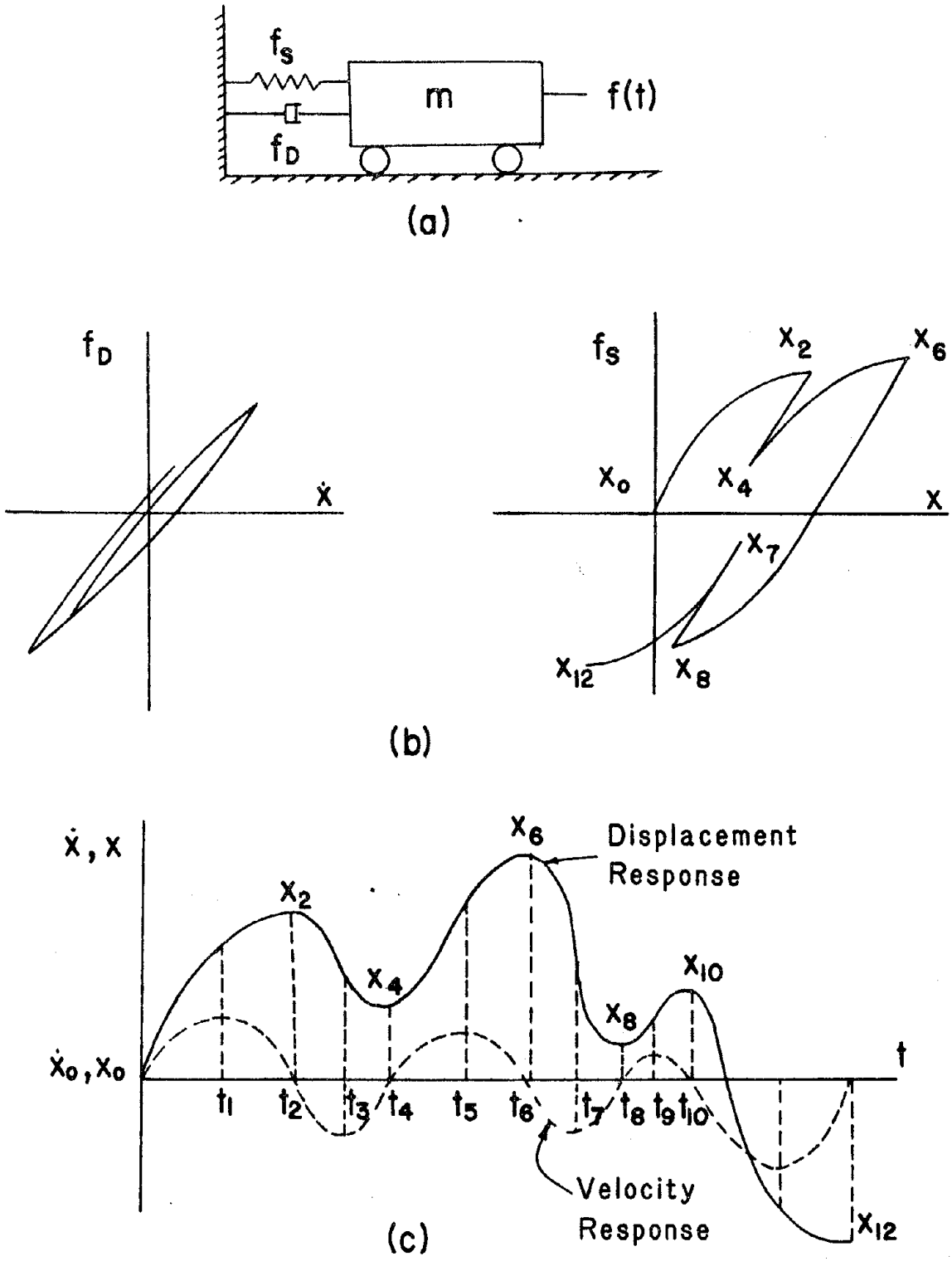

Figure 1: System model

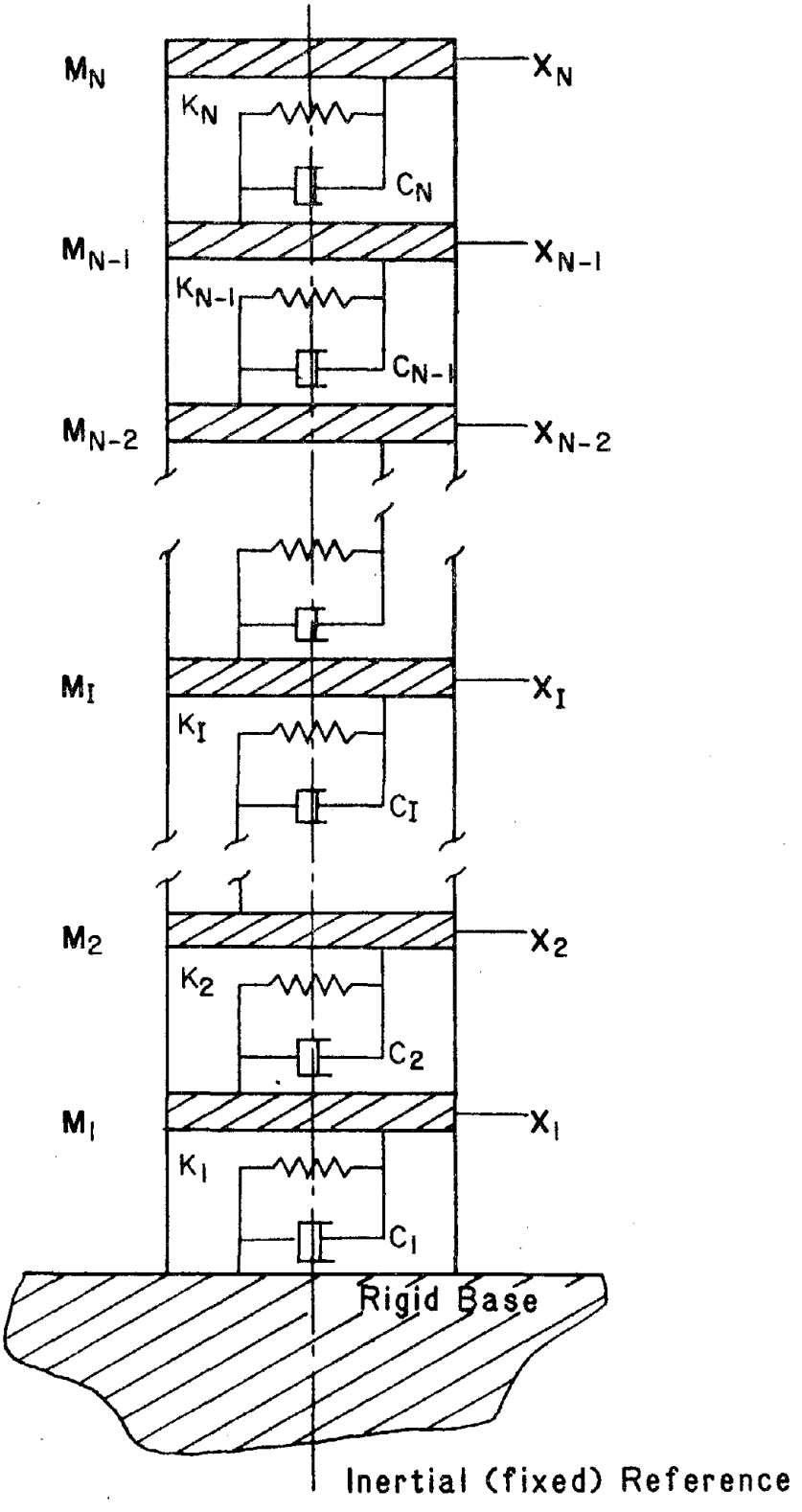

Figure 2: Lumped – Mass System

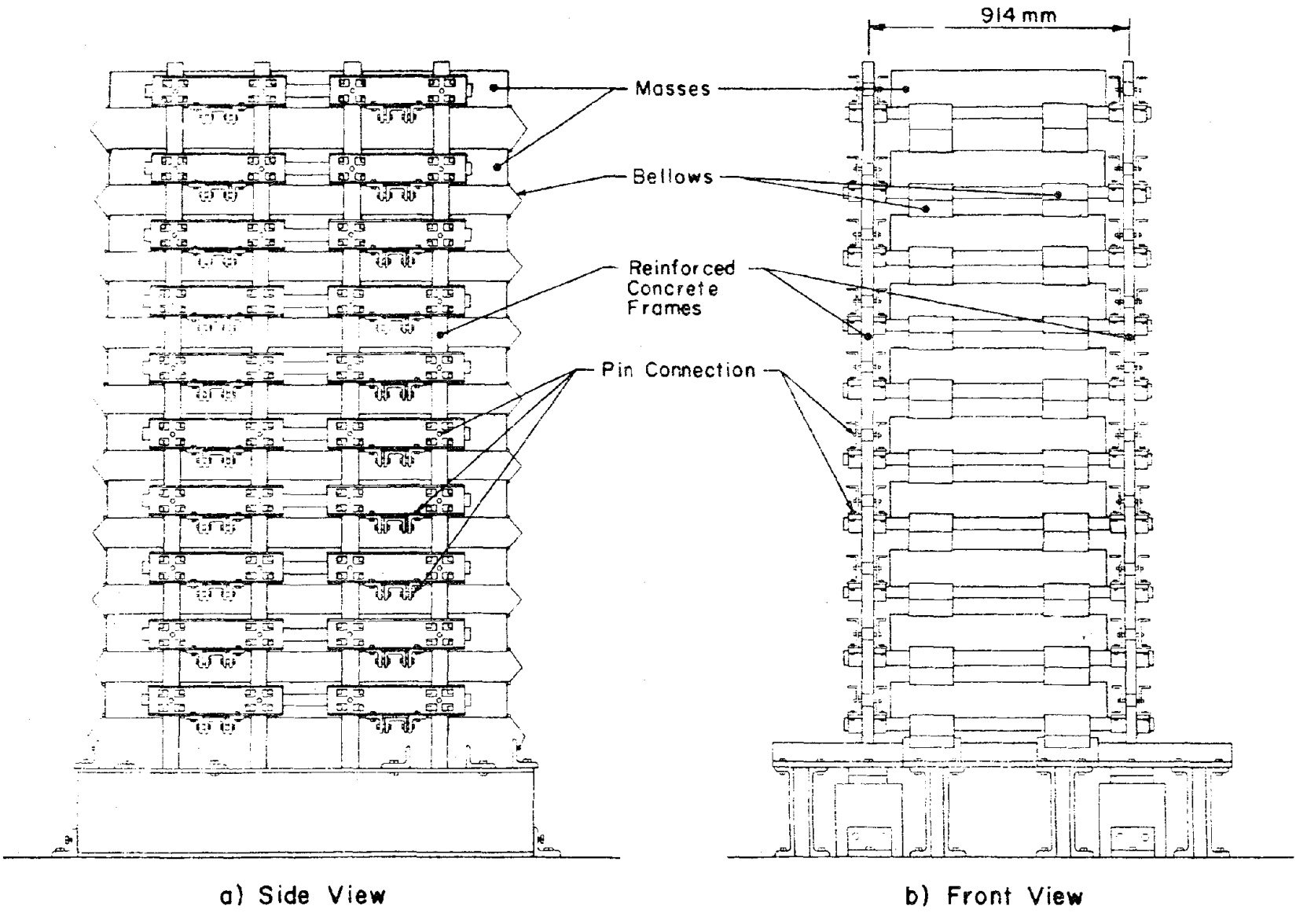

Figure 3 - Test Structure
(Healey & Sozen [3]).

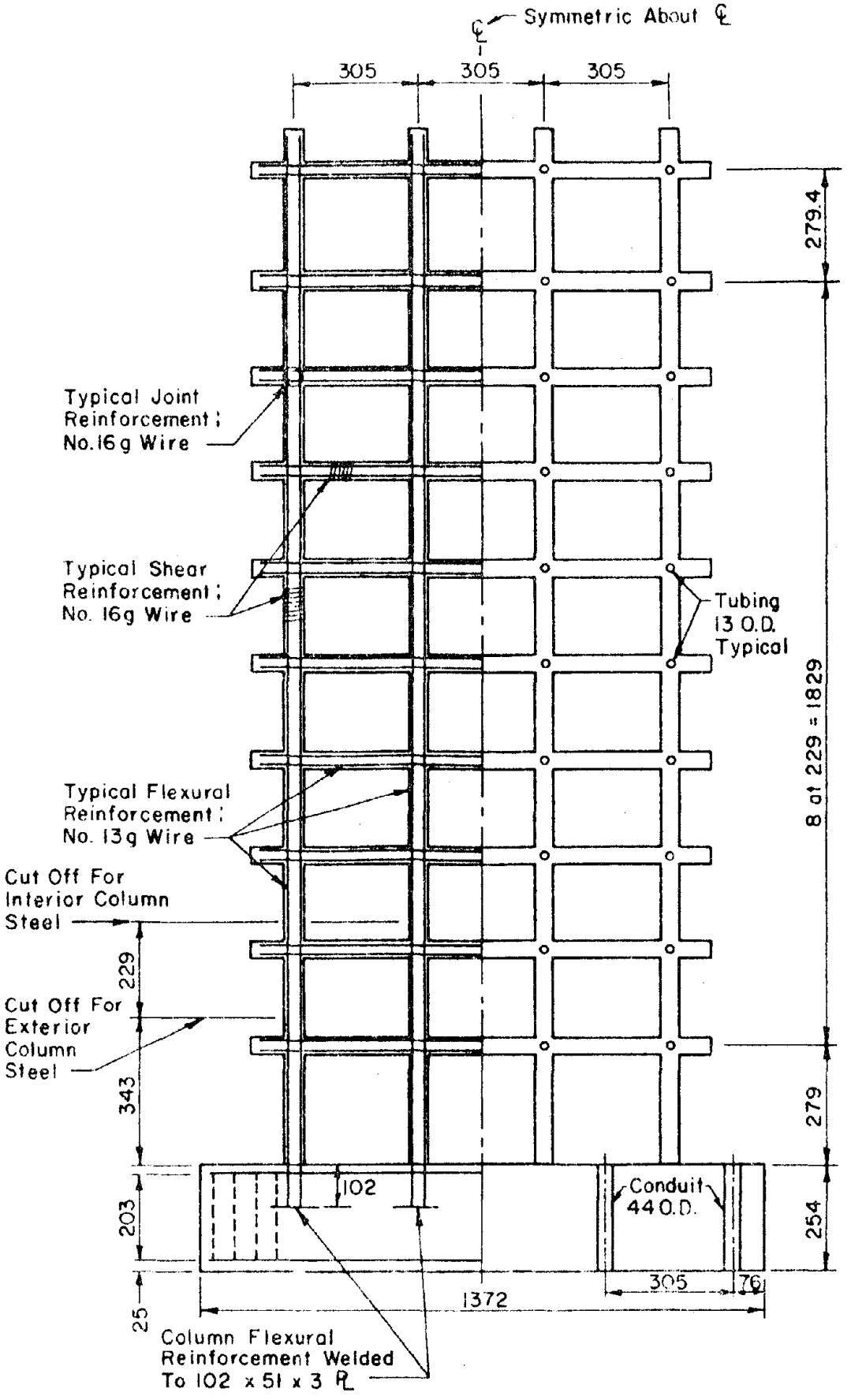

Figure 4: Reinforcement Detail and Dimensions of the Test Structure (Healey and Sozen [3])

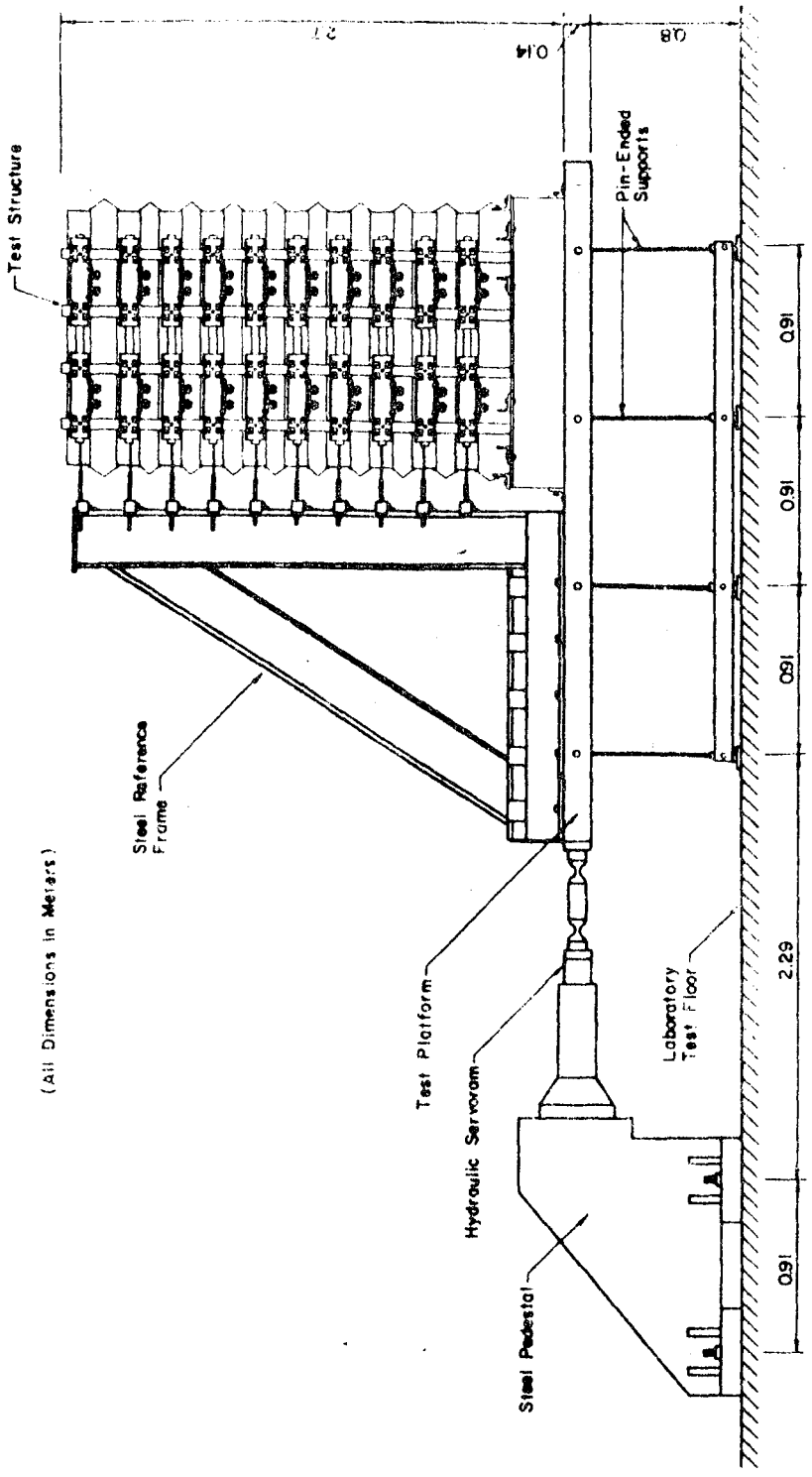

Figure 5: Test Setup (Healey and Sozen [3]).

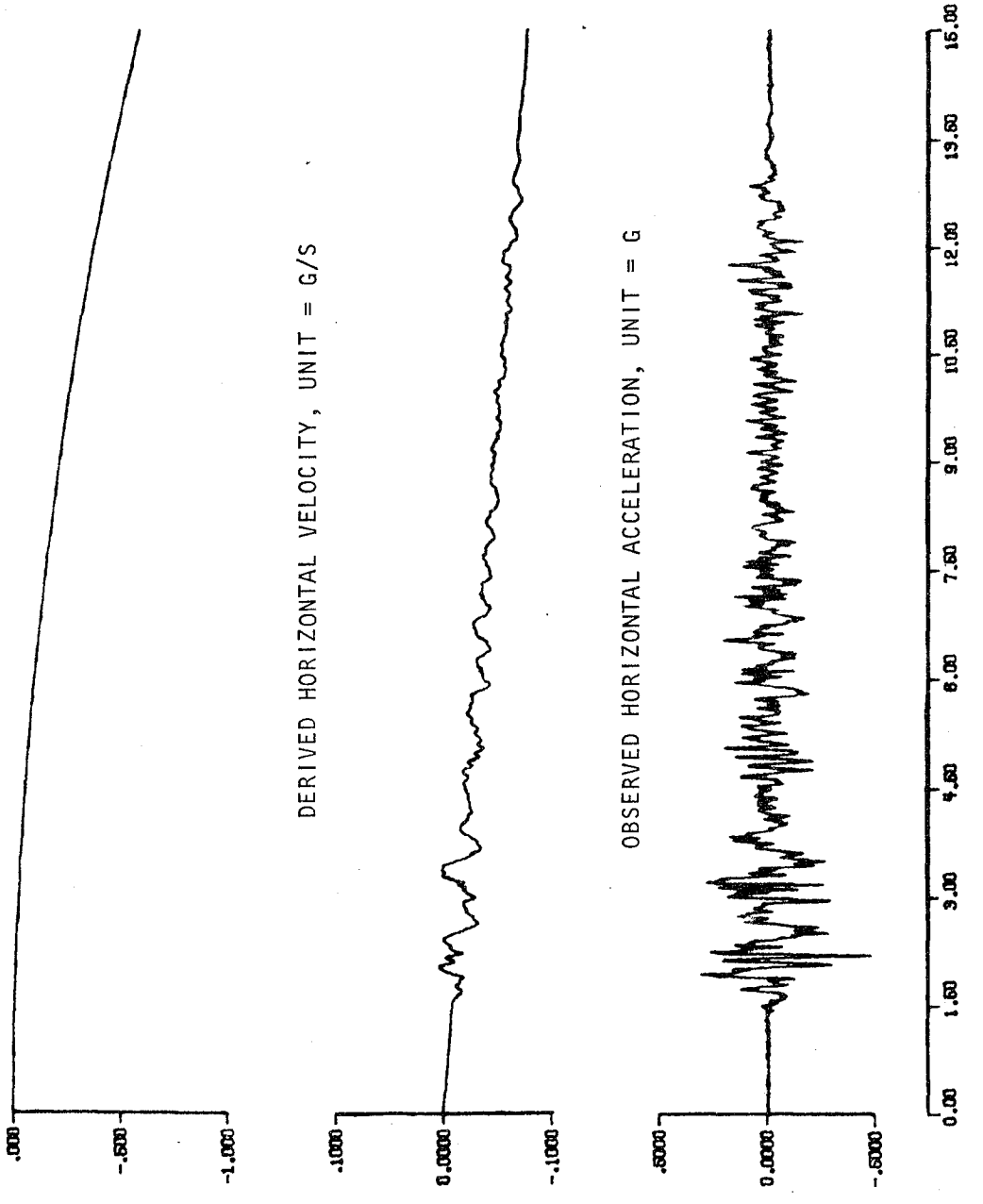

Figure 6: Second-Level Absolute Acceleration, Velocity, and Displacement, RUN 1.

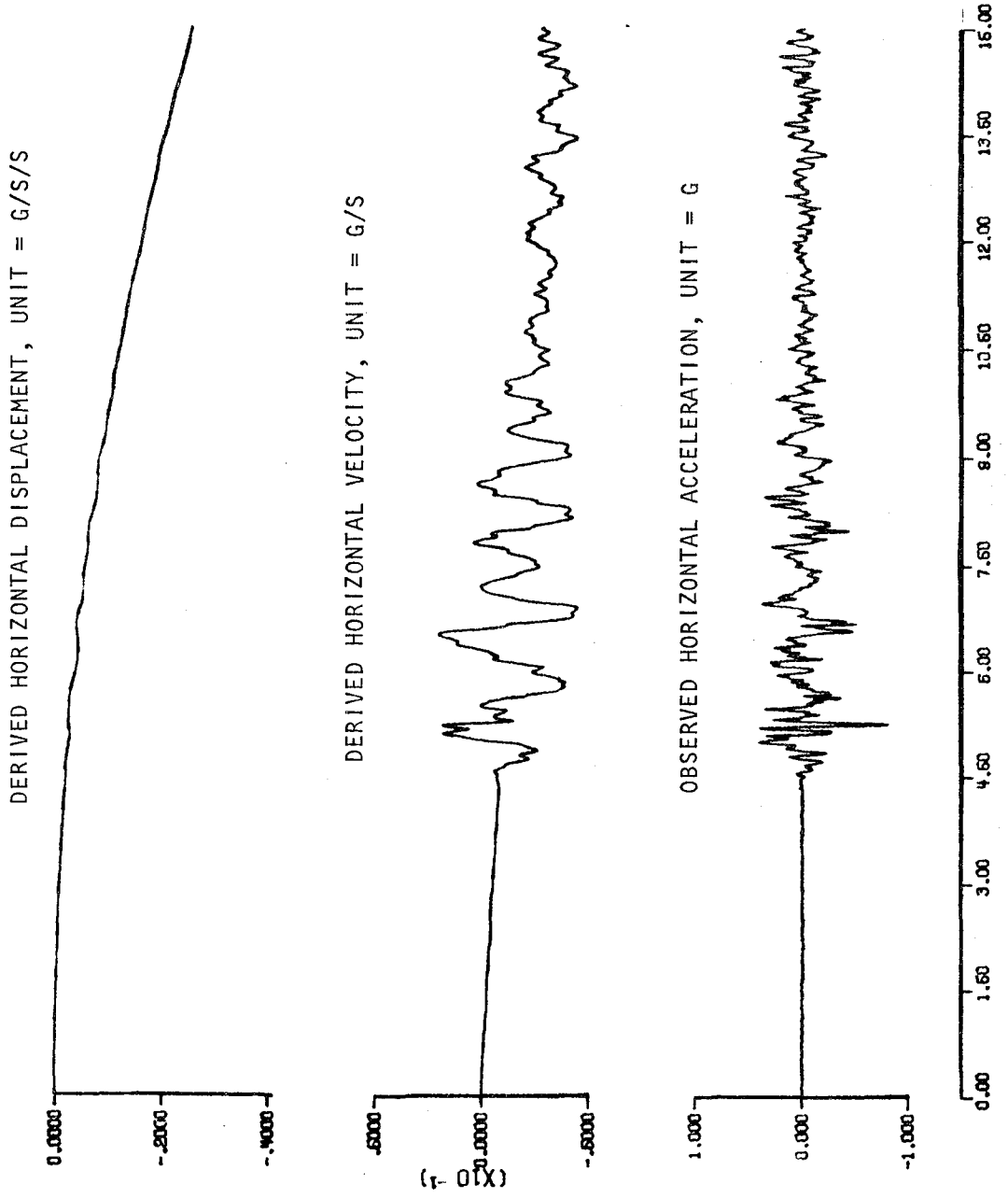

Figure 7: Fourth-Level Absolute Acceleration, Velocity, and Displacement, RUN 2

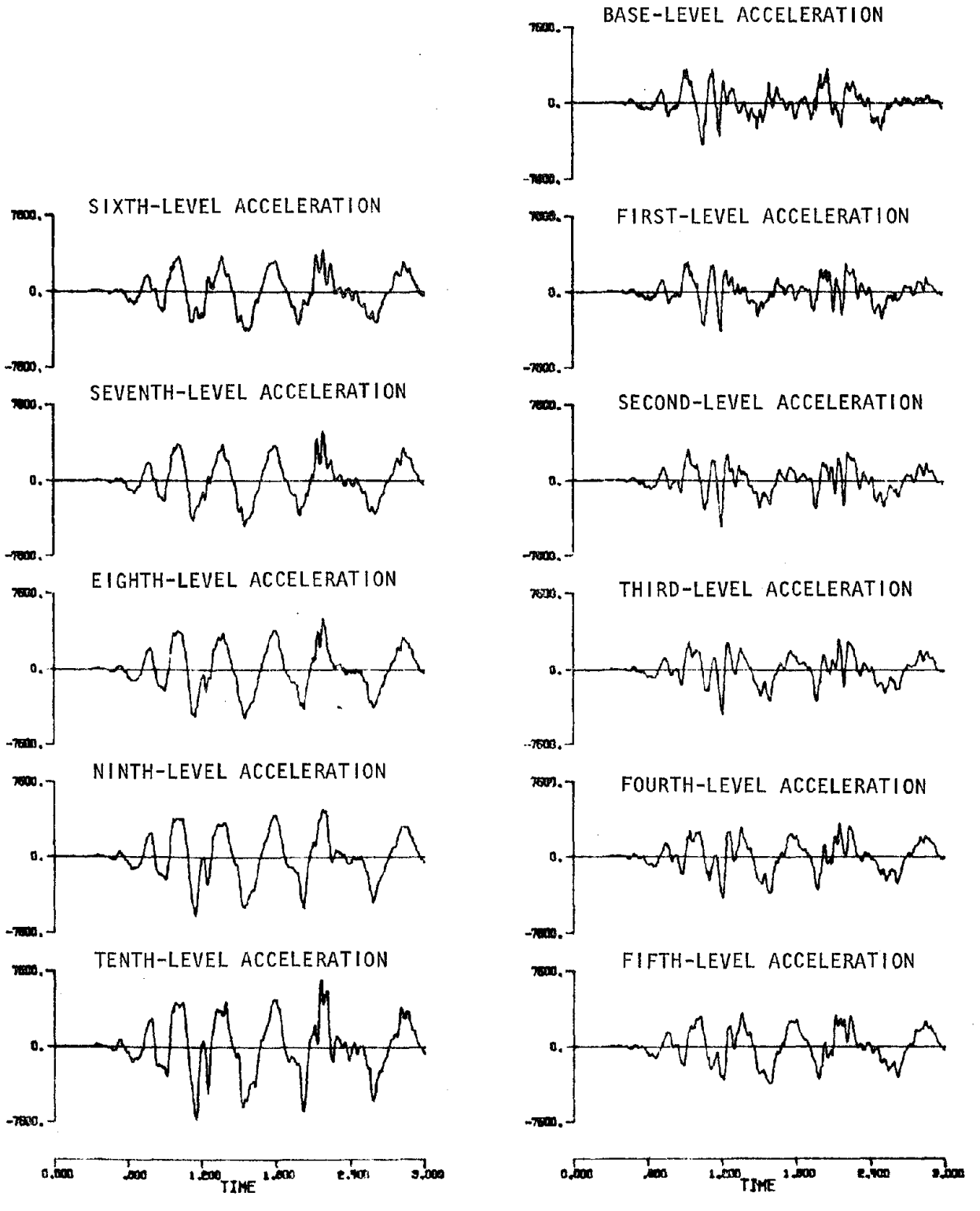

Figure 8: Absolute Acceleration Response (Unit = MM/S/S), RUN 1

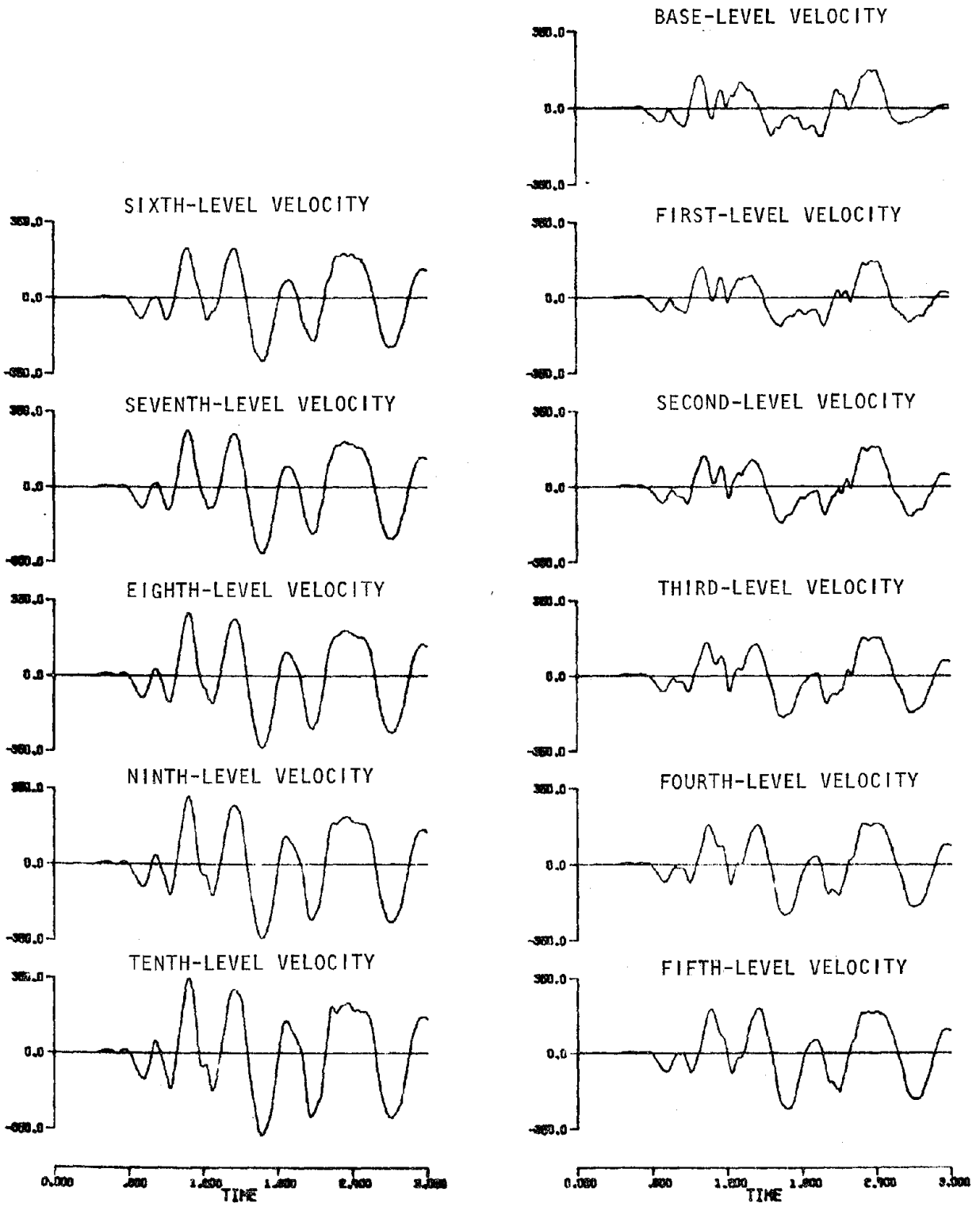

Figure 9: Absolute Velocity Response (Unit = MM/S), RUN 1.

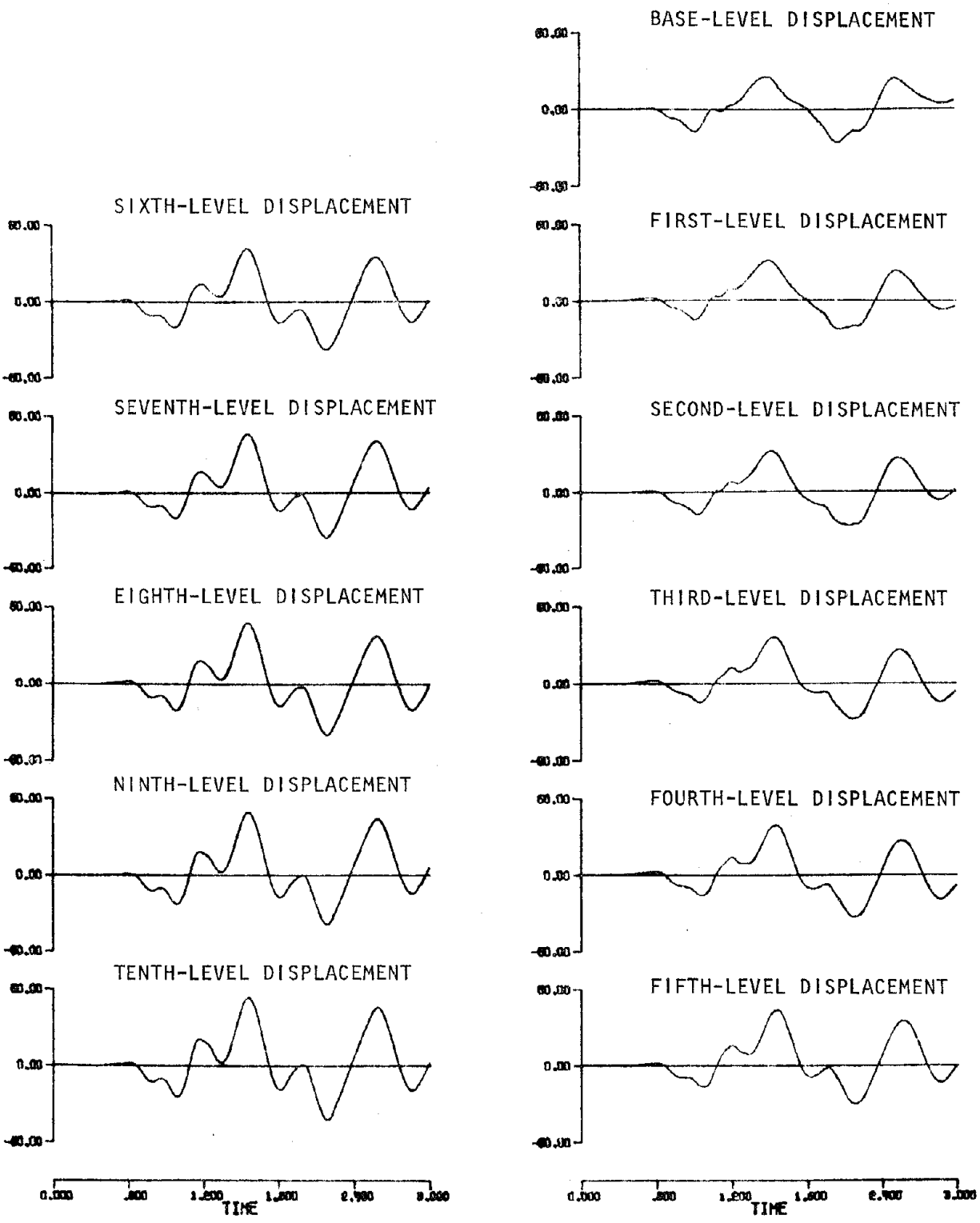

Figure 10: Absolute Displacement Response (Unit = MM), RUN 1.

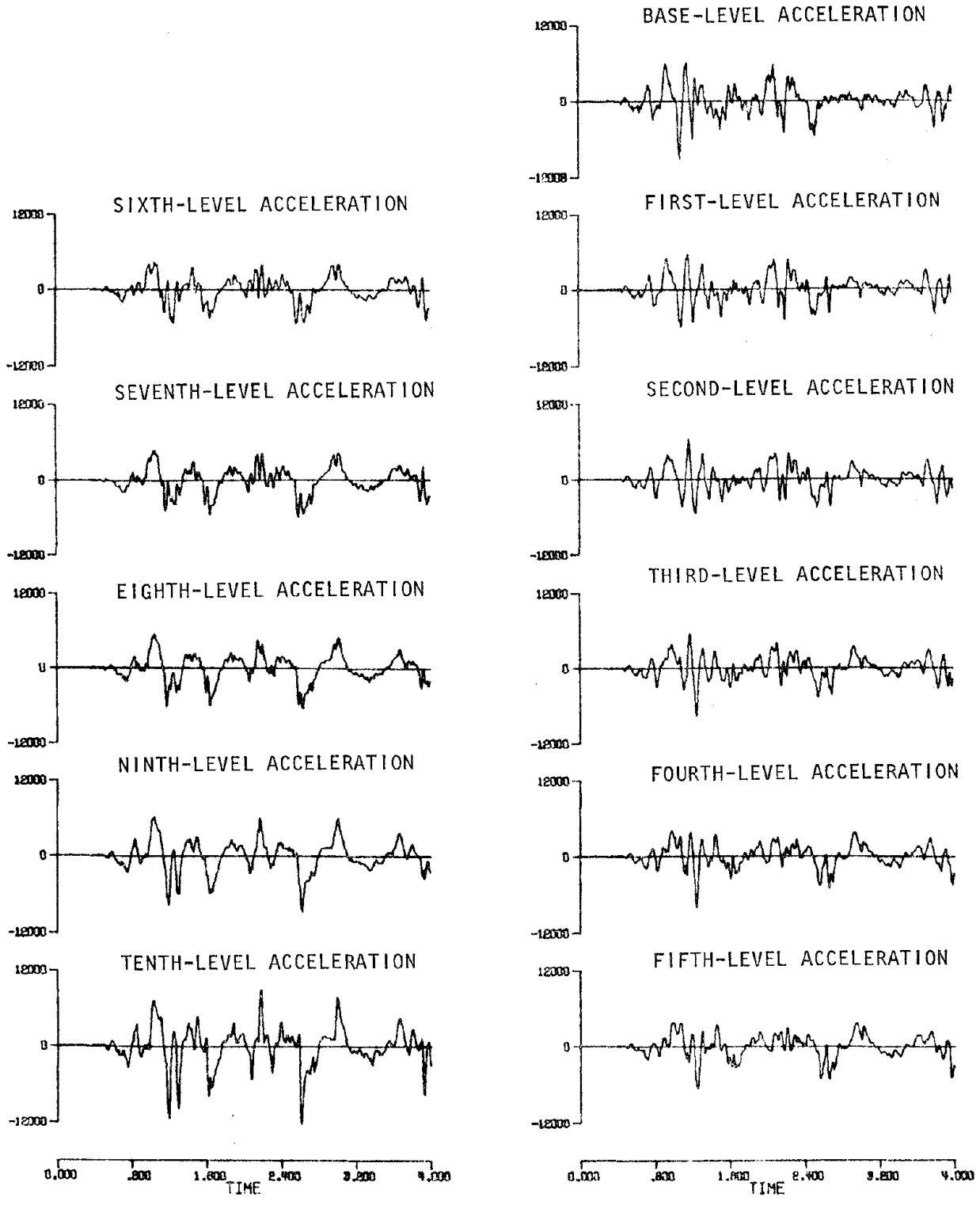

Figure 11: Absolute Acceleration Response (Unit = MM/S/S), RUN 2.

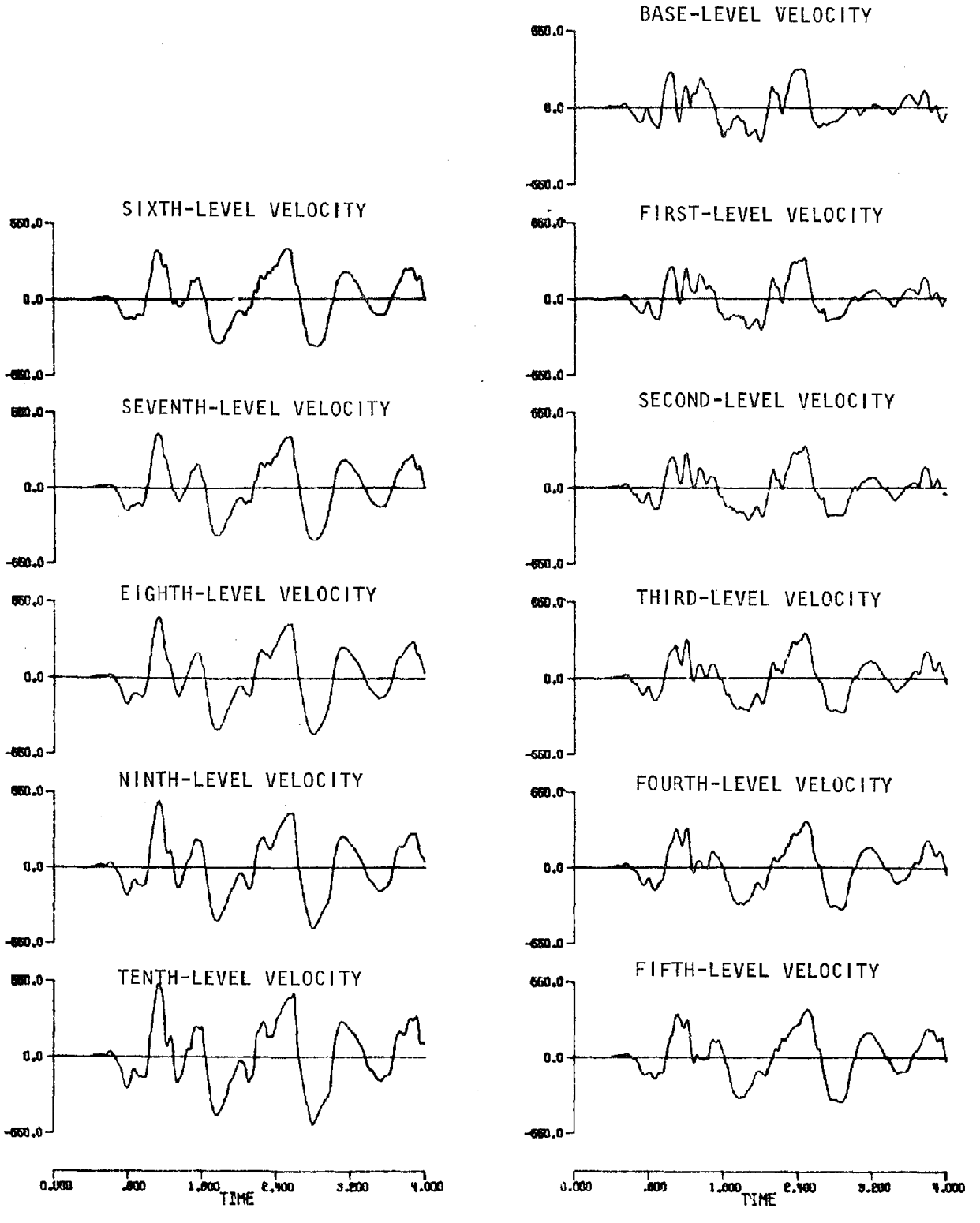

Figure 12: Absolute Velocity Response (Unit = MM/S), RUN 2.

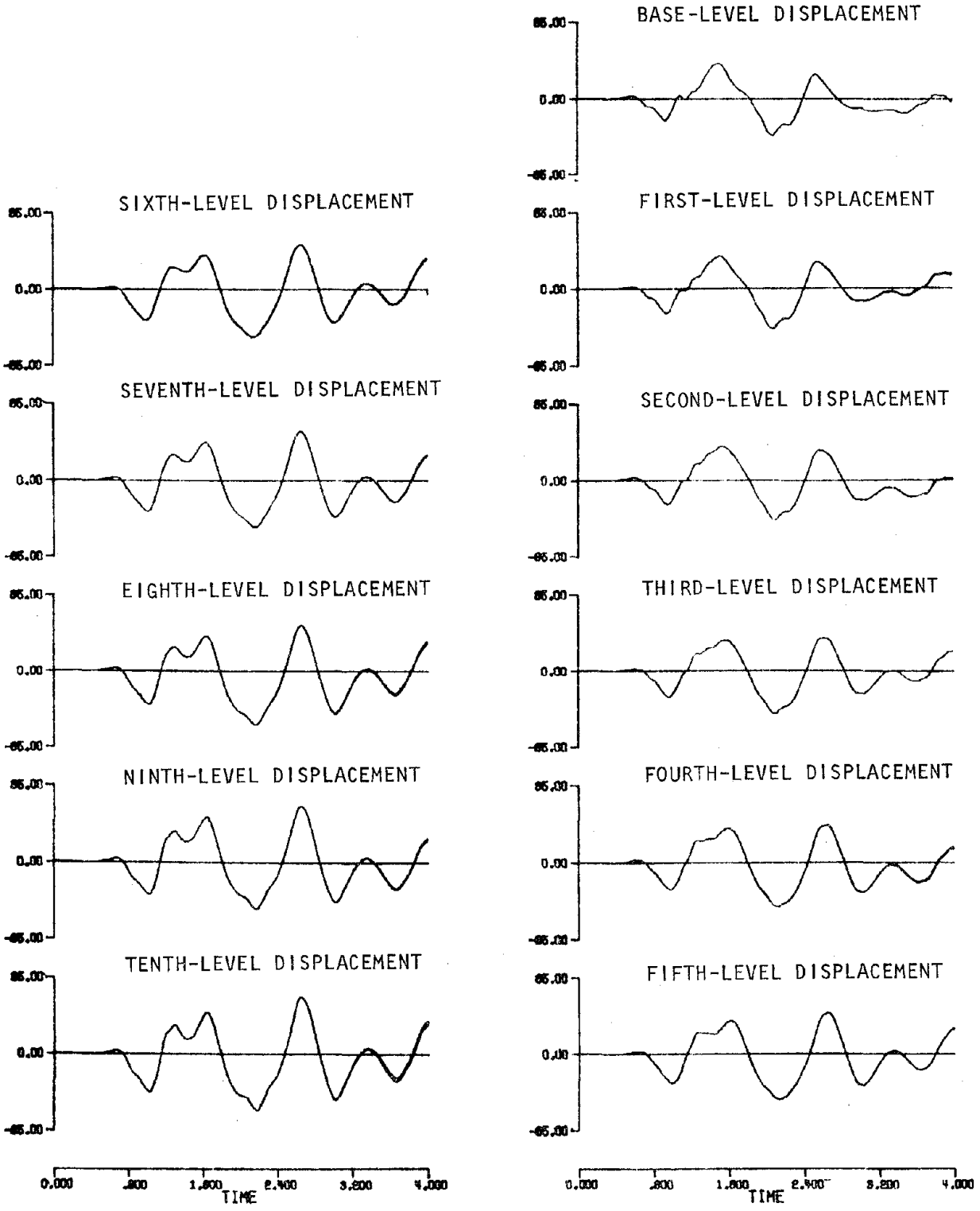

Figure 13: Absolute Displacement Response (Unit = MM), RUN 2.

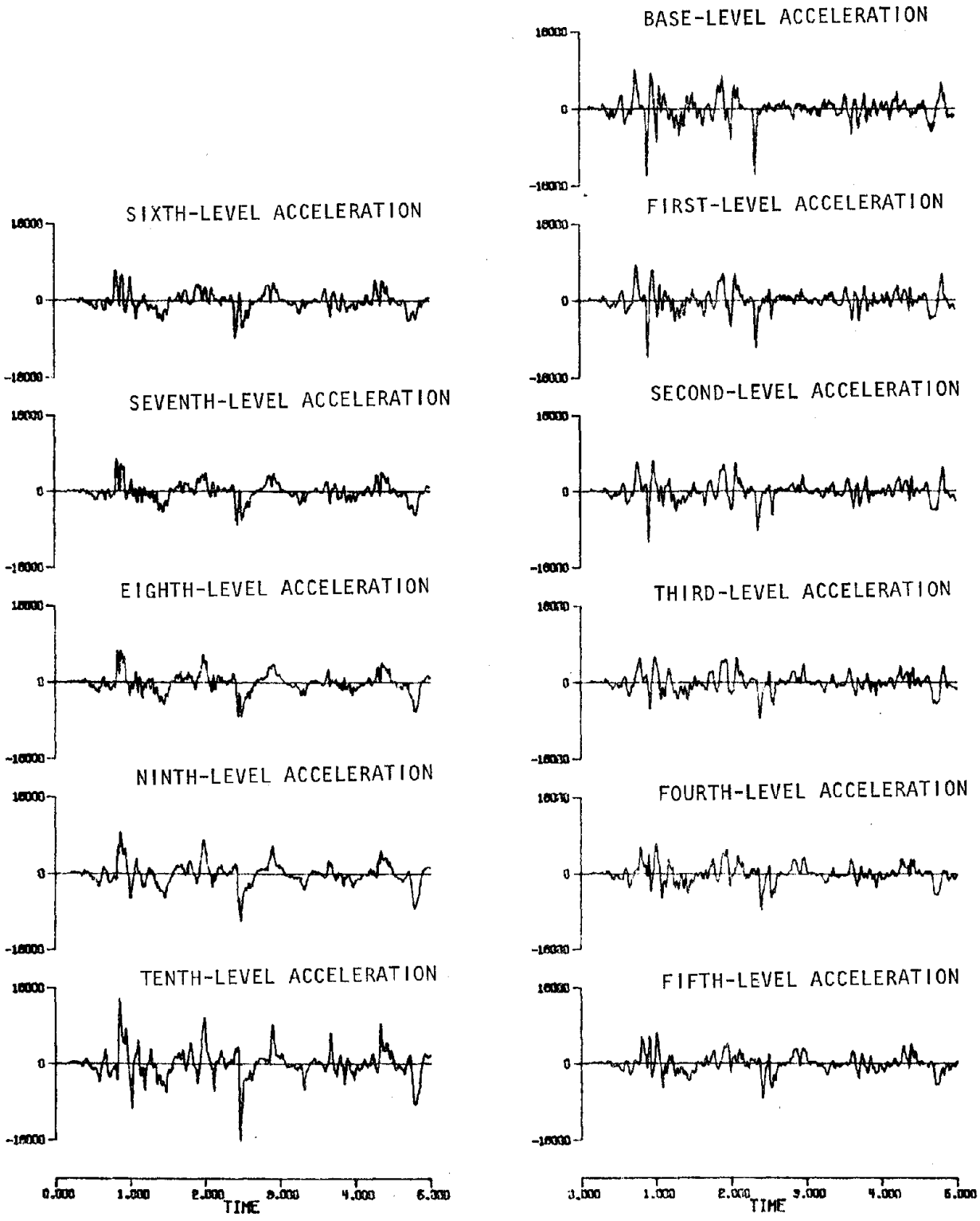

Figure 14: Absolute Acceleration Response (Unit = MM), RUN 3.

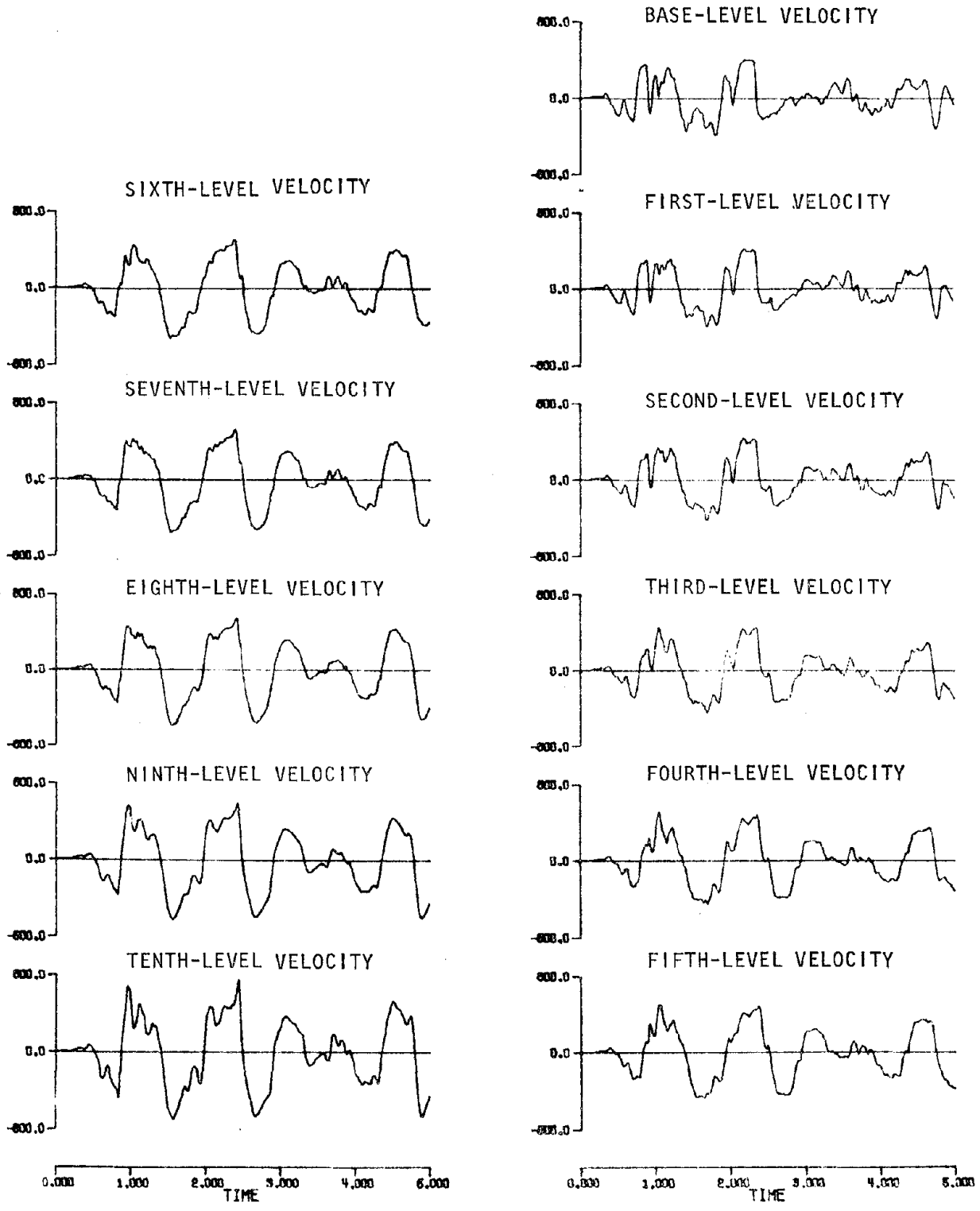

Figure 15: Absolute Velocity Response (Unit = MM/S), RUN 3.

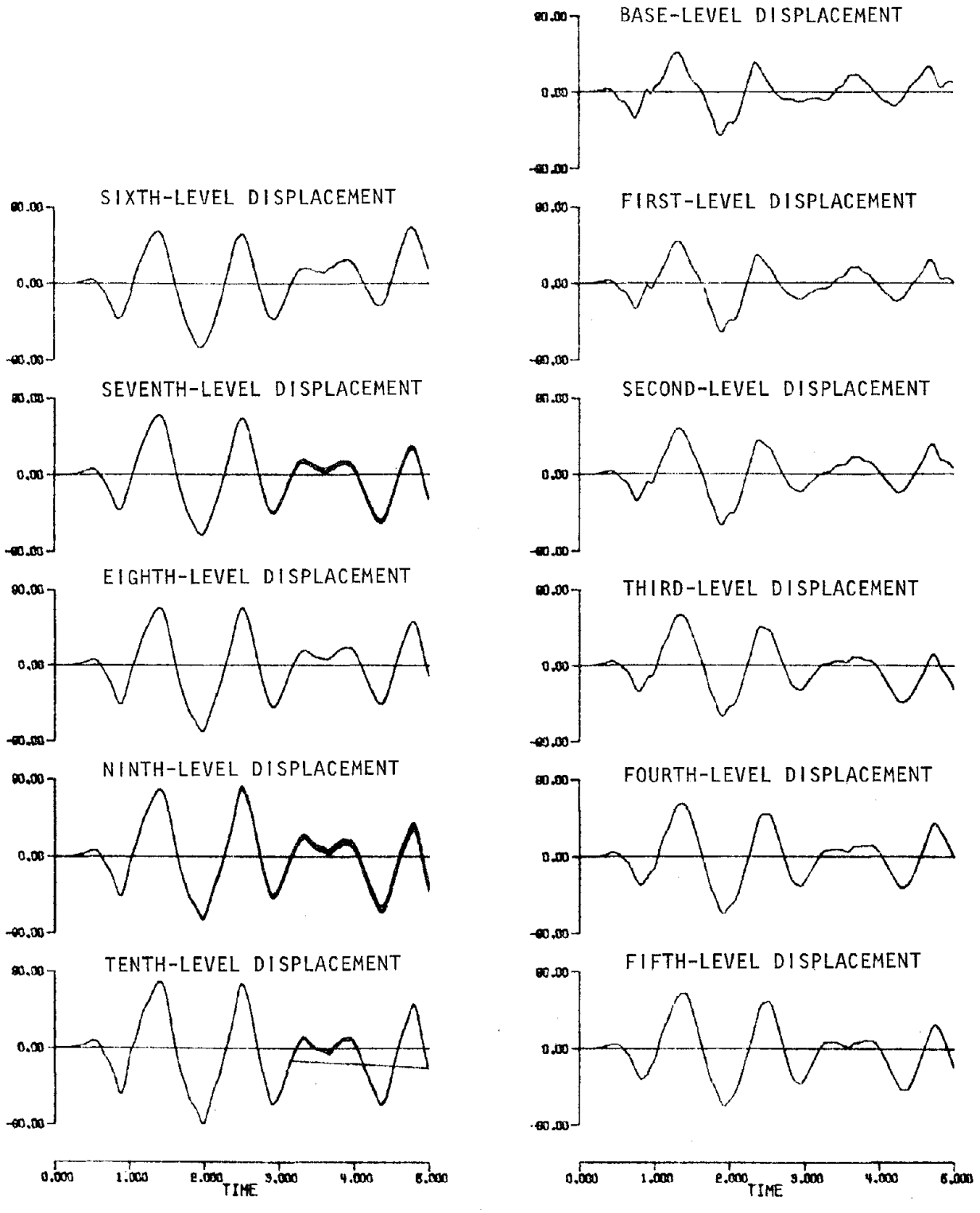

Figure 16: Absolute Displacement Response (Unit = MM), RUN 3.

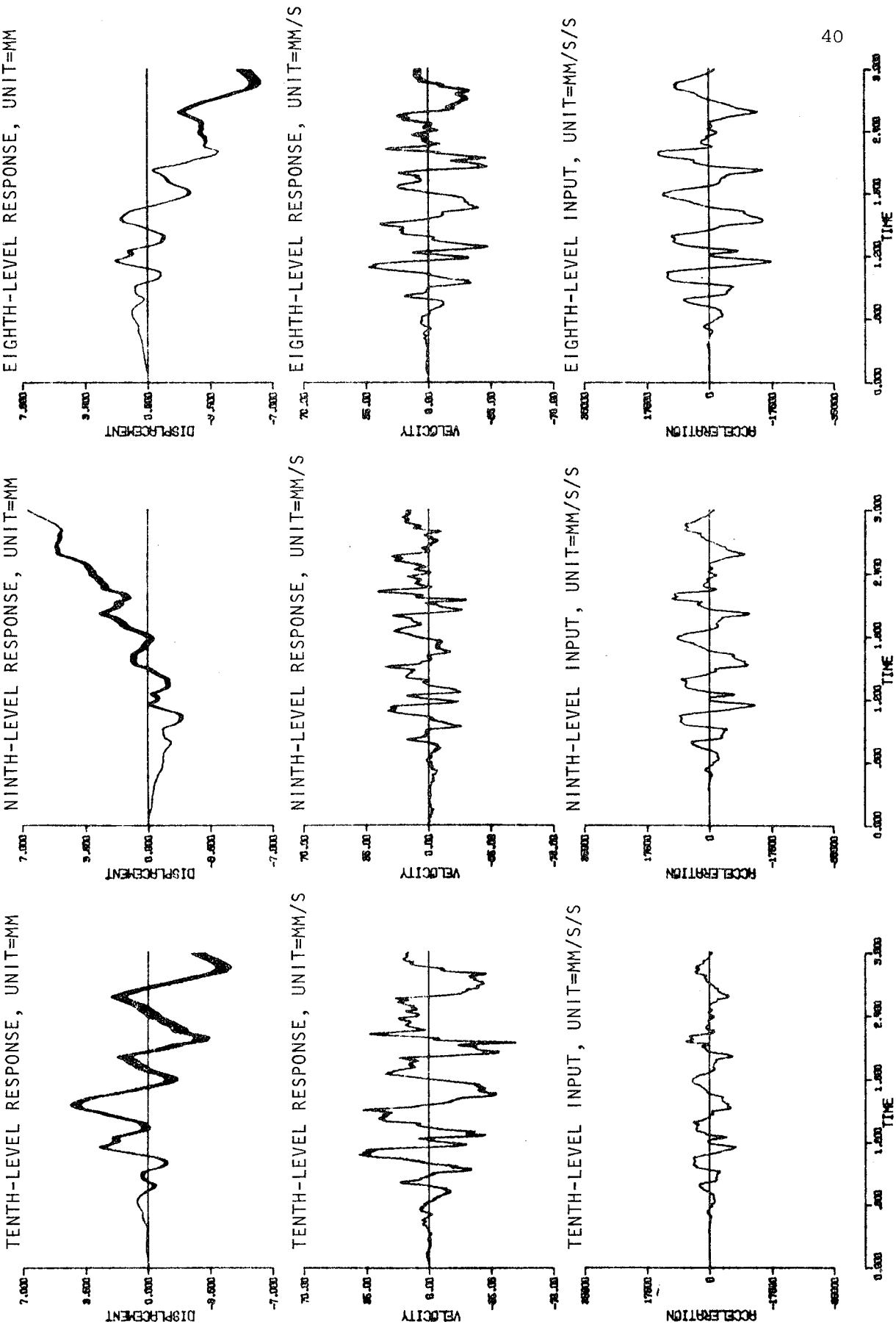

Figure 17: Inter-Story Horizontal Response, RUN 1.

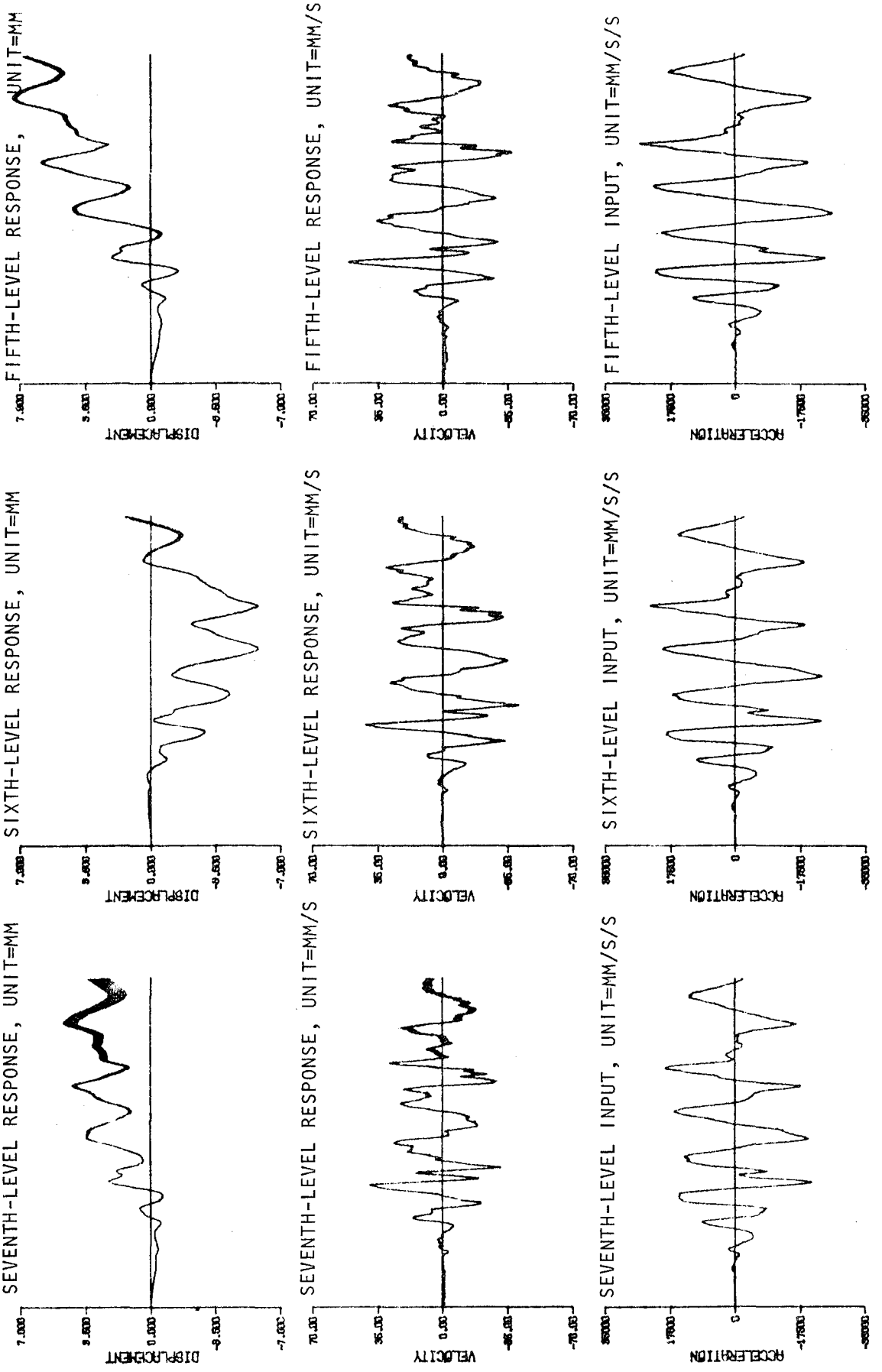

Figure 17 (Contd): Inter-Story Horizontal Responses, RUN 1.

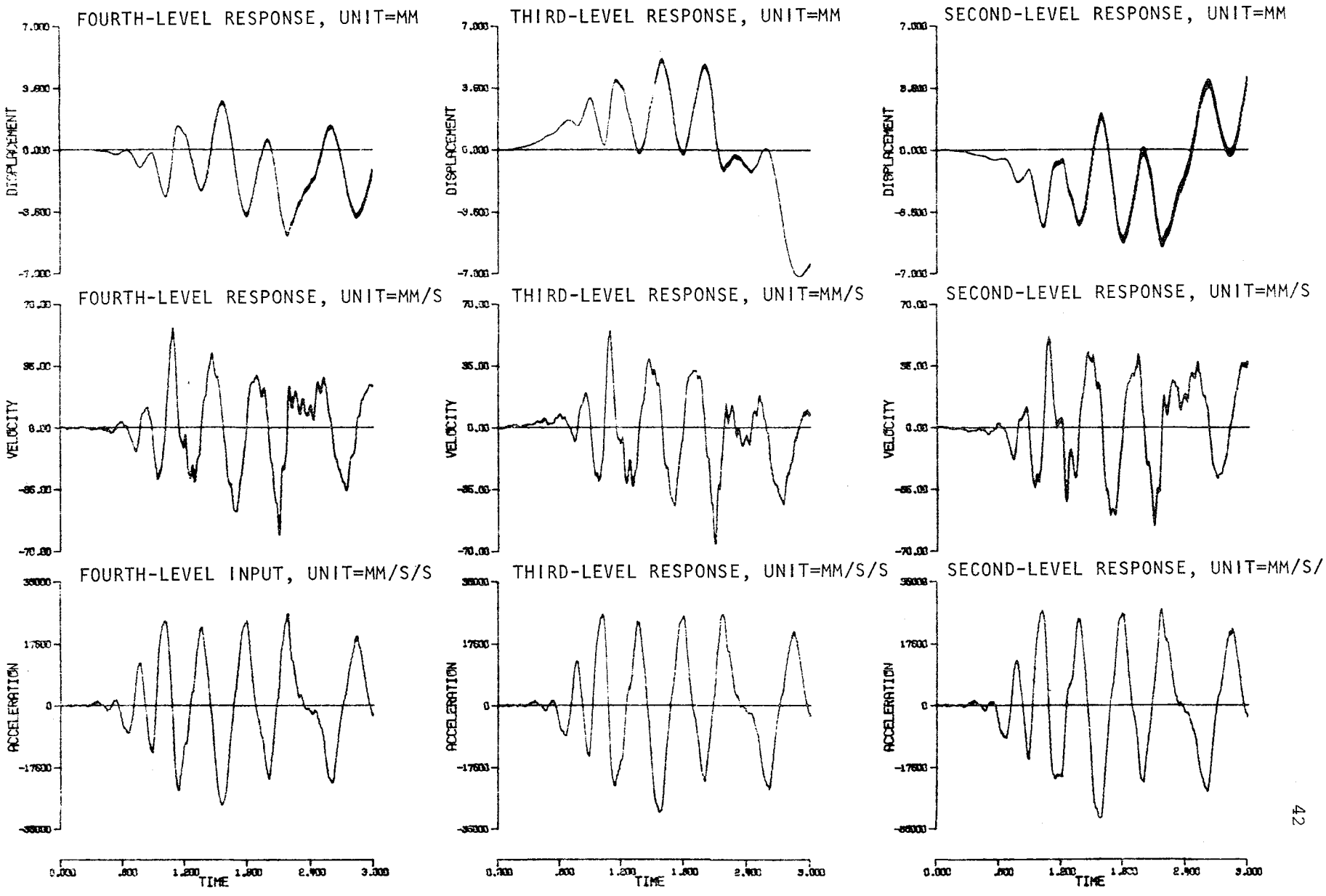

Figure 17 (Cont.): Inter-Story Horizontal Responses, RUN 1

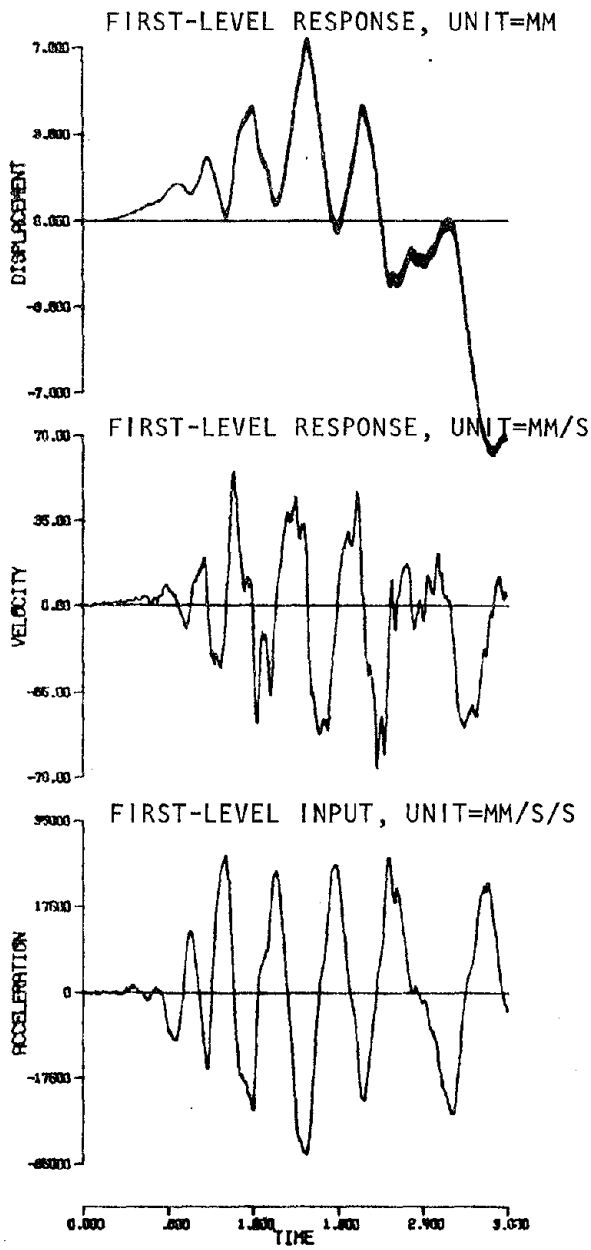

Figure 17 (Cont.): Inter-Story Horizontal Responses, RUN 1.

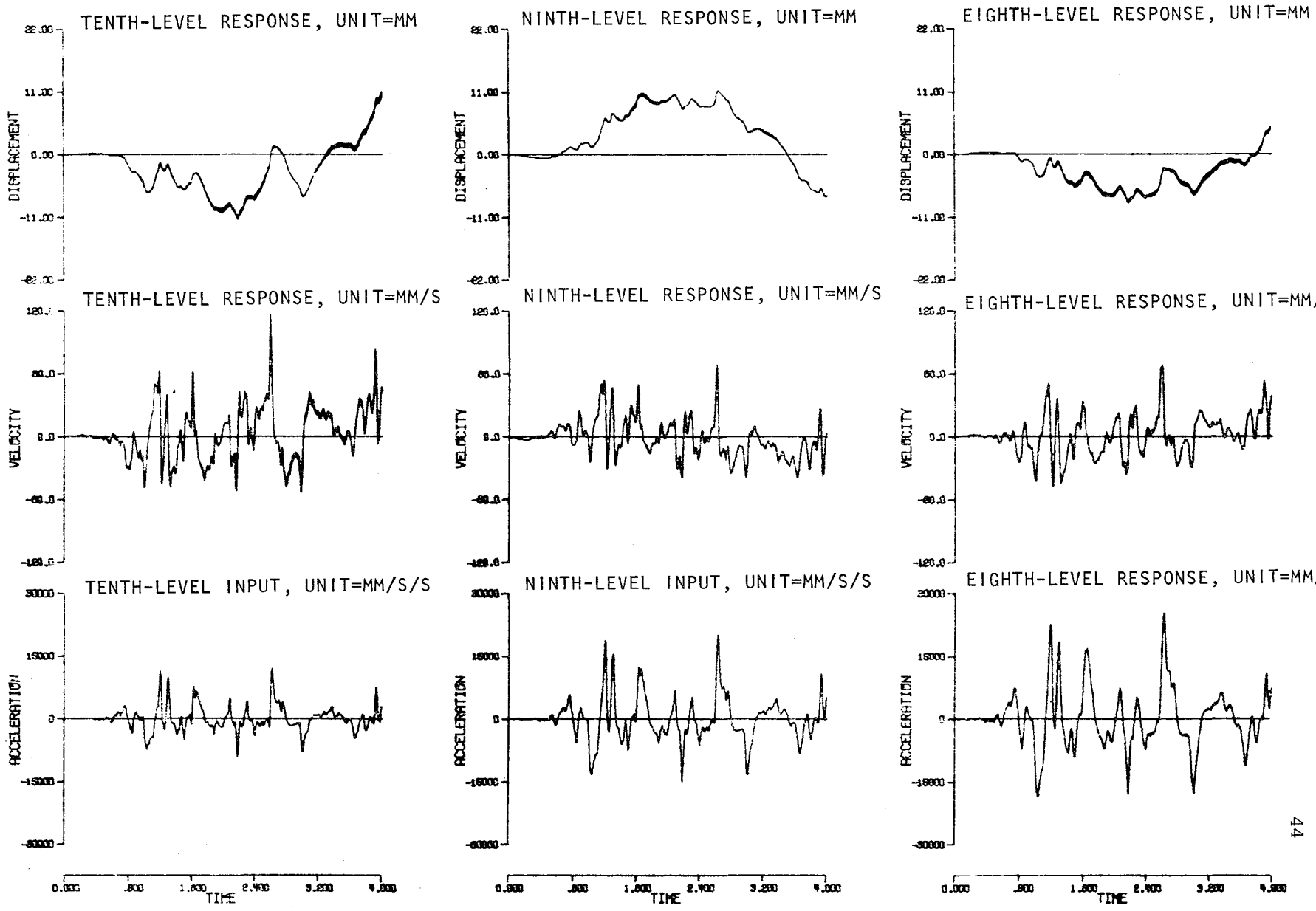

Figure 18: Inter-Story Horizontal Responses, RUN 2.

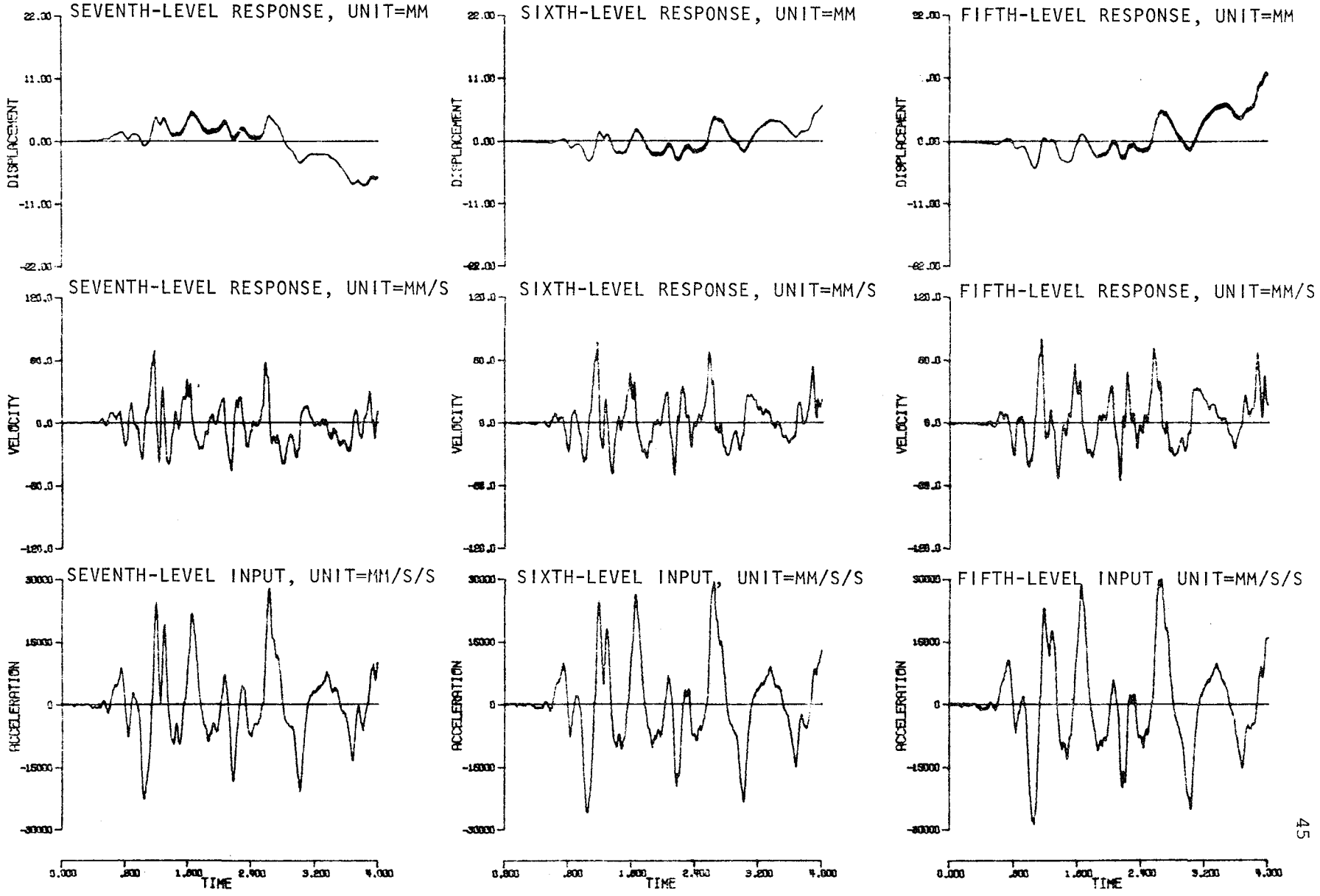

Figure 18 (Cont.): Inter-Story Horizontal Responses, RUN 2.

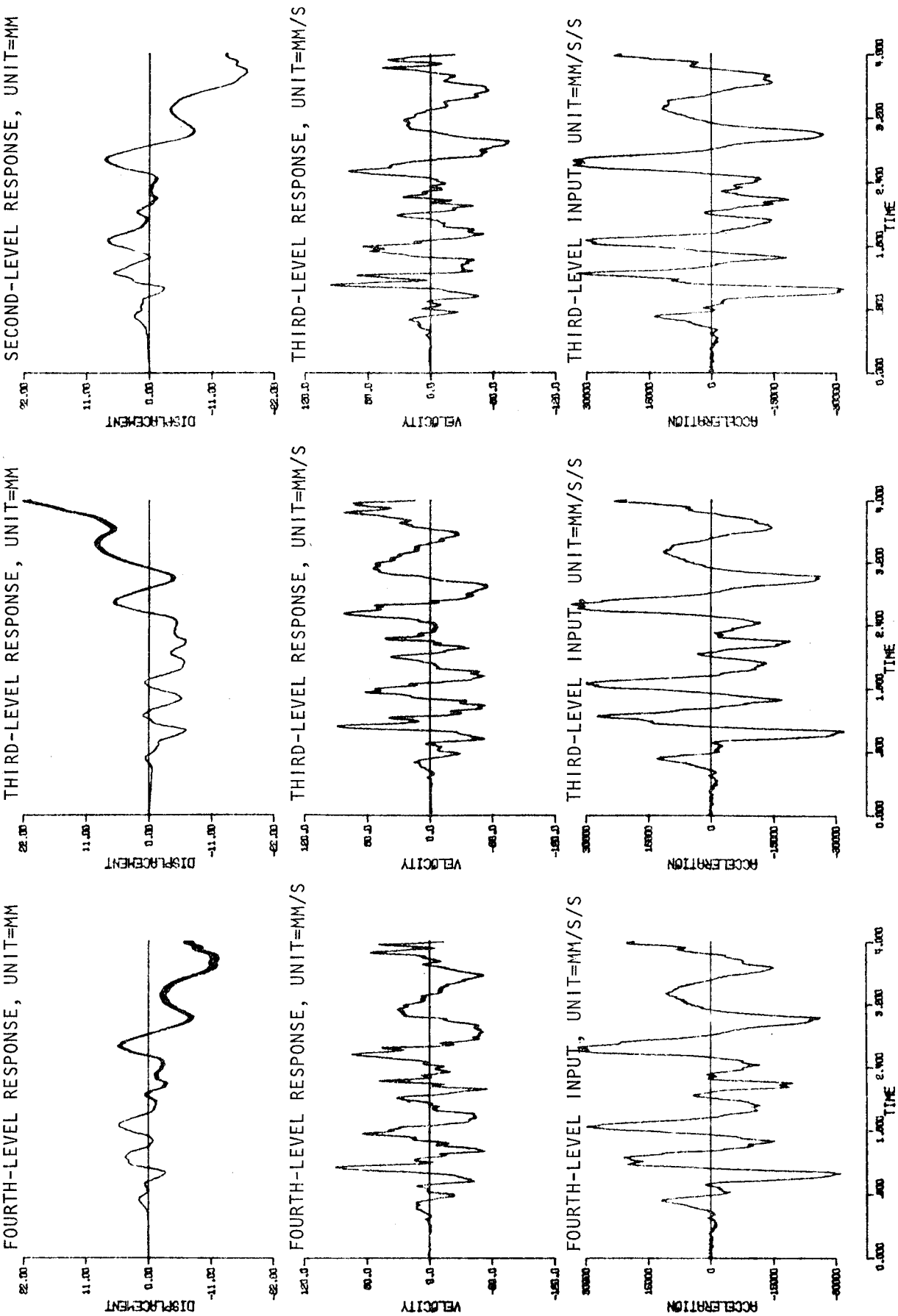

Figure 18 (Cont.): Inter-Story Horizontal Response, RUN 2.

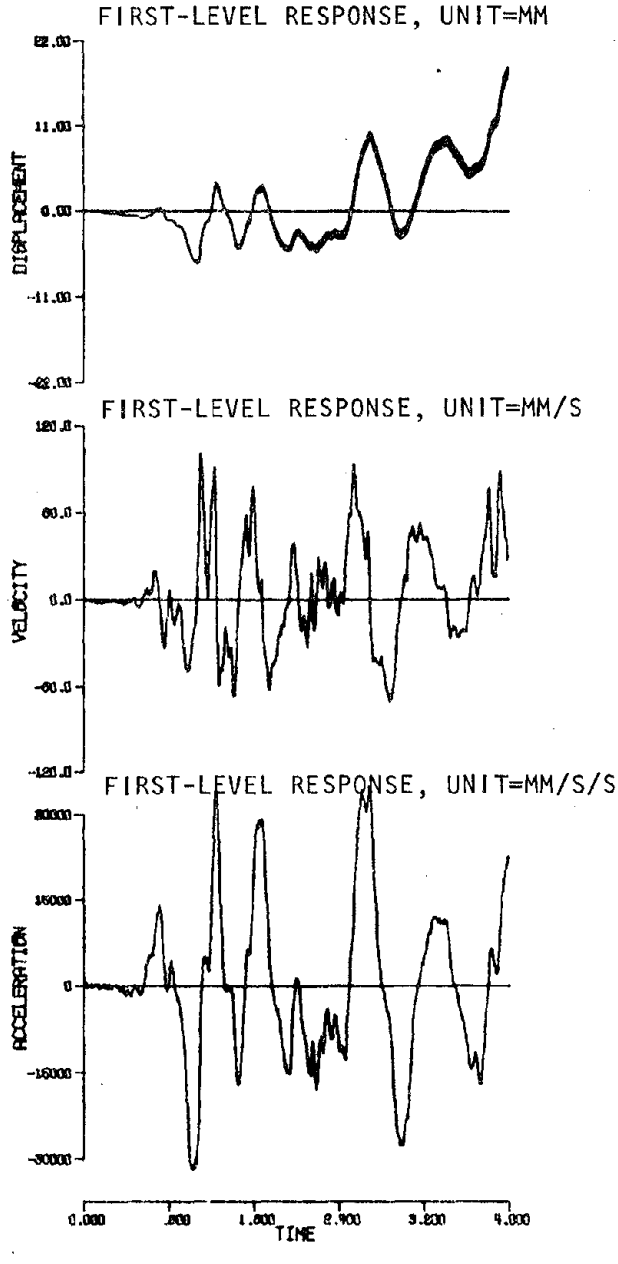

Figure 18 (Cont.): Inter-Story Horizontal Responses, RUN 2.

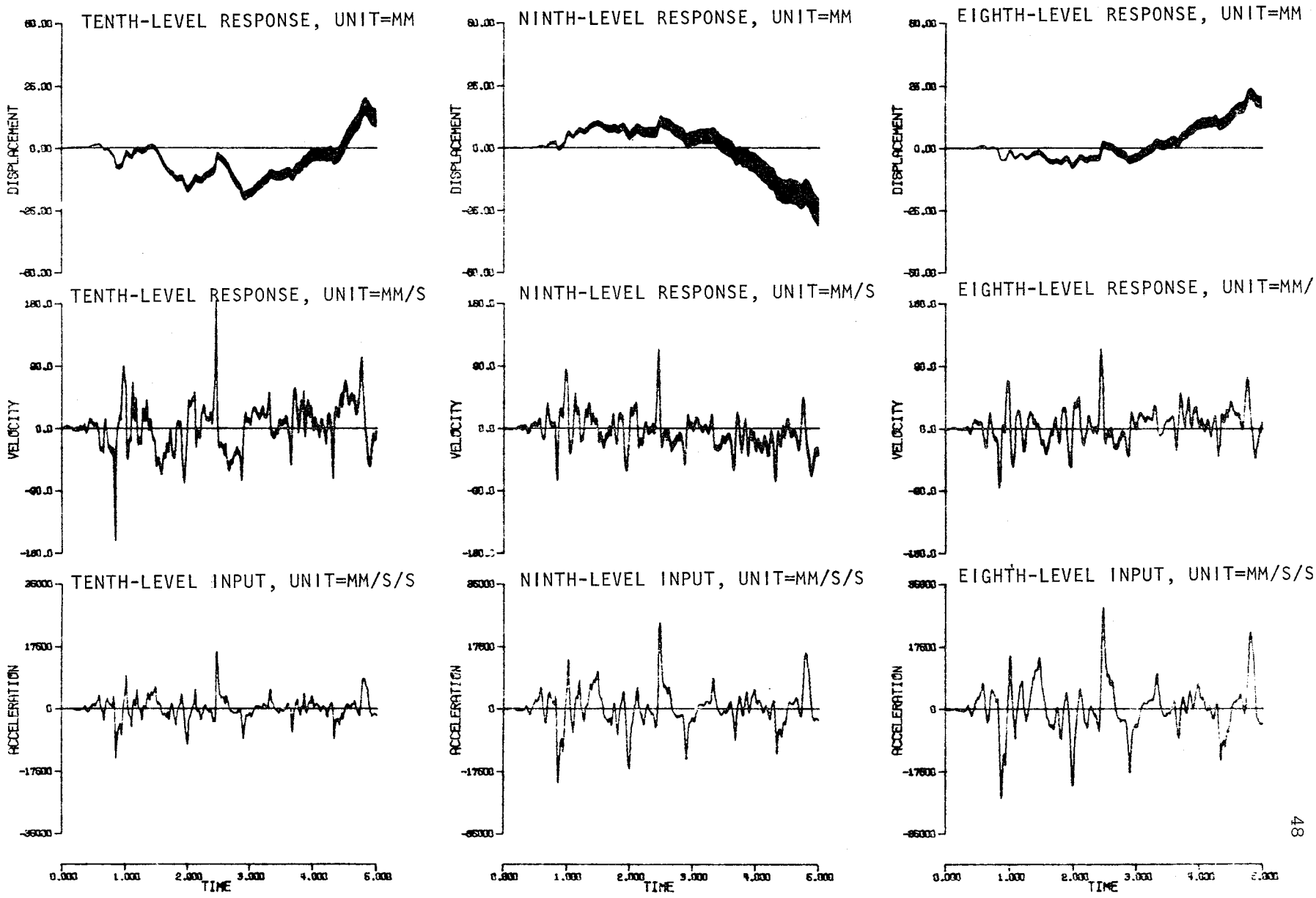

Figure 19: Inter-Story Horizontal Responses, RUN 3.

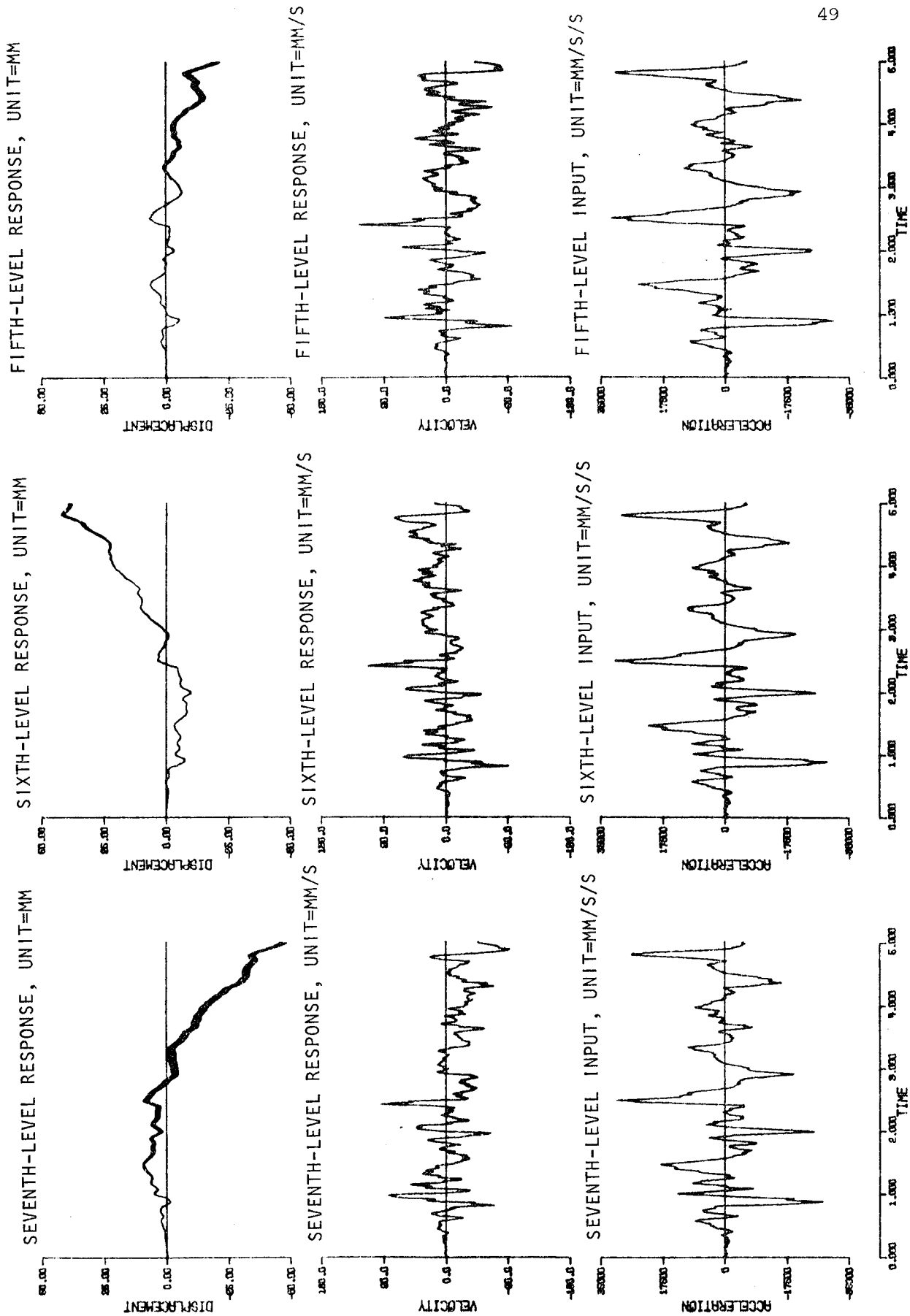

Figure 19 (Cont.): Inter-Story Horizontal Responses, RUN 3.

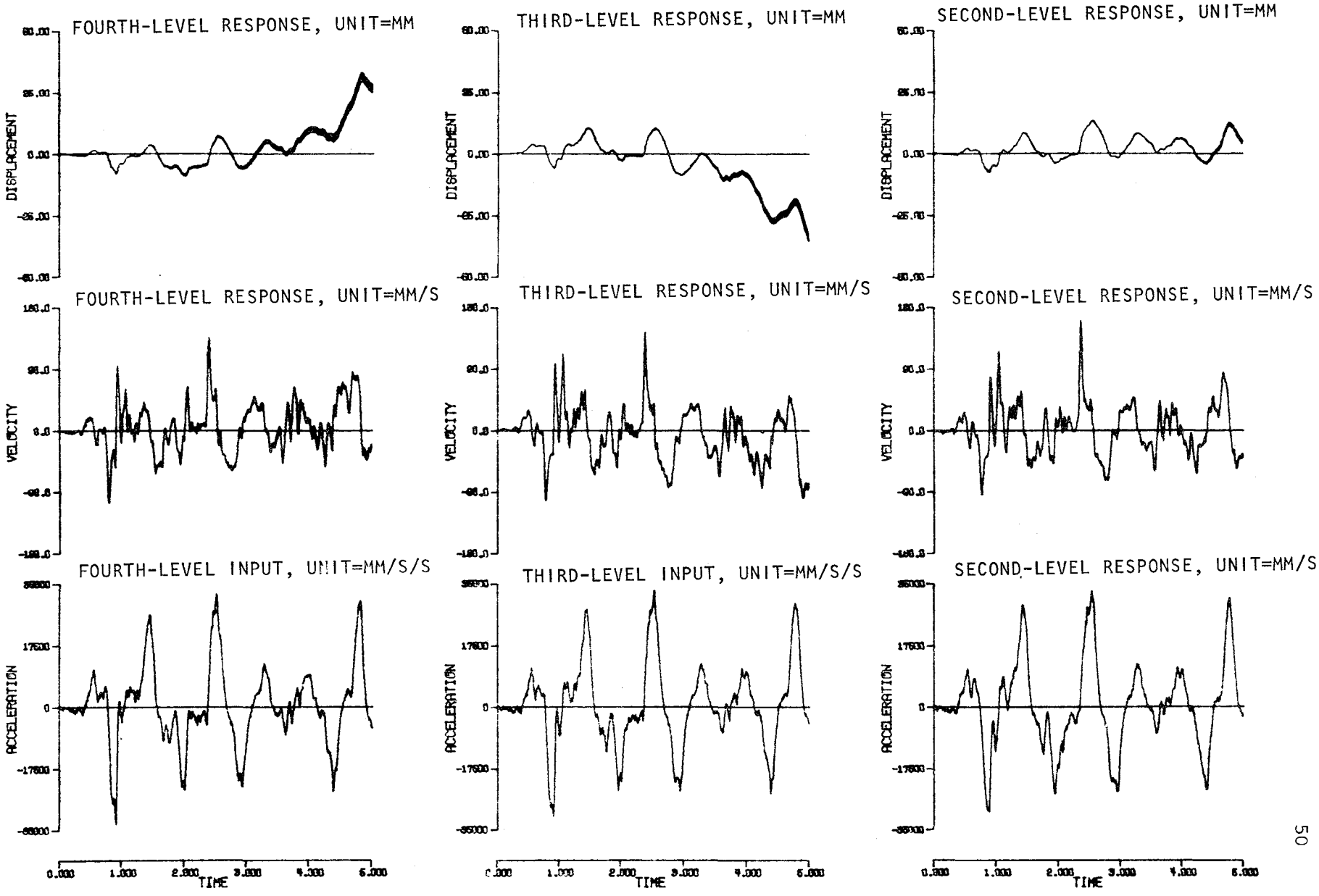

Figure 19 (Cont.): Inter-Story Horizontal Responses, RUN 3.

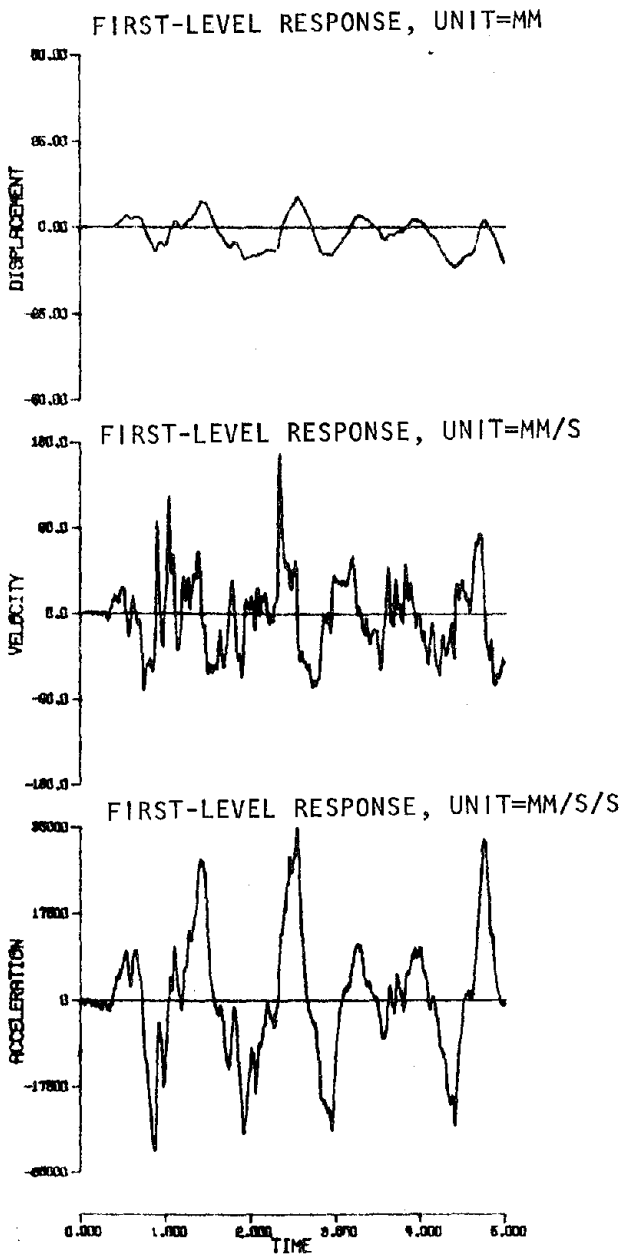

Figure 19 (Cont.): Inter-Story Horizontal Responses, RUN 3.

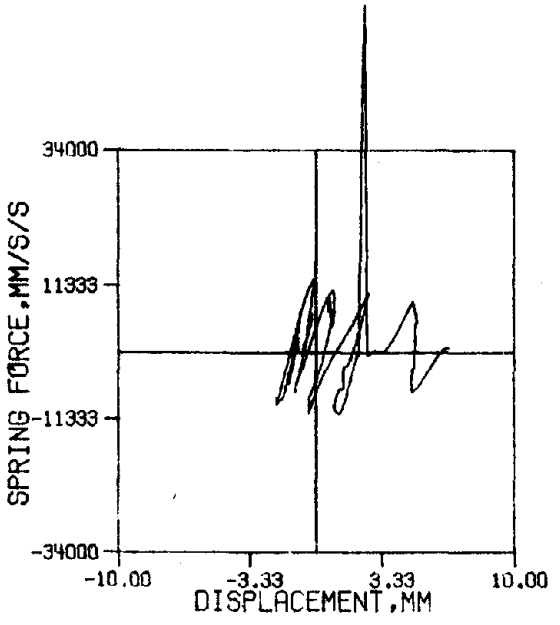

(b) NINTH FLOOR

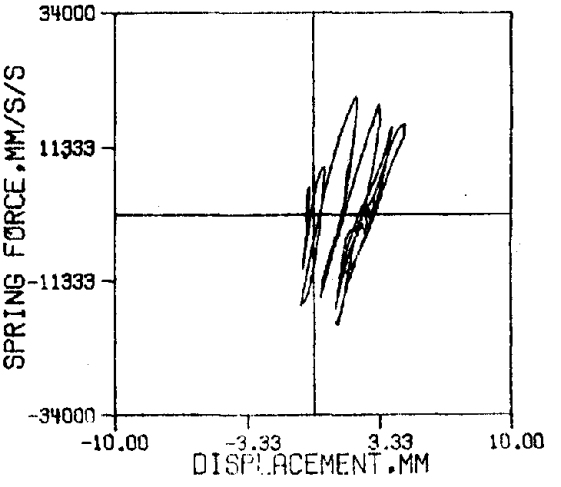

(d) SEVENTH FLOOR

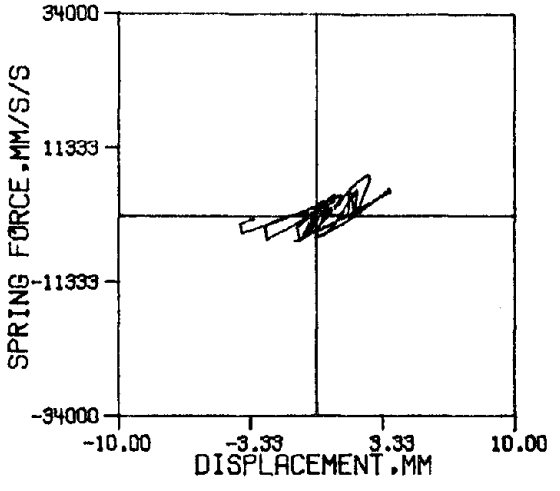

(a) TENTH FLOOR

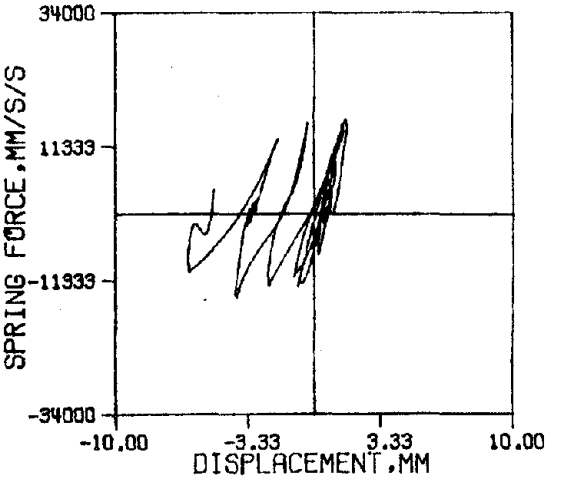

(c) EIGHTH FLOOR

Figure 20: Identified Hysteretic-Behavior of Floors Where the Damping is Neglected, RUN 1.

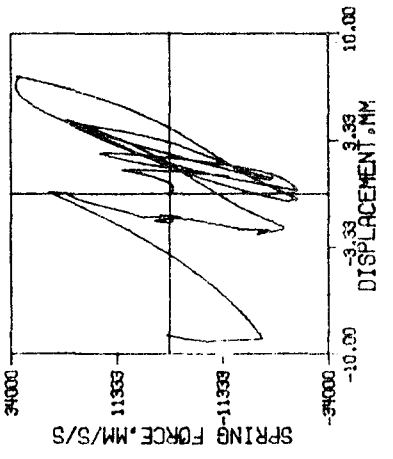

(f) FIFTH FLOOR

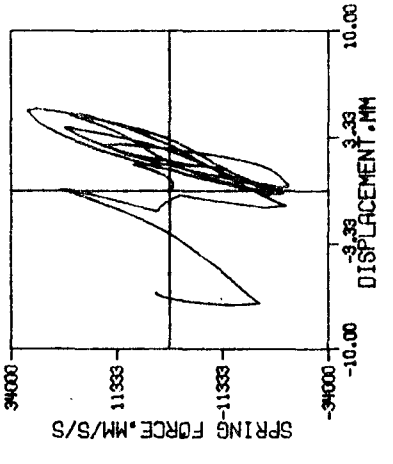

(h) THIRD FLOOR

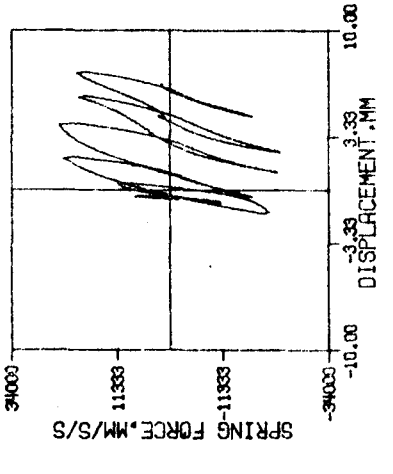

(j) FIRST FLOOR

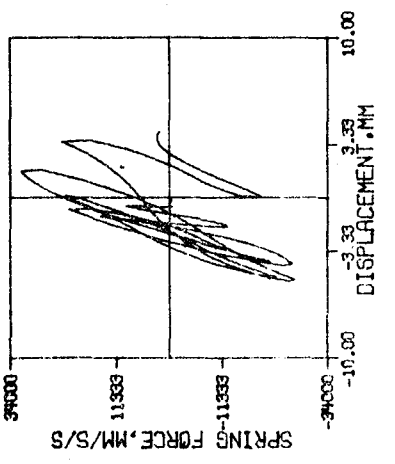

(e) SIXTH FLOOR

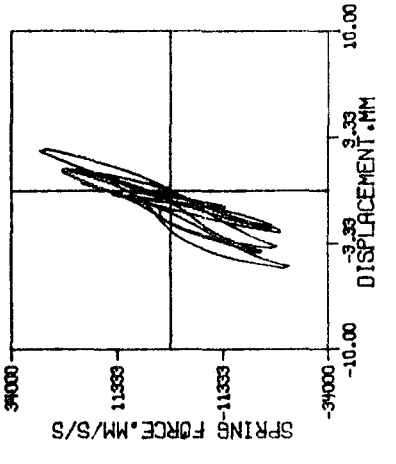

(g) FOURTH FLOOR

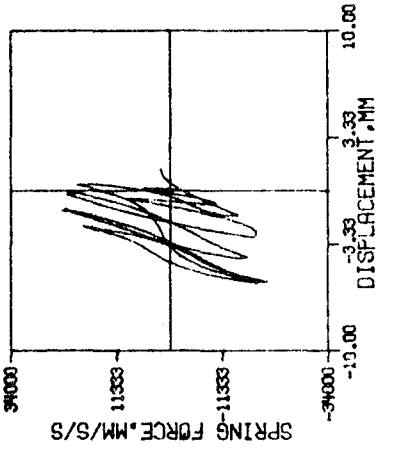

(i) SECOND FLOOR

Figure 20 (Cont.): Identified Hysteretic Behavior of Floors Where the Damping is Ignored, RUN 1.

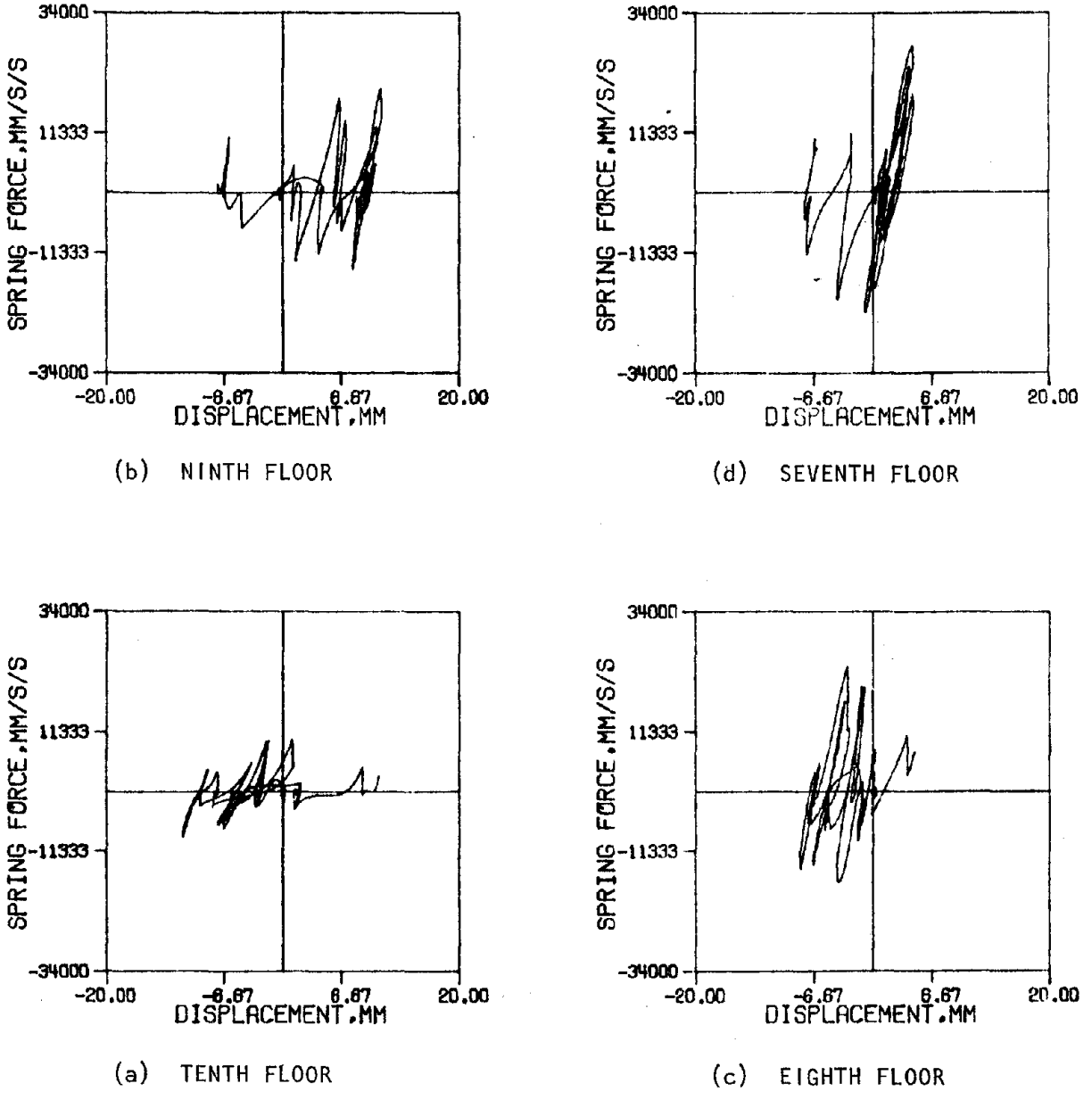

Figure 21: Identified Hysteretic Behavior of Floors Where the Damping is Ignored, RUN 2.

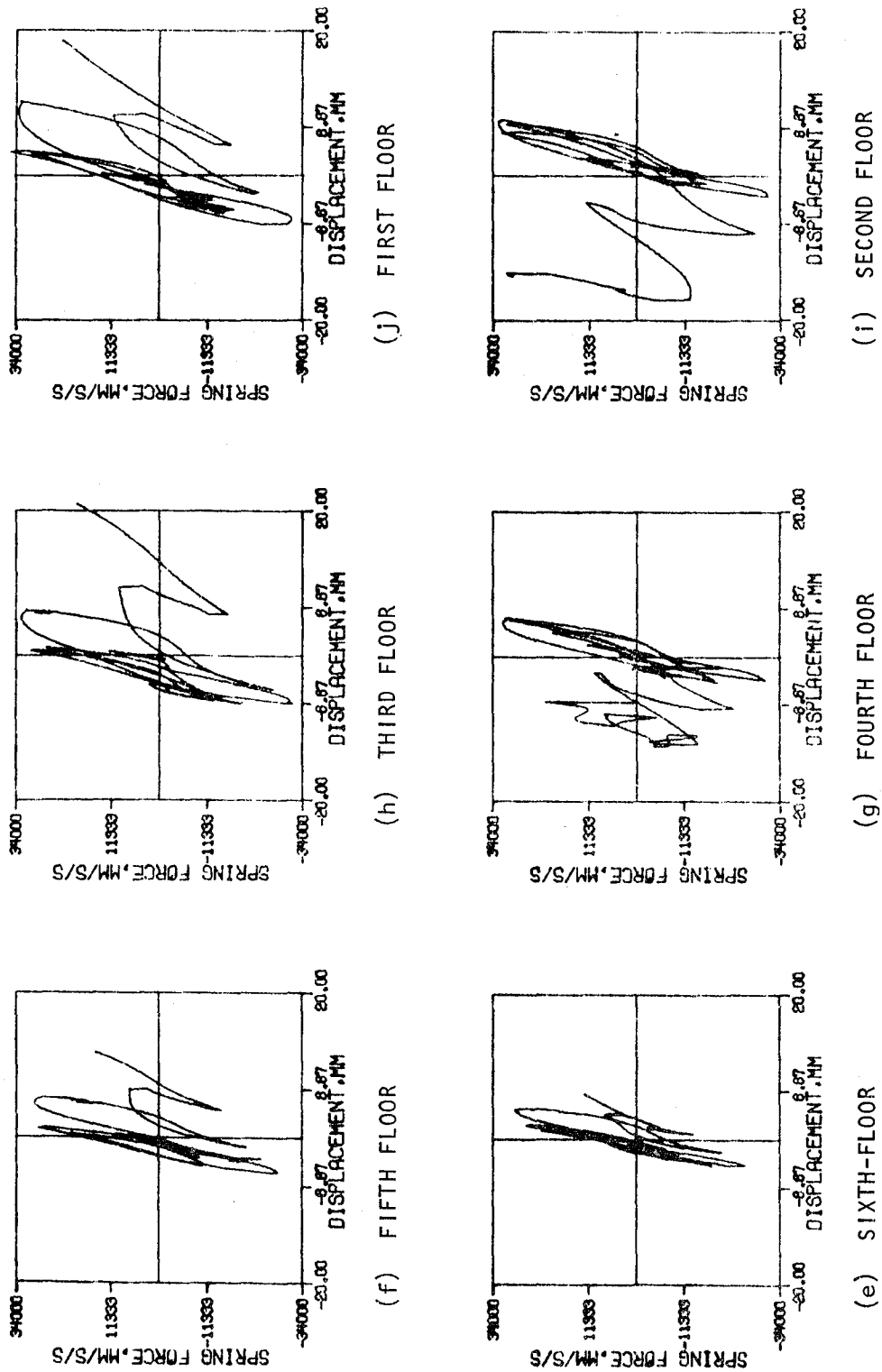

Figure 21 (Cont.): Identified Hysteretic Behavior of Floors Where the Damping is Ignored, RUN 2.

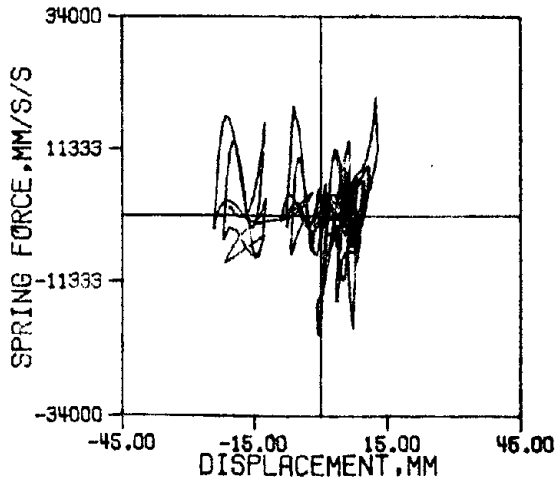

(b) NINTH FLOOR

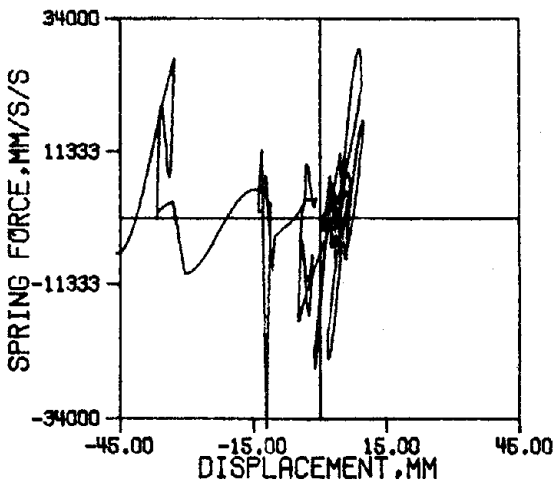

(d) SEVENTH FLOOR

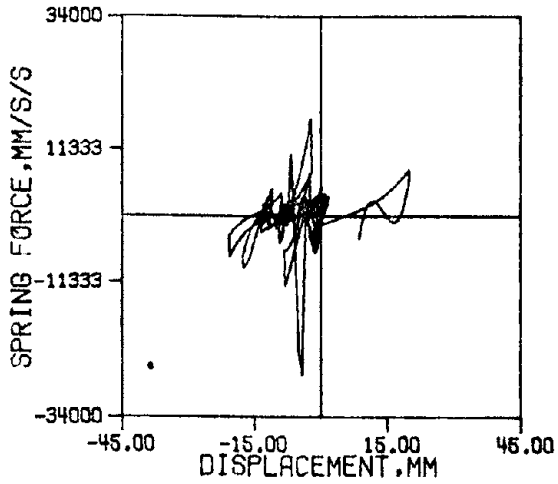

(a) TENTH FLOOR

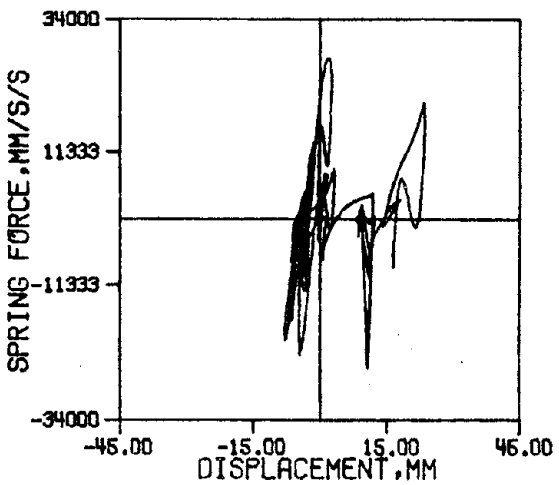

(c) EIGHTH FLOOR

Figure 22: Identified Hysteretic Behavior of Floors Where Damping is Ignored, RUN 3.

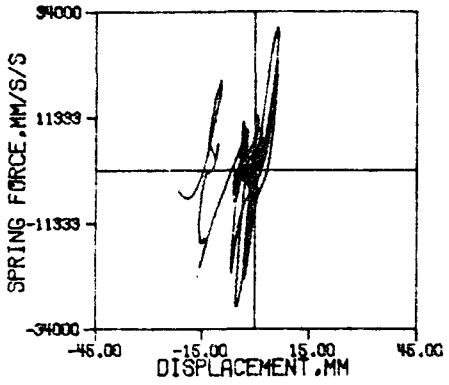

(f) FIFTH FLOOR

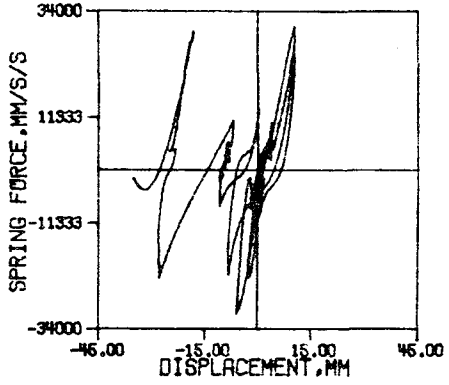

(h) THIRD FLOOR

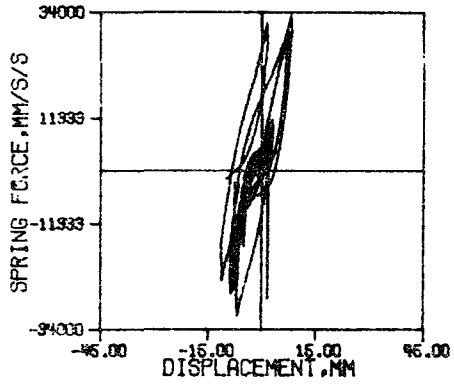

(j) FIRST FLOOR

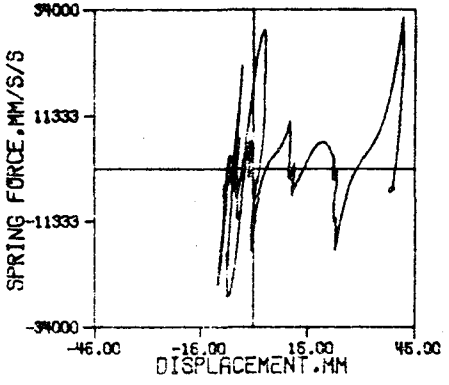

(e) SIXTH FLOOR

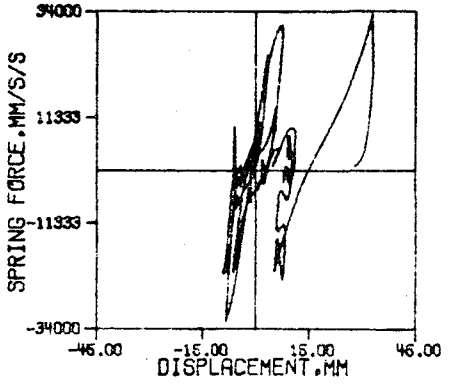

(g) FOURTH FLOOR

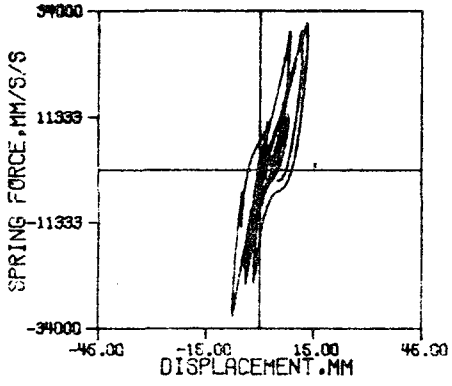

(i) SECOND FLOOR

Figure 22 (Cont.): Identified Hysteretic Behavior of Floor Where the Damping is Ignored, RUN 3.

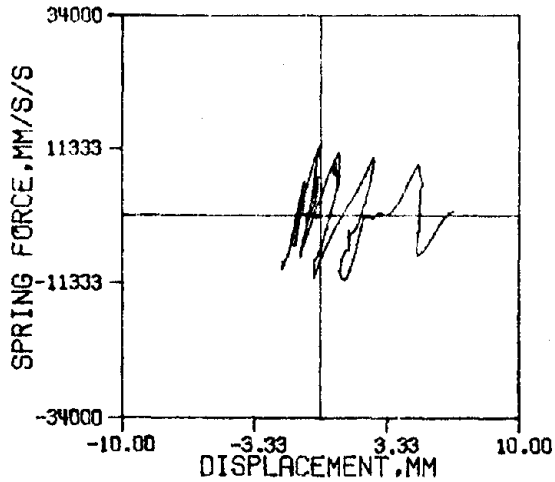

(b) NINTH FLOOR

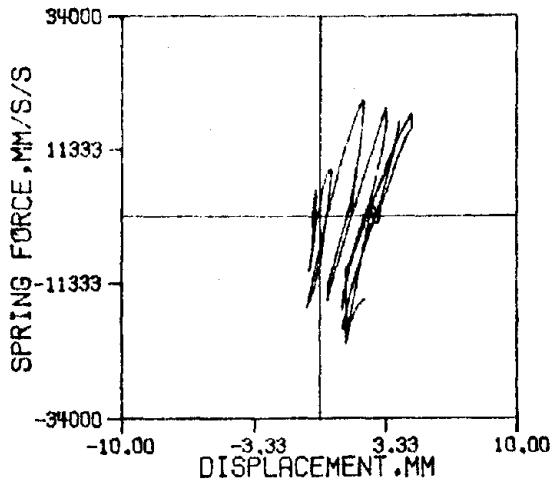

(d) SEVENTH FLOOR

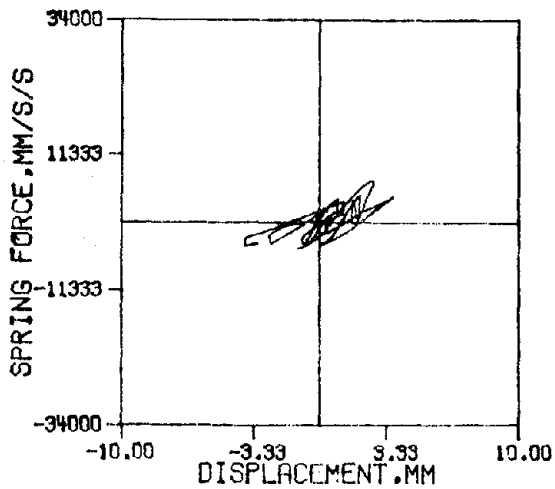

(a) TENTH FLOOR

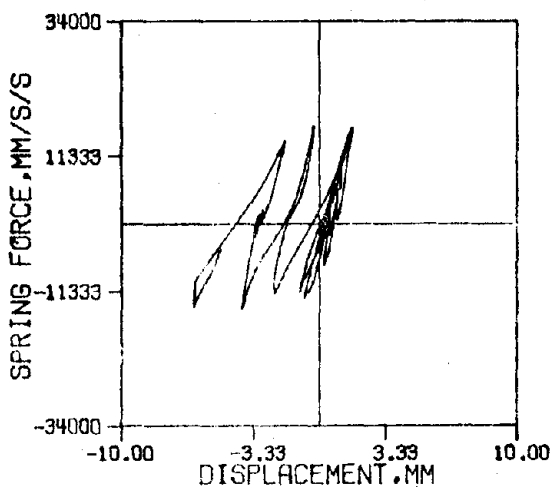

(c) EIGHTH FLOOR

Figure 23: Identified Hysteretic Behavior of Floors Where the Damping has a Linear-Viscous Form, RUN 1.

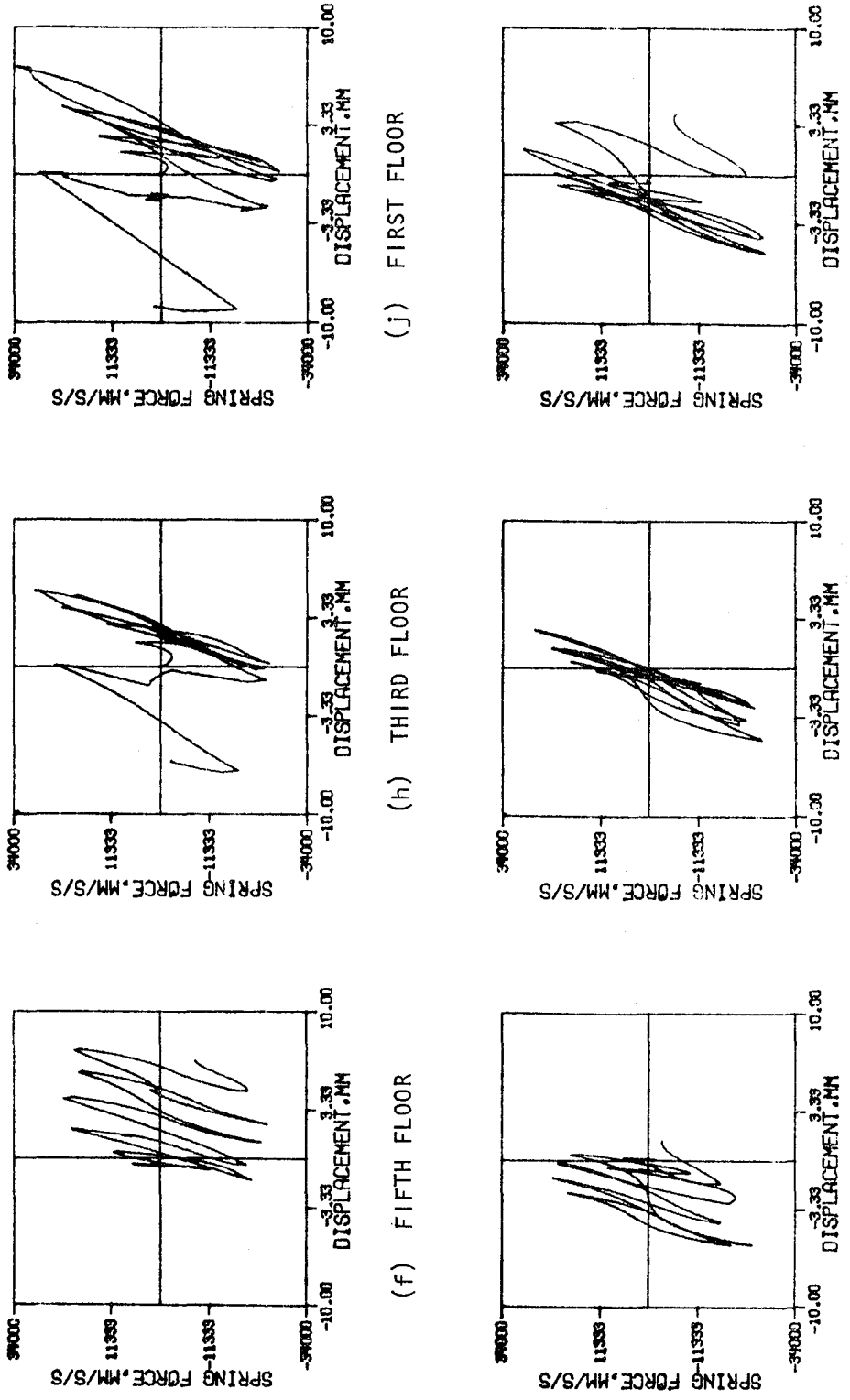

Figure 23 (Cont.): Identified Hysteretic Behavior of Floors Where the Damping has a Linear-Viscous Form, RUN 1.

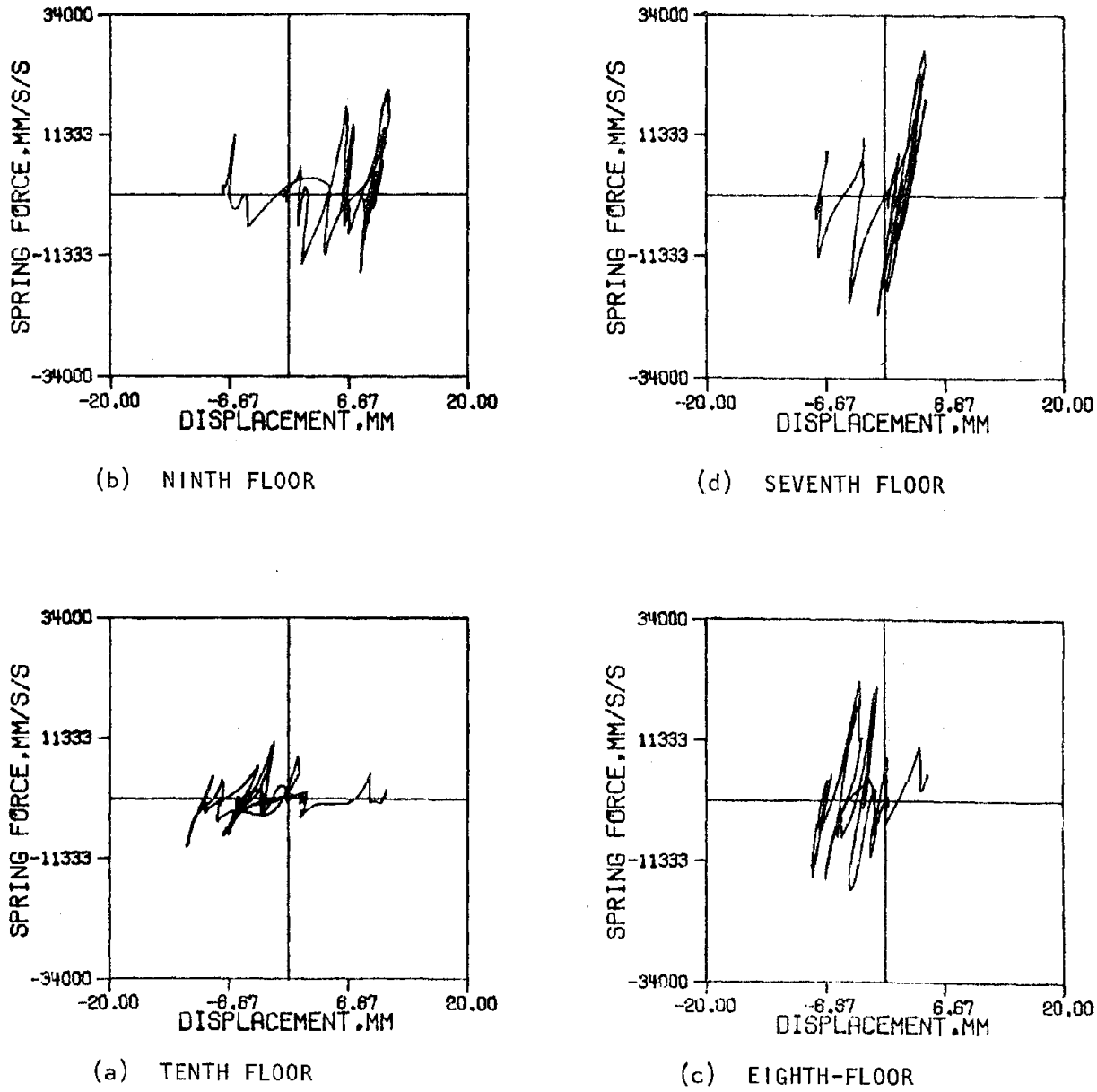

Figure 24: Identified Hysteretic Behavior of Floors Where the Damping has a Linear-Viscous Form, RUN 2.

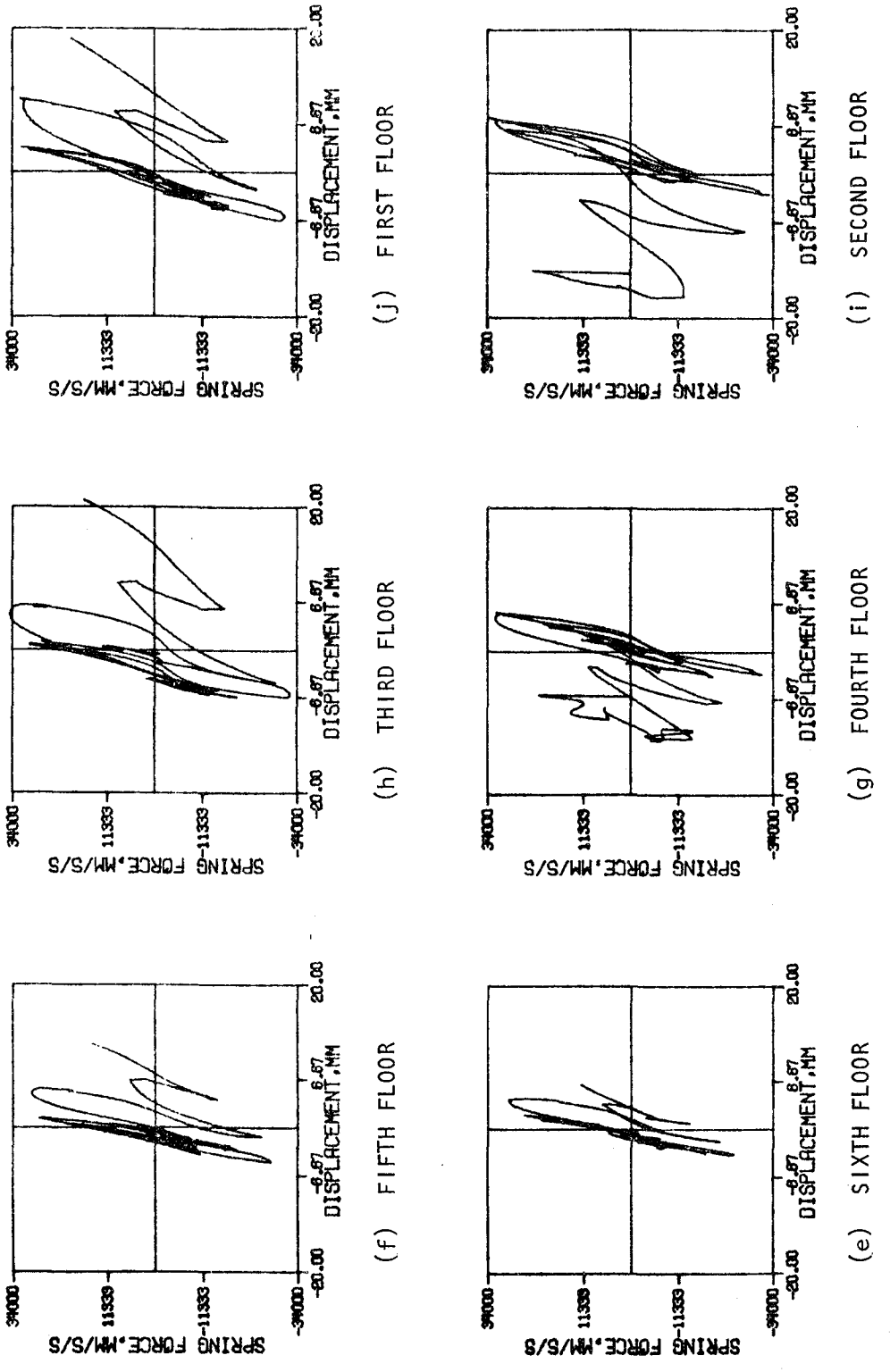

Figure 24 (Cont.): Identified Hysteretic Behavior of Floors Where Damping has a Linear-Viscous Form, RUN 2.

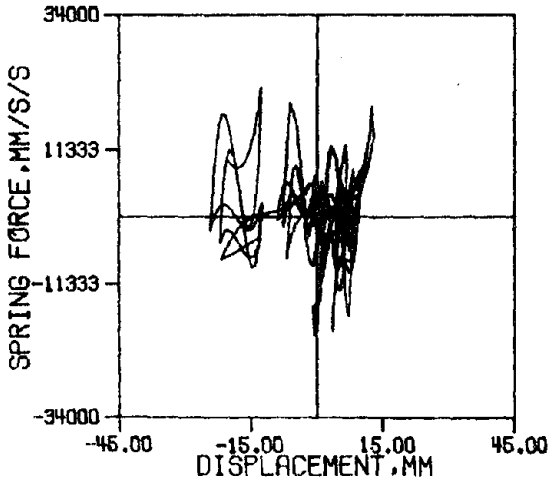

(b) NINTH FLOOR

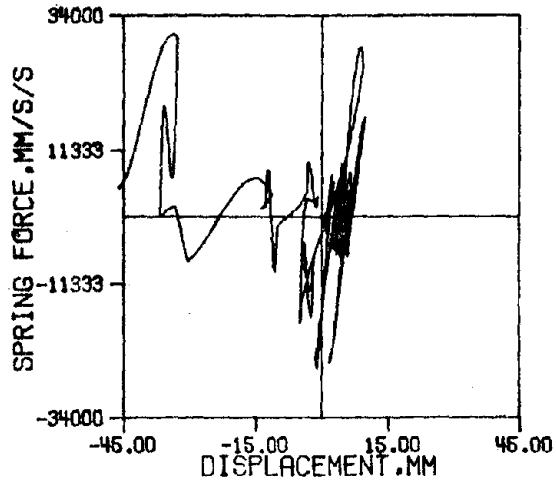

(d) SEVENTH FLOOR

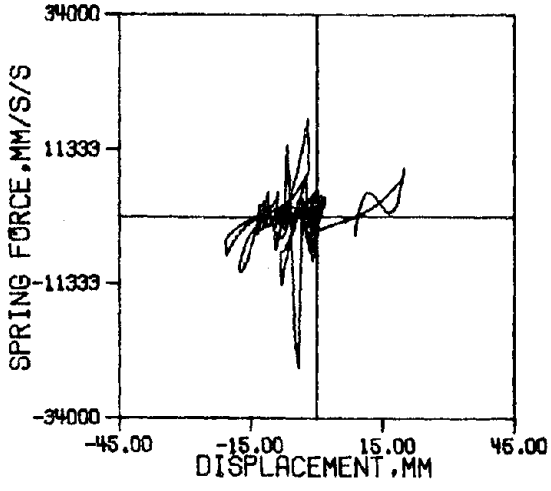

(a) TENTH FLOOR

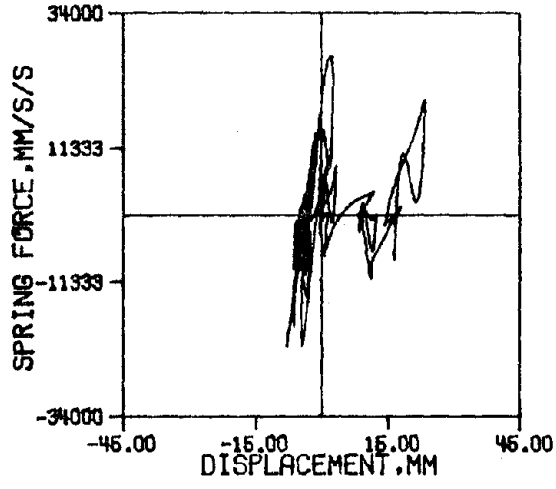

(c) EIGHTH FLOOR

Figure 25: Identified Hysteretic Behavior of Floors Where Damping Has a Linear-Viscous Form, RUN 3.

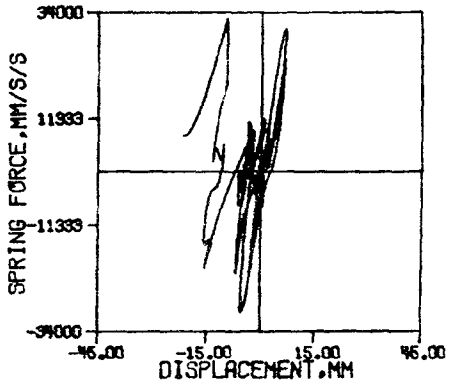

(f) FIFTH FLOOR

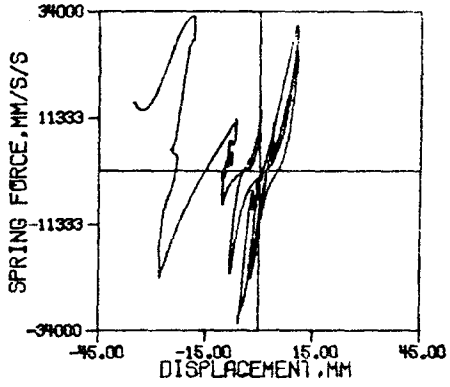

(h) THIRD FLOOR

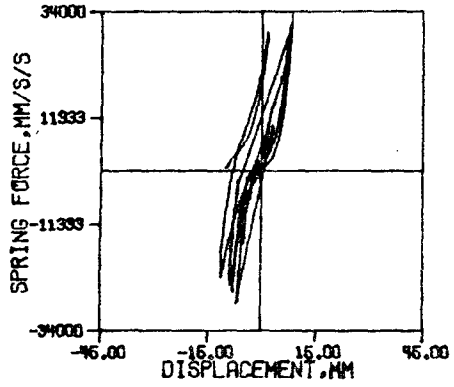

(j) FIRST FLOOR

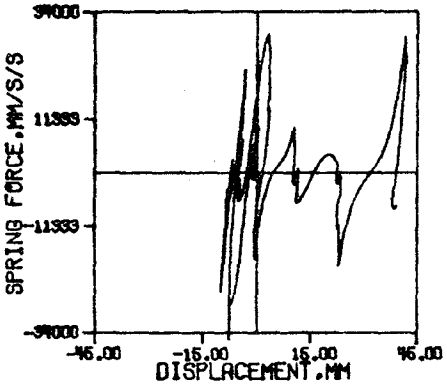

(e) SIXTH FLOOR

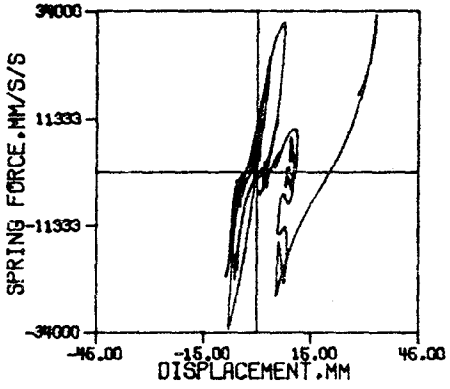

(g) FOURTH FLOOR

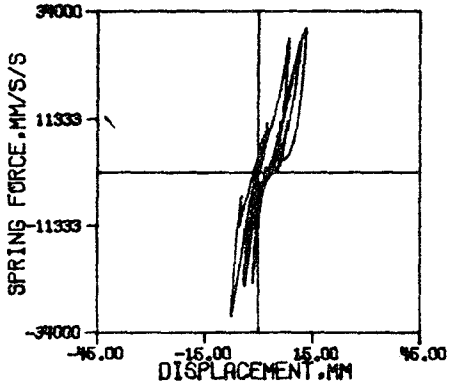

(i) SECOND FLOOR

Figure 25 (Cont.): Identified Hysteretic Behavior of Floors Where The Damping Has a Linear-Viscous Form, RUN 3.

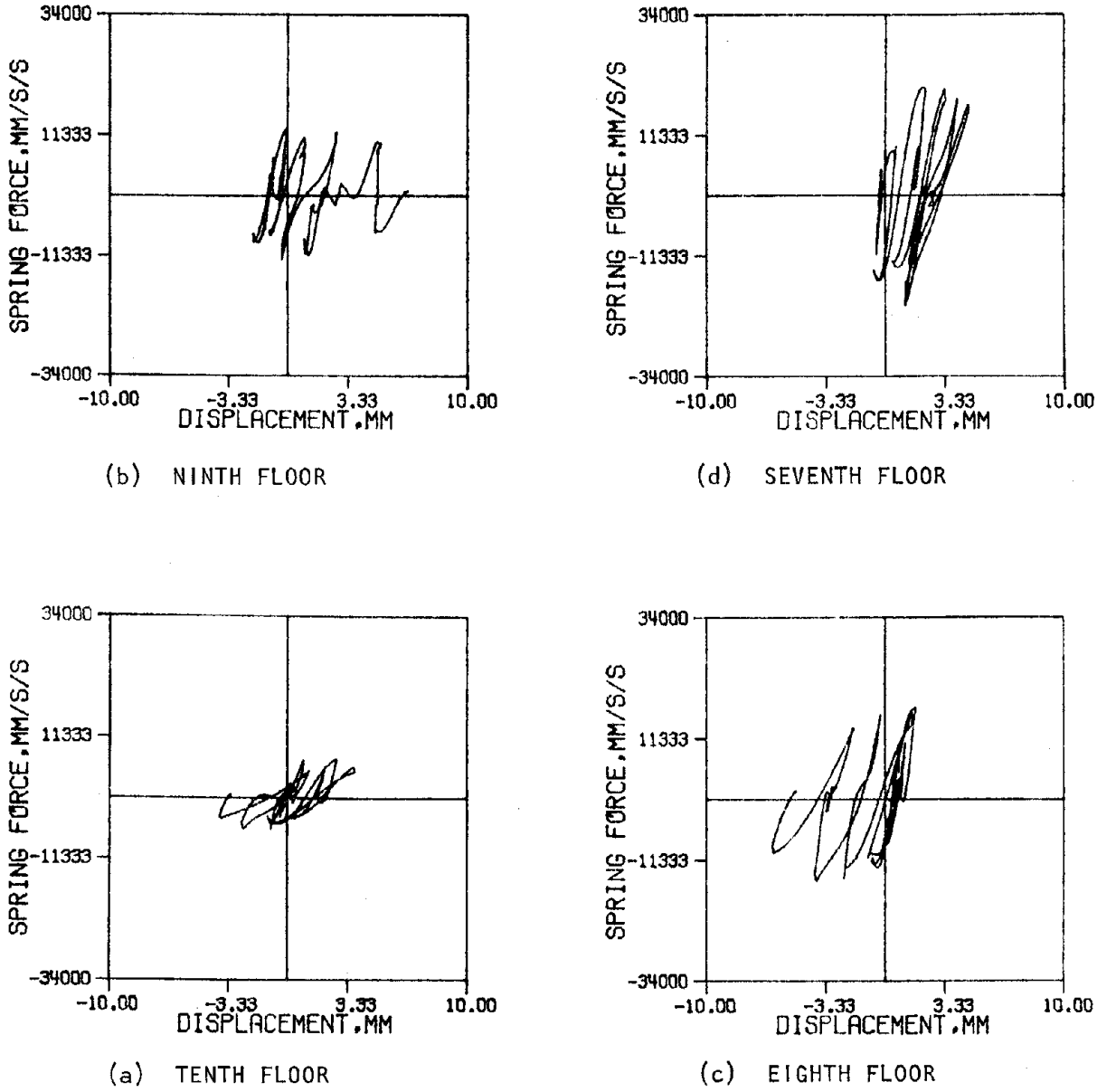

Figure 26: Identified Hysteretic Behavior of Floors Where Damping Has a (Restricted) Linear-Viscous Damping, RUN 1.

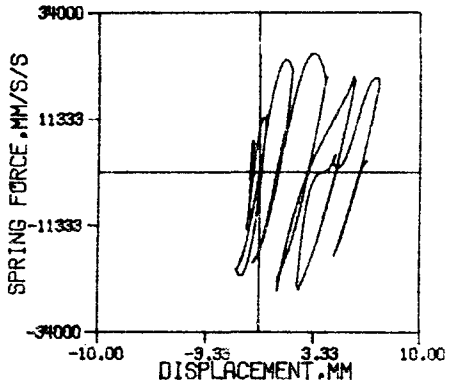

(f) FIFTH FLOOR

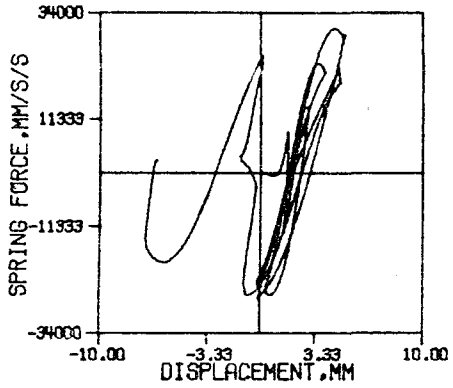

(h) THIRD FLOOR

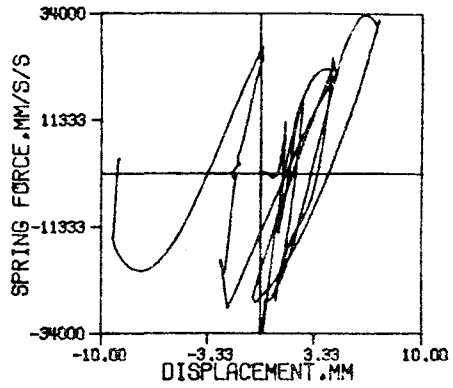

(j) FIRST FLOOR

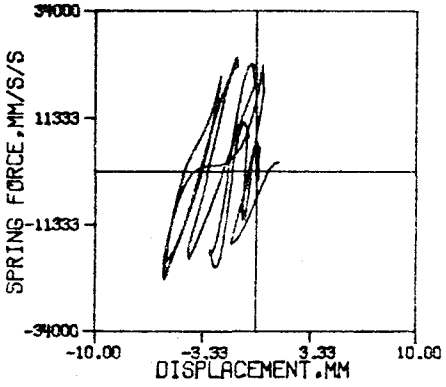

(e) SIXTH FLOOR

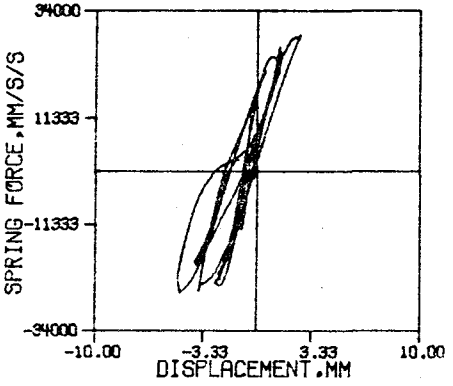

(g) FOURTH FLOOR

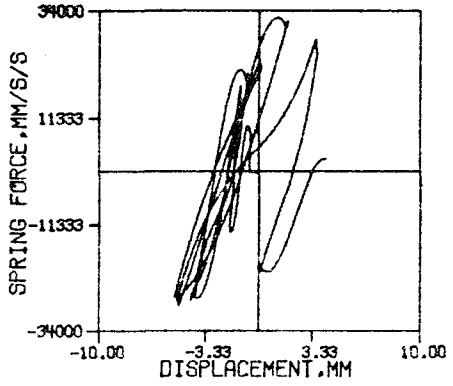

(i) SECOND FLOOR

Figure 26 (Cont.): Identified Hysteretic Behavior of Floors Where Damping has a (Restricted) Linear-Viscous Form, RUN 1.

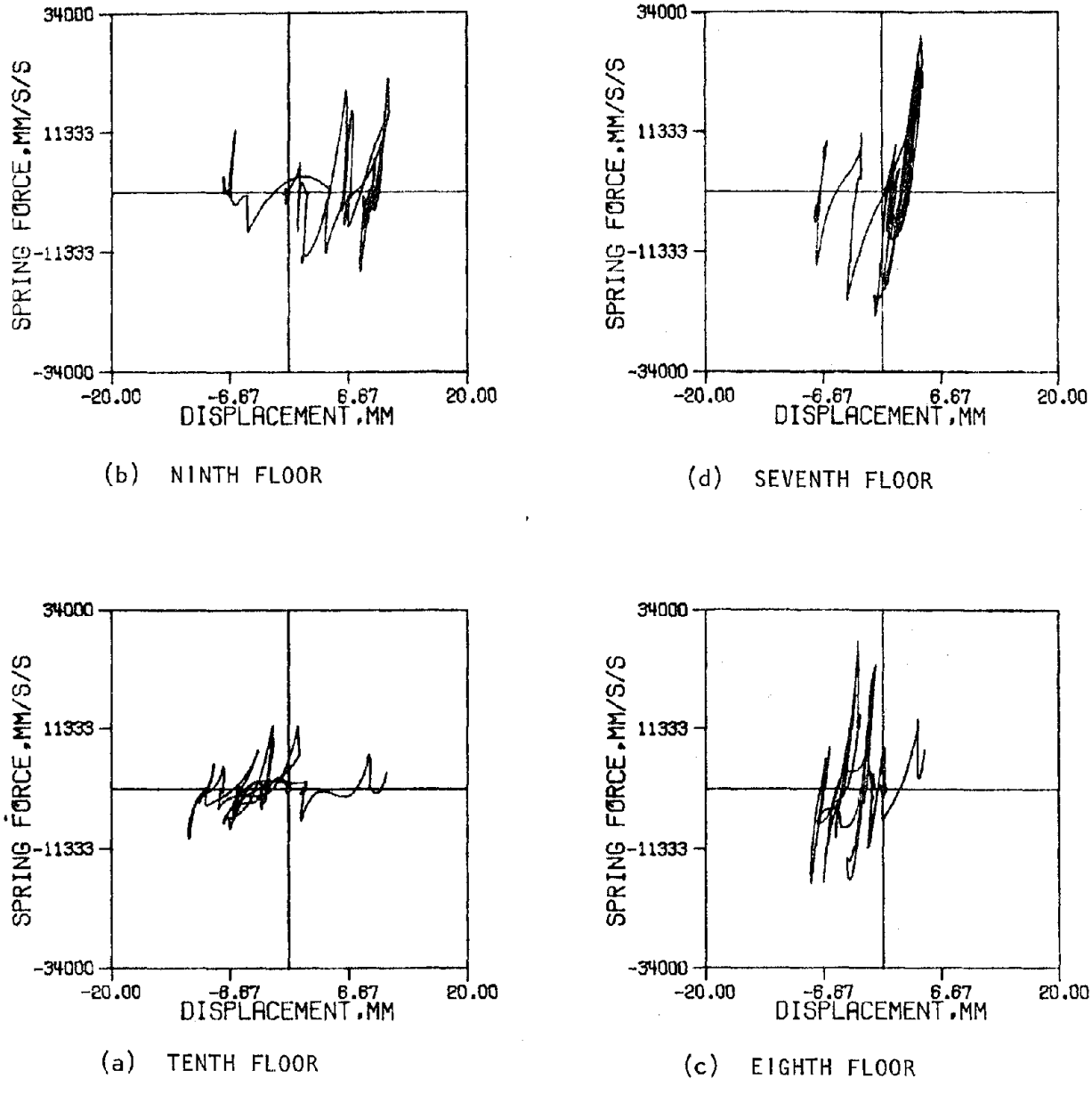

Figure 27: Identified Hysteretic Behavior of Floors Where Damping has a (Restricted) Linear-Viscous Form, RUN 2.

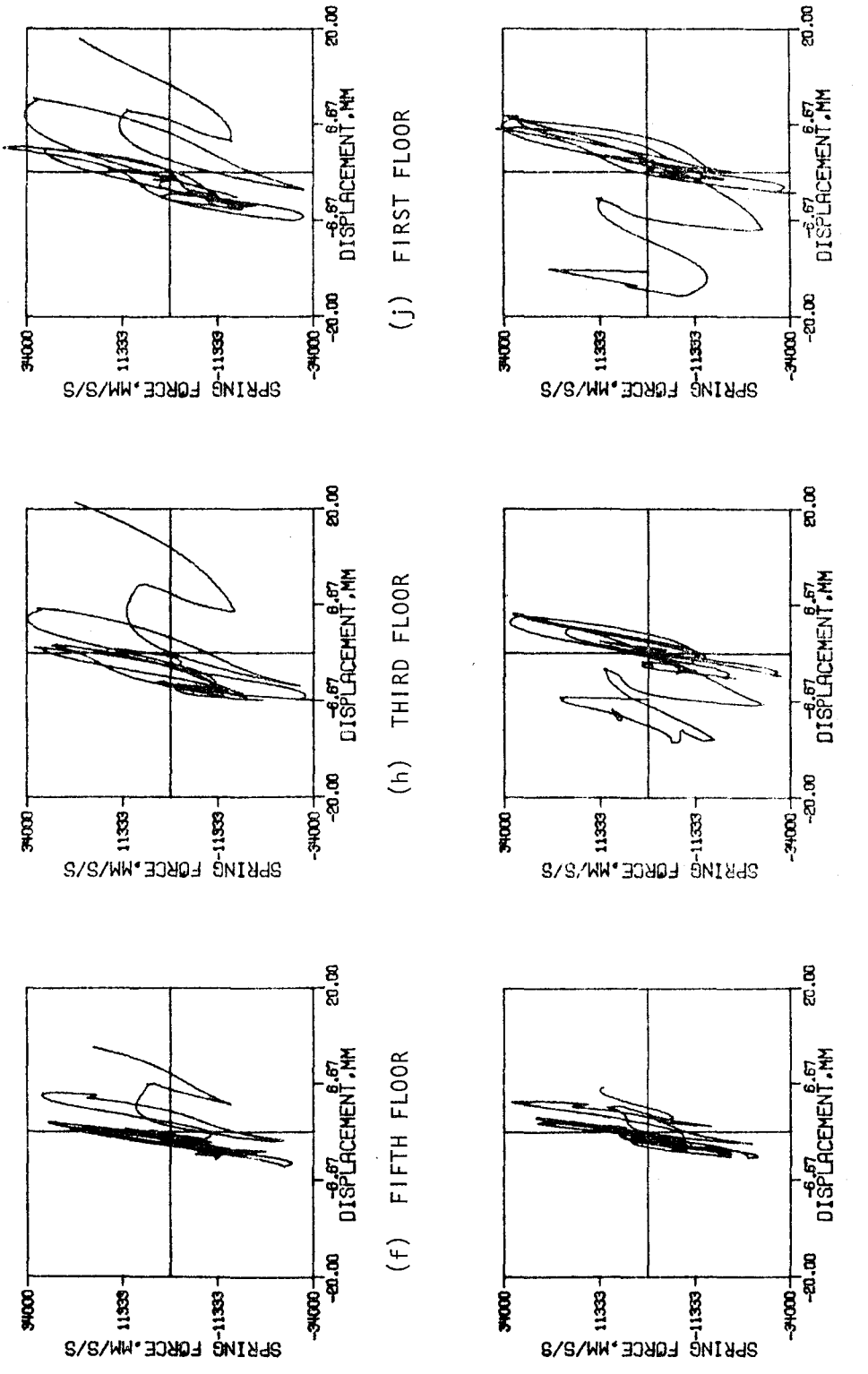

Figure 27 (Cont.): Identified Hysteretic Behavior of Floors Where Damping has a (Restricted) Linear-Viscous Form, RUN 2.

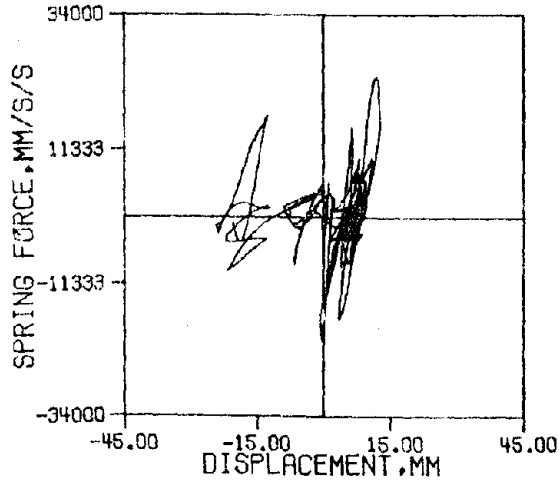

(b) NINTH FLOOR

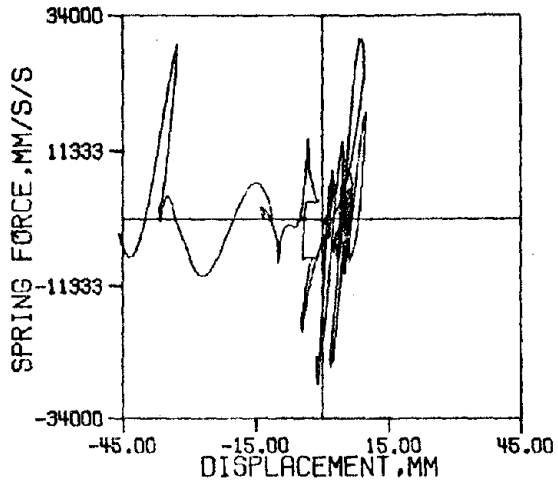

(d) SEVENTH FLOOR

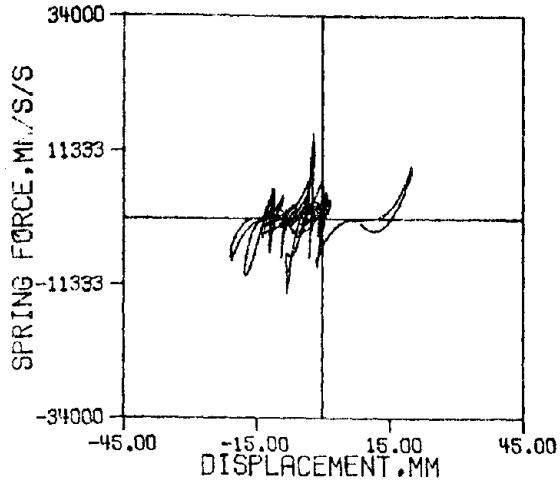

(a) TENTH FLOOR

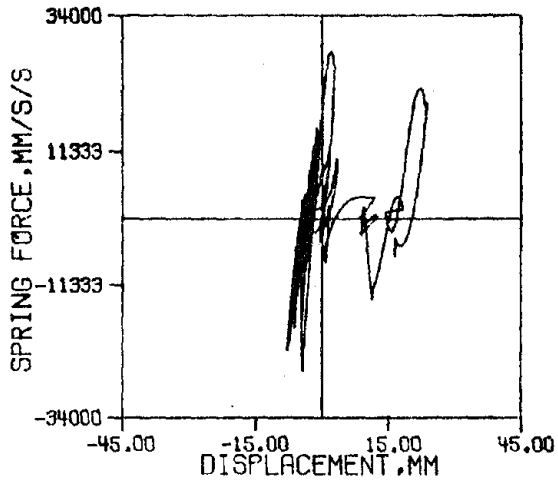

(c) EIGHTH FLOOR

Figure 28: Identified Hysteretic Behavior of Floors Where Damping has a (Restricted) Linear-Viscous Form, RUN 3.

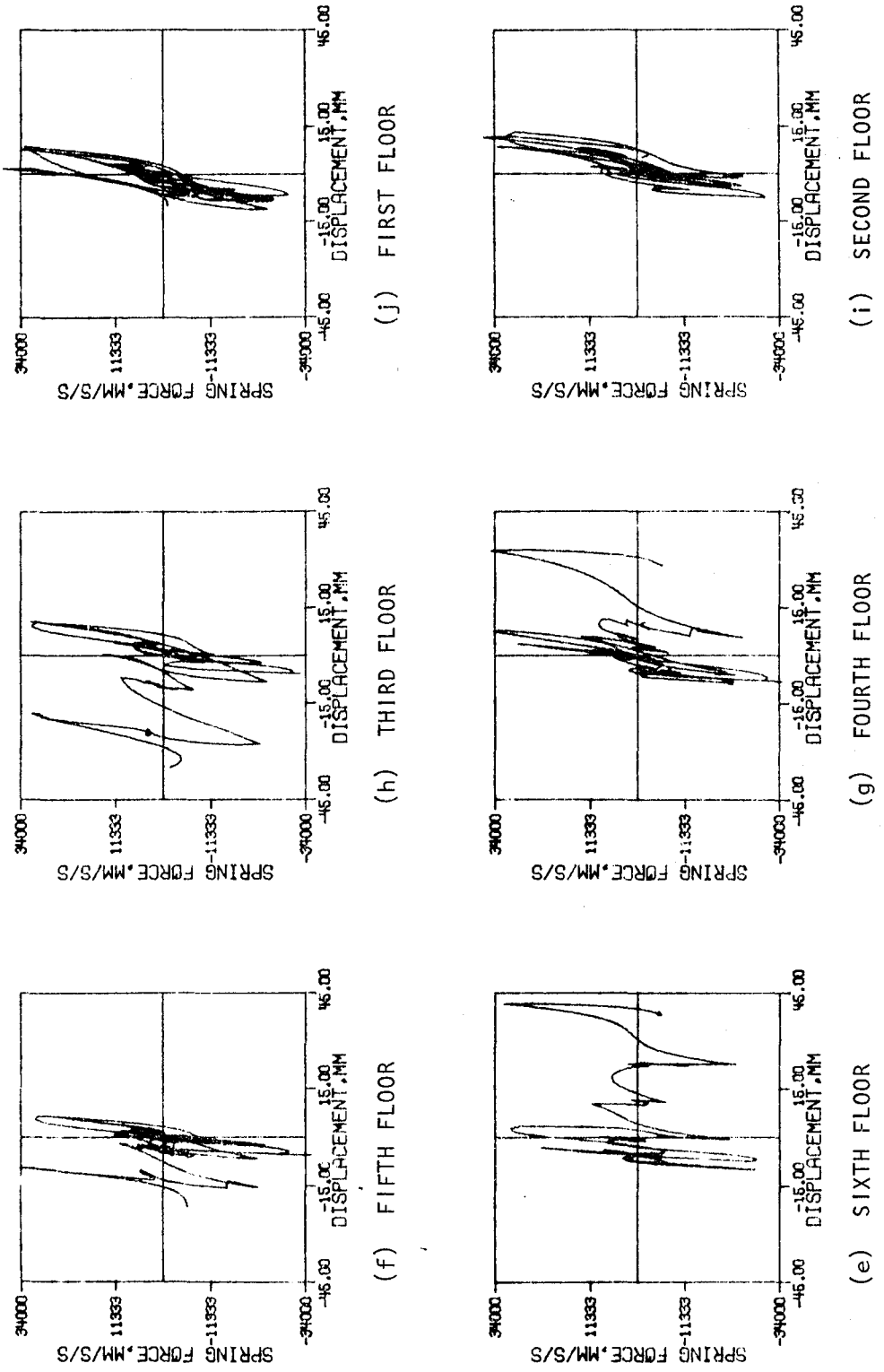

Figure 28 (Cont.): Identified Hysteretic Behavior of Floors Where Damping has a (Restricted) Linear-Viscous Form, RUN 3.

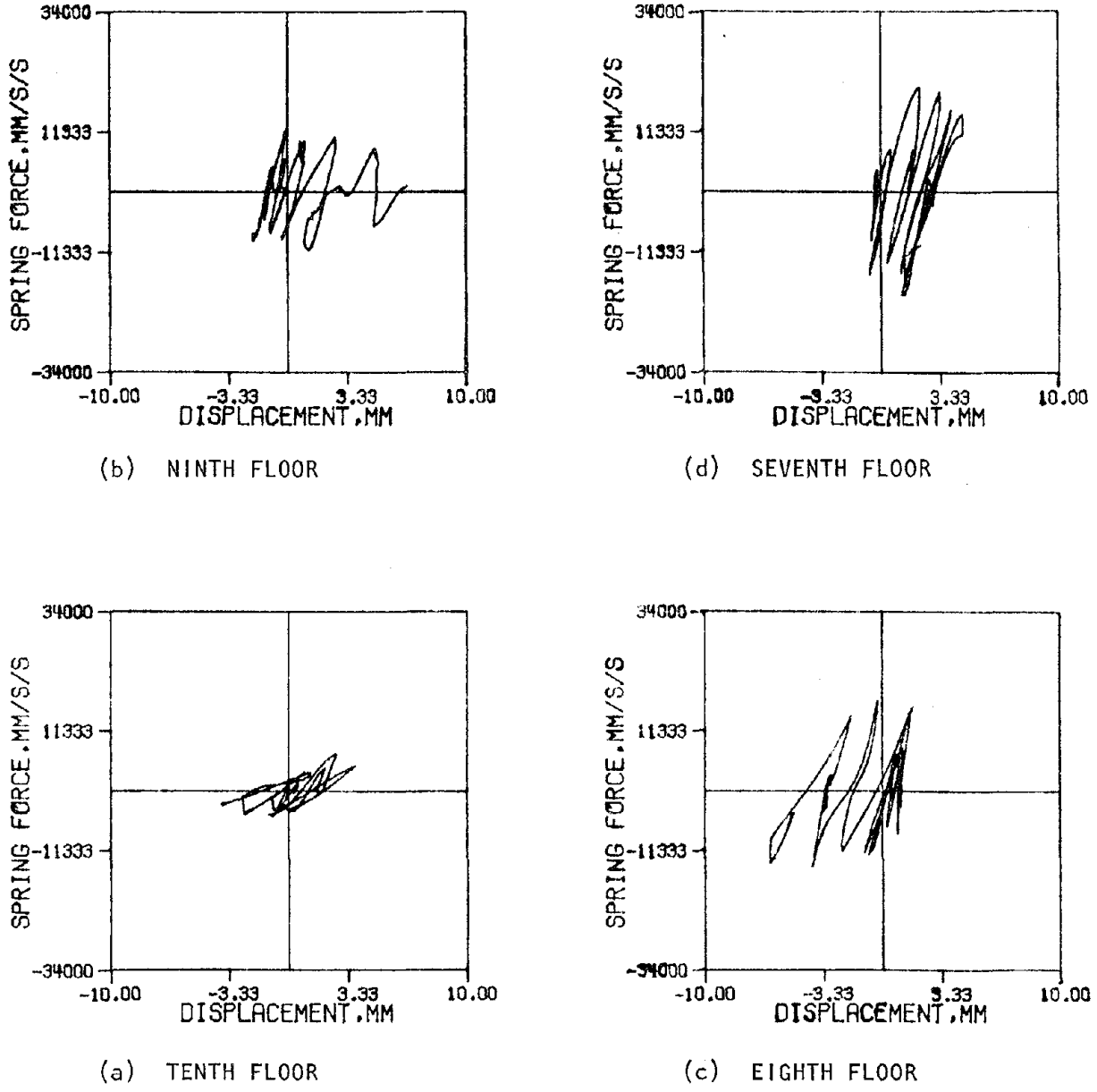

Figure 29: Identified Hysteretic Behavior of Floors Where Damping has a Symmetrical-Cubic Form, RUN 1.

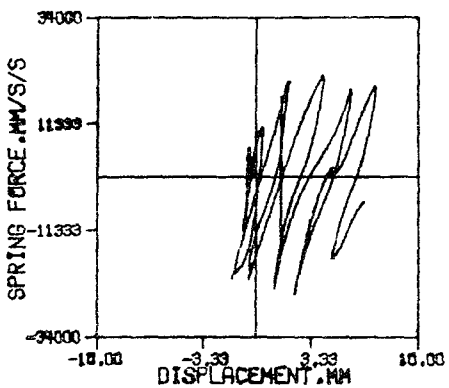

(f) FIFTH FLOOR

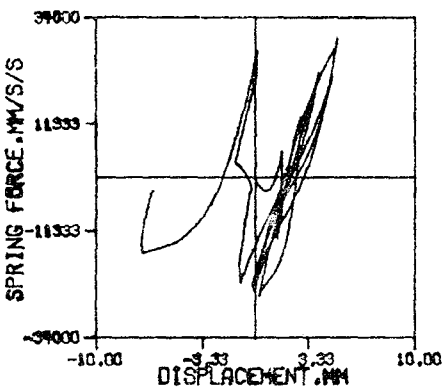

(h) THIRD FLOOR

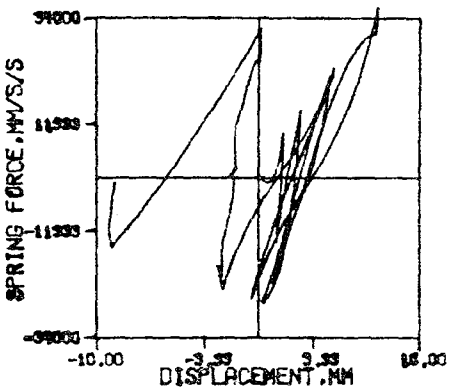

(j) FIRST FLOOR

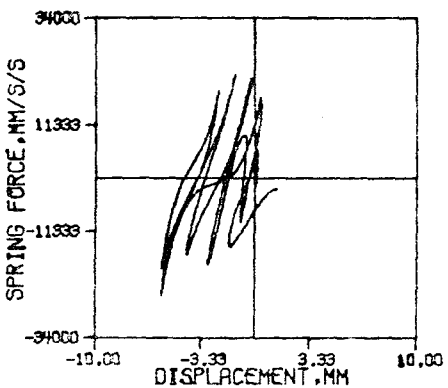

(e) SIXTH FLOOR

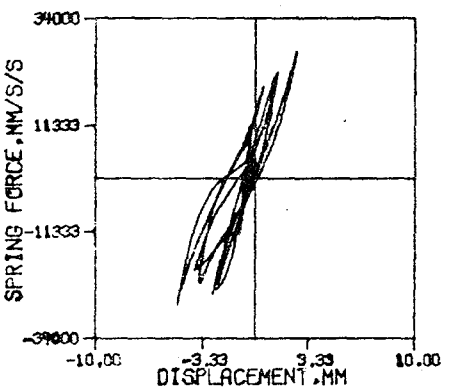

(g) FOURTH FLOOR

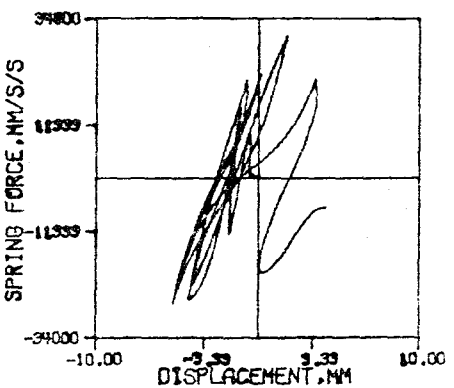

(i) SECOND FLOOR

Figure 29 (Cont.): Identified Hysteretic Behavior of Floors Where Damping has a Symmetrical-Cubic Form, RUN 1.

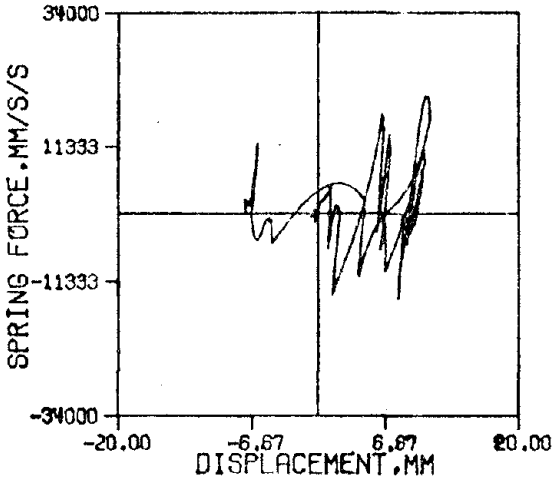

(b) NINTH FLOOR

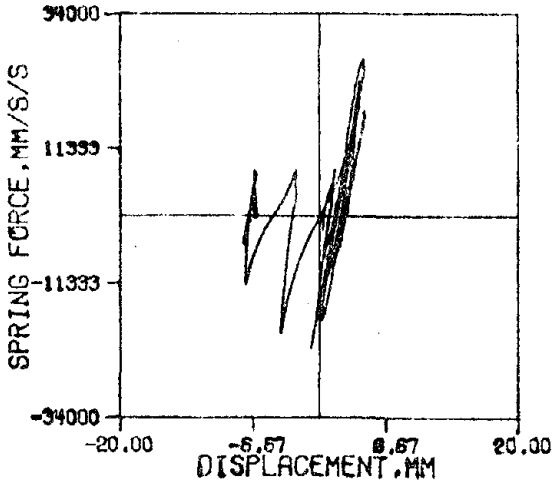

(d) SEVENTH FLOOR

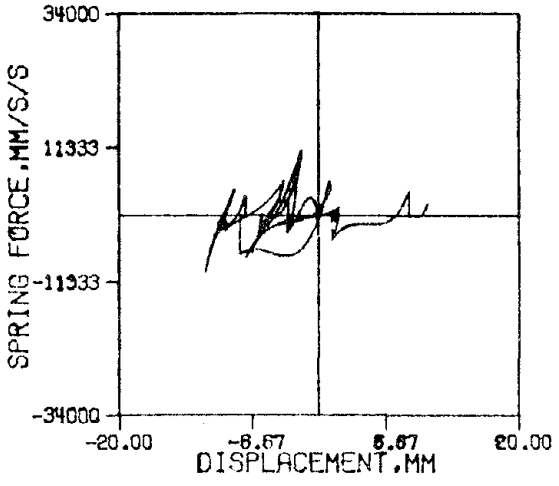

(a) TENTH FLOOR

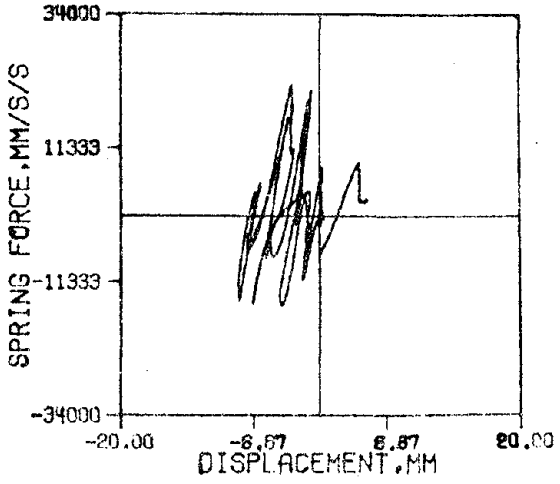

(c) EIGHTH FLOOR

Figure 30: Identified Hysteretic Behavior of Floors Where Damping Has a Symmetrical-Cubic Form, RUN 2.

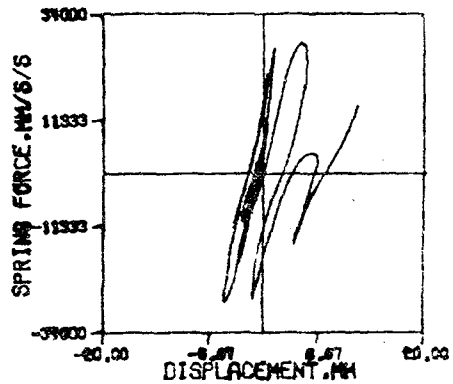

(f) FIFTH FLOOR

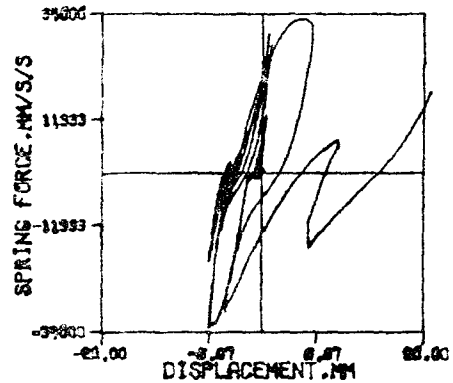

(h) THIRD FLOOR

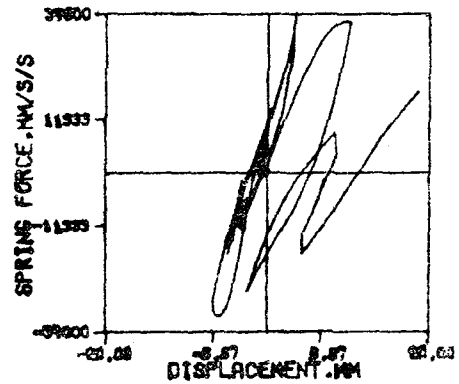

(j) FIRST FLOOR

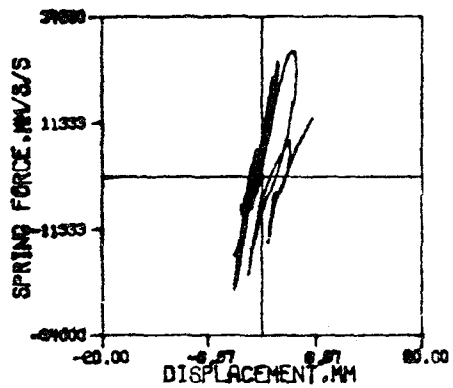

(e) SIXTH FLOOR

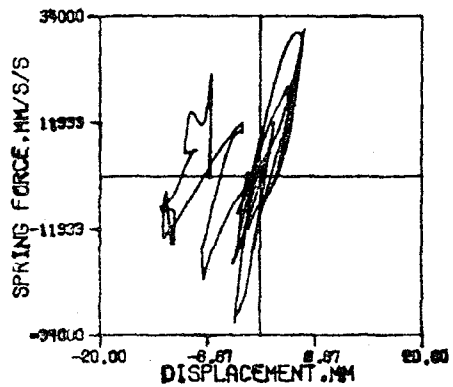

(g) FOURTH FLOOR

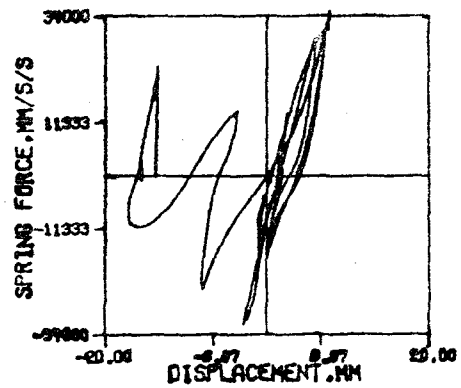

(i) SECOND FLOOR

Figure 30 (Cont.): Identfied Hysteretic Behavior of Floors Where Damping has a Symmetrical-Cubic Form, RUN 2.

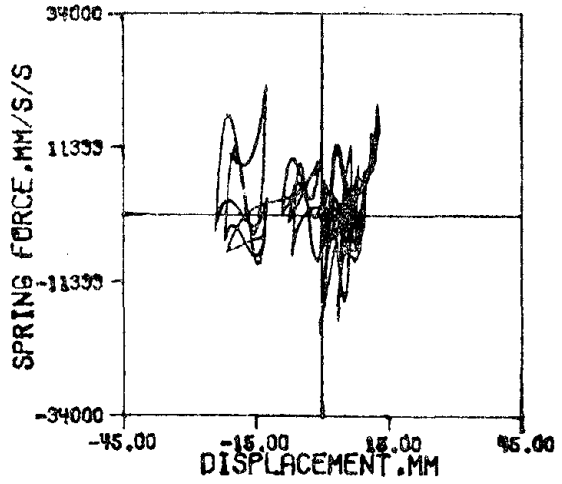

(b) NINTH FLOOR

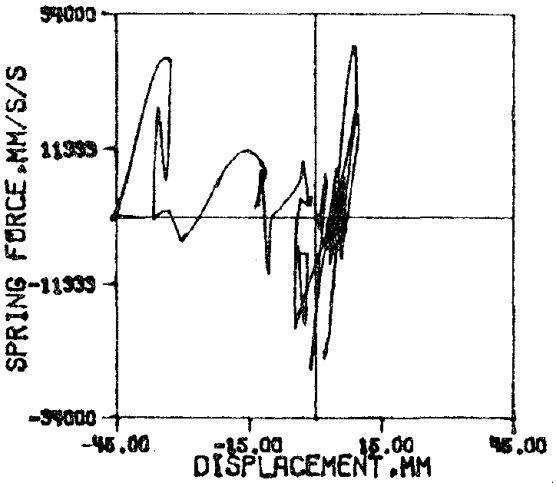

(d) SEVENTH FLOOR

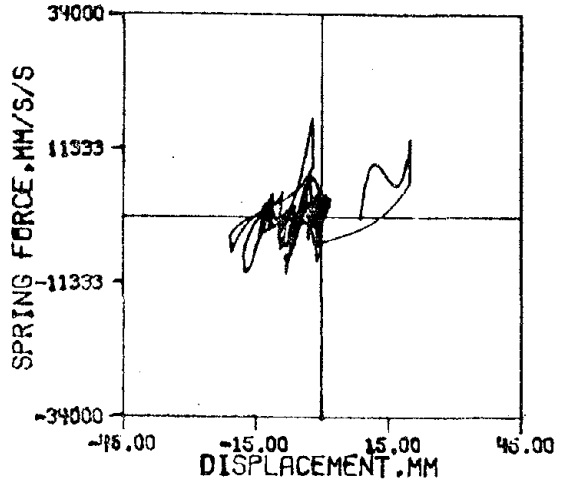

(a) TENTH FLOOR

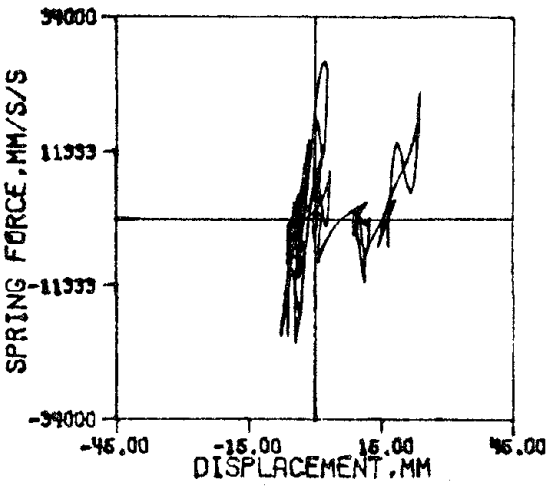

(c) EIGHTH FLOOR

Figure 31: Identified Hysteretic Behavior of Floors Where Damping Has a Symmetrical-Cubic Form, RUN 3.

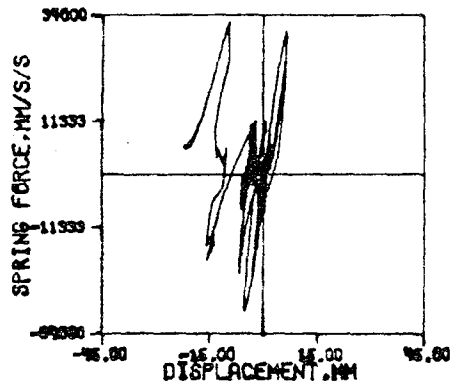

(f) FIFTH FLOOR

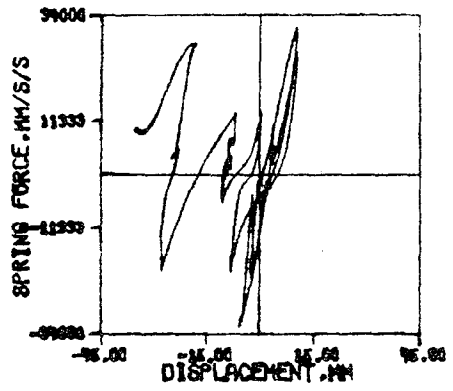

(h) THIRD FLOOR

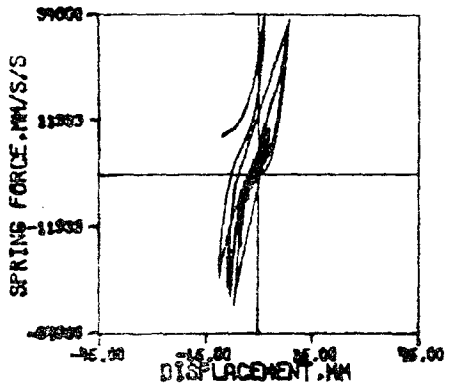

(j) FIRST FLOOR

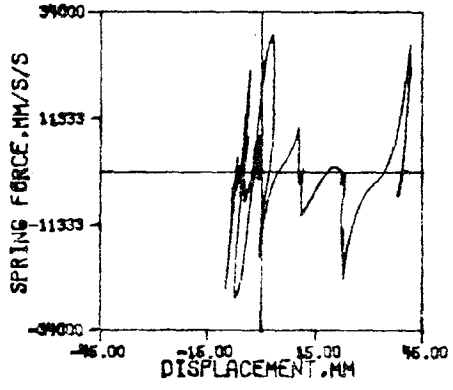

(e) SIXTH FLOOR

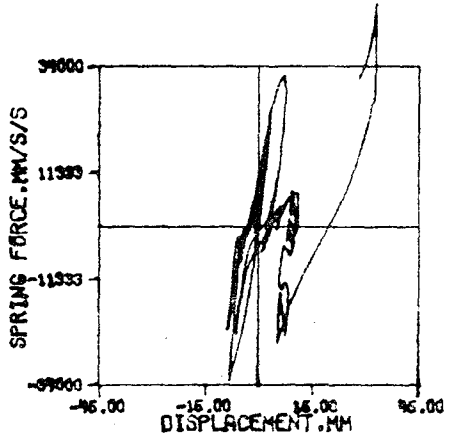

(g) FOURTH FLOOR

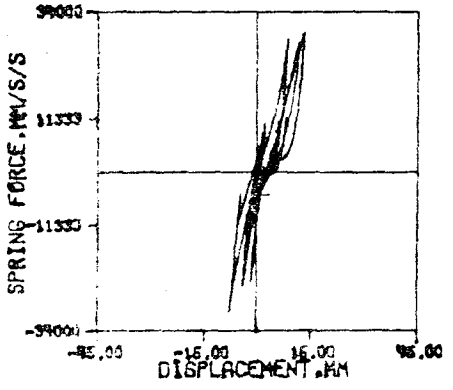

(i) SECOND FLOOR

Figure 31 (Cont.): Identified Hysteretic Behavior of Floors Where Damping Has a Symmetrical-Cubic Form, RUN 3.

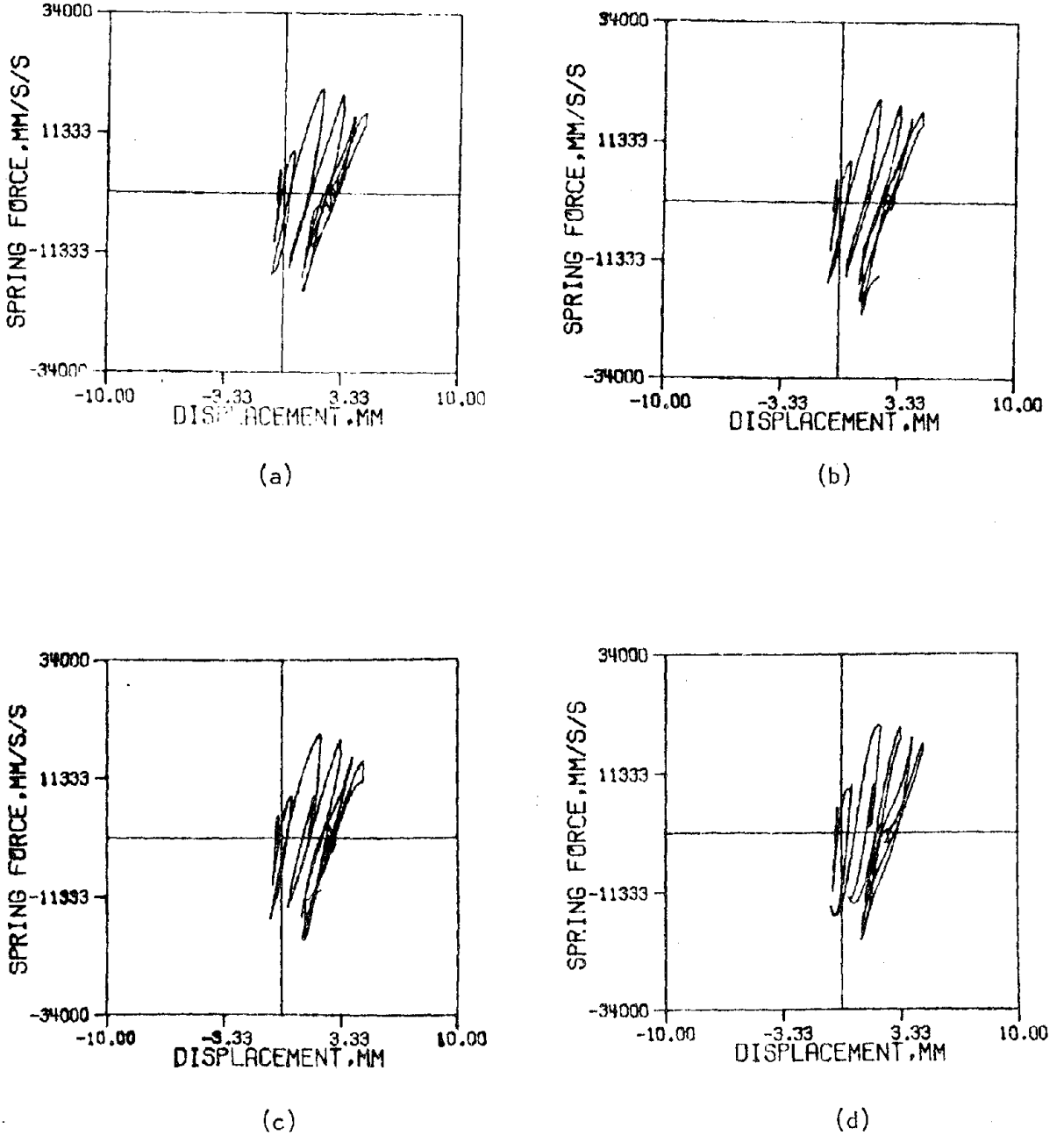

Figure 32: A Comparison of the Spring Force-Displacement Curves for a System Whose Damping Force Was Represented by (a) Zero, (b) Linear, (c) Cubic (Symmetrical), and (d) Restricted Linear Viscous Form (Seventh Floor, RUN 1).

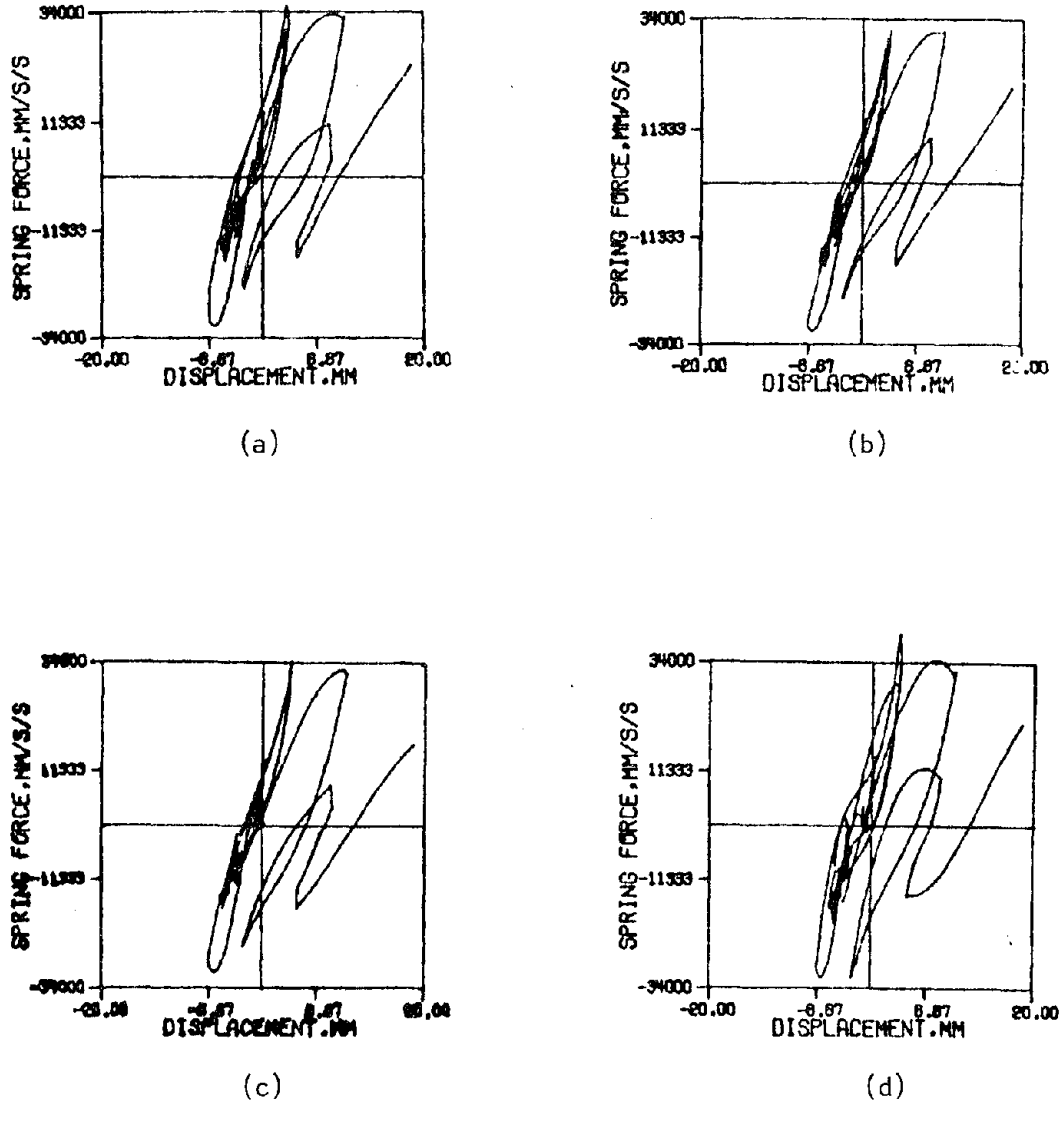

Figure 33: A Comparison of the Spring Force-Displacement Curves For A System Whose Damping Force was Represented by (a) Zero, (b) Linear, (c) Cubic (Symmetrical), and (d) Restricted Linear Viscous Form (First Floor, RUN 2).

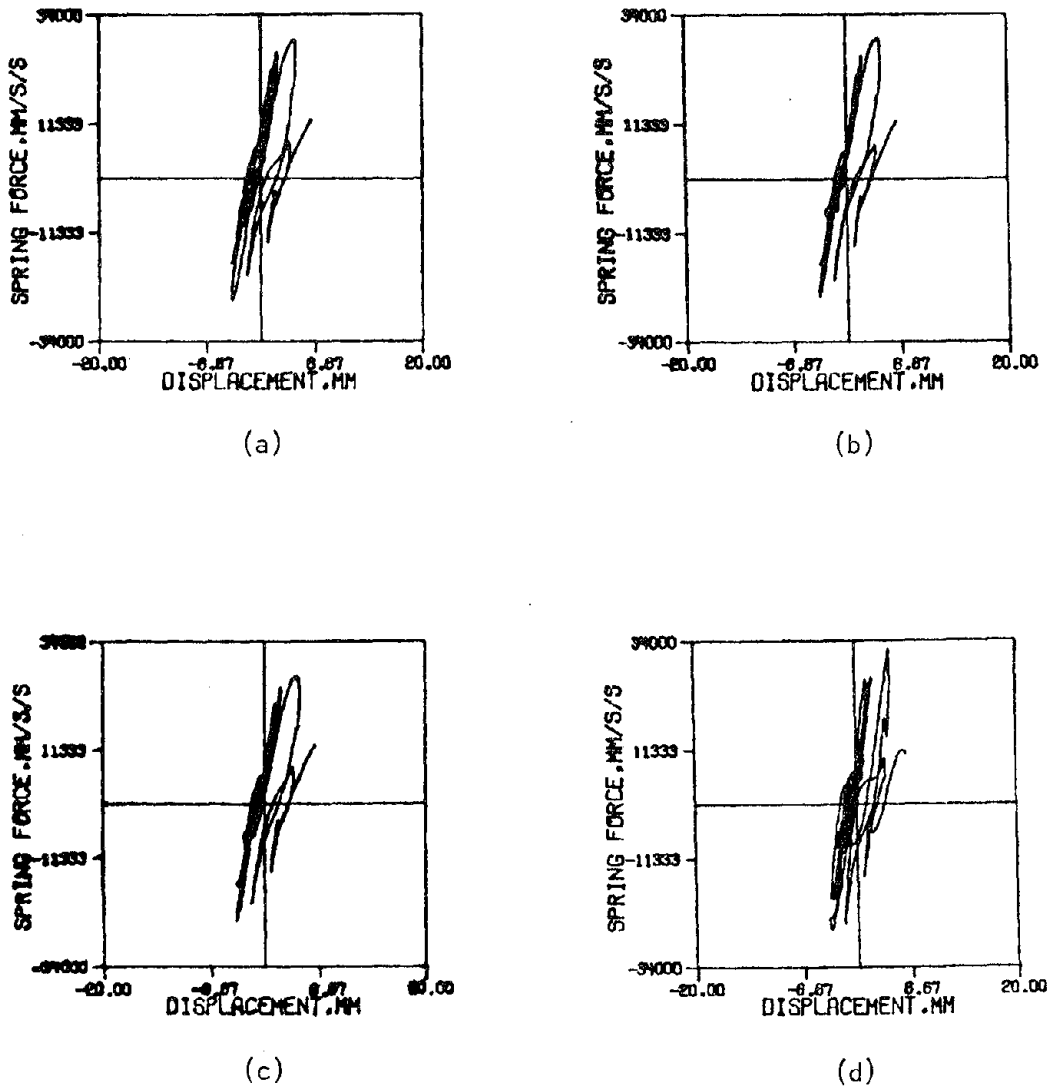

Figure 34: A Comparison of the Spring Force-Displacement Curves For a System Whose Damping Force was Represented by (a) Zero, (b) Linear, and (c) Cubic (Symmetrical), and (d) Restricted Linear Viscous Form (Sixth Floor, RUN 2).

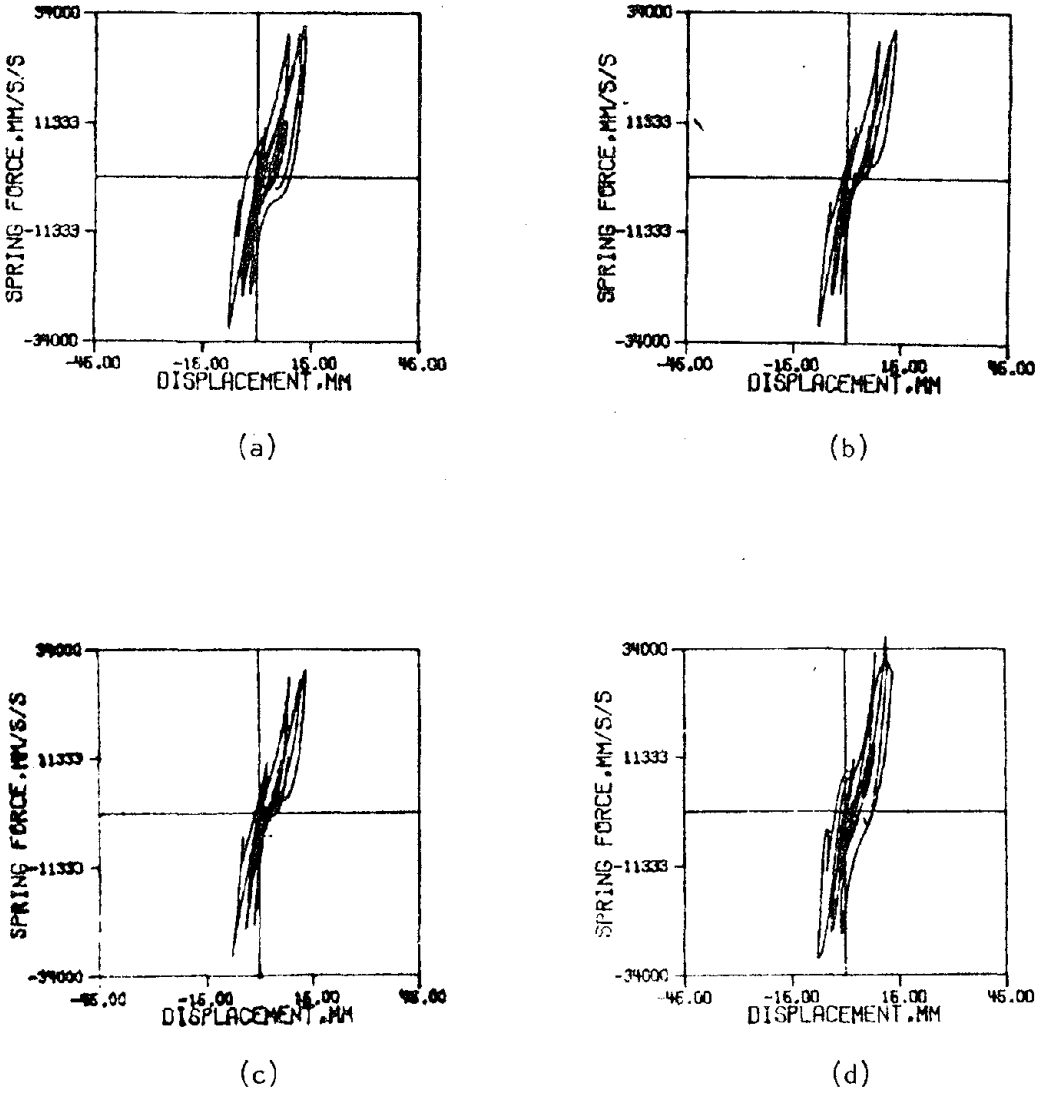

Figure 35: A Comparison of the Spring Force-Displacement Curves for a System Whose Damping Force was Represented by (a) Zero, (b) Linear, (c) Symmetrical Cubic, and (d) Restricted Linear Viscous Forms (Second Floor, RUN 3).

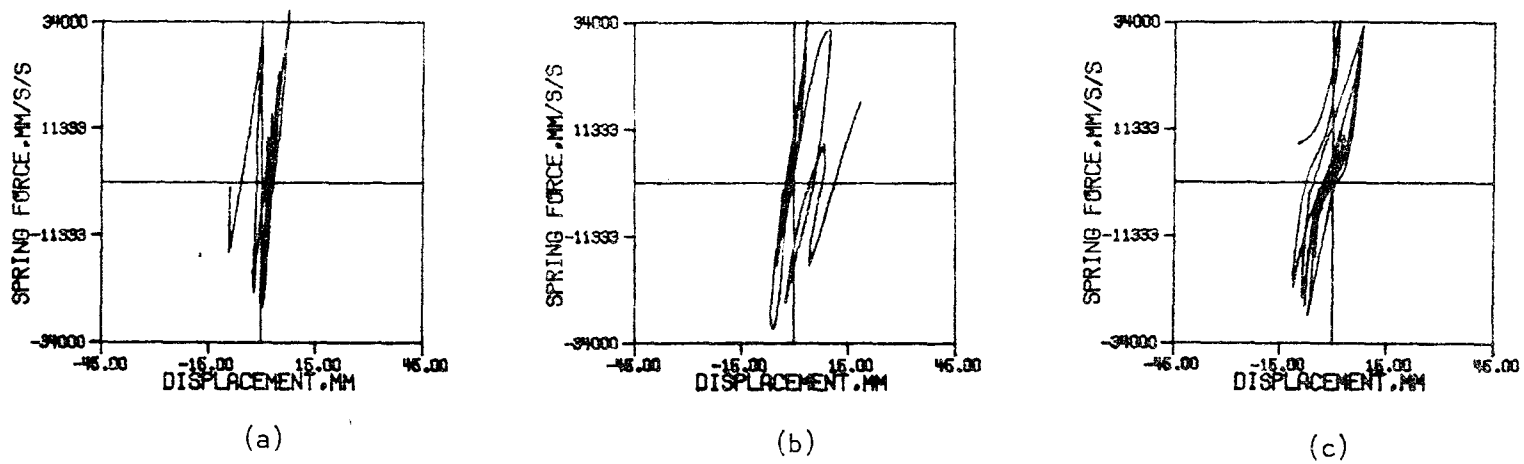

Figure 36: A Comparison of the First-Floor Response Due to (a) Test Run 1, (b) Test Run 2, and (c) Test Run 3.

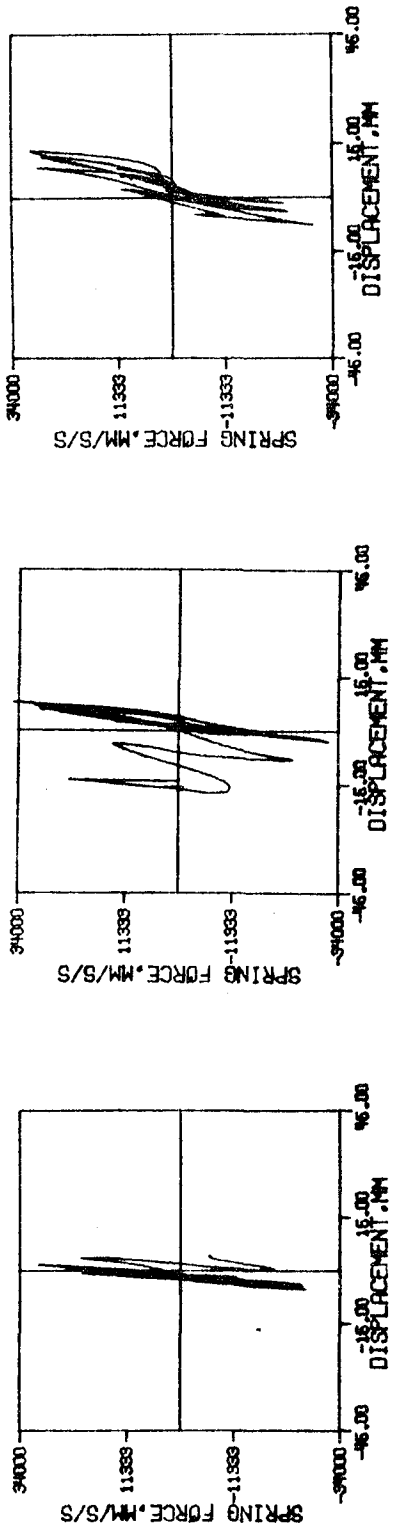

Figure 37: A Comparison of the Second-Floor Response Due to (a) Test Run 1, (b) Test Run 2, and (c) Test Run 3.

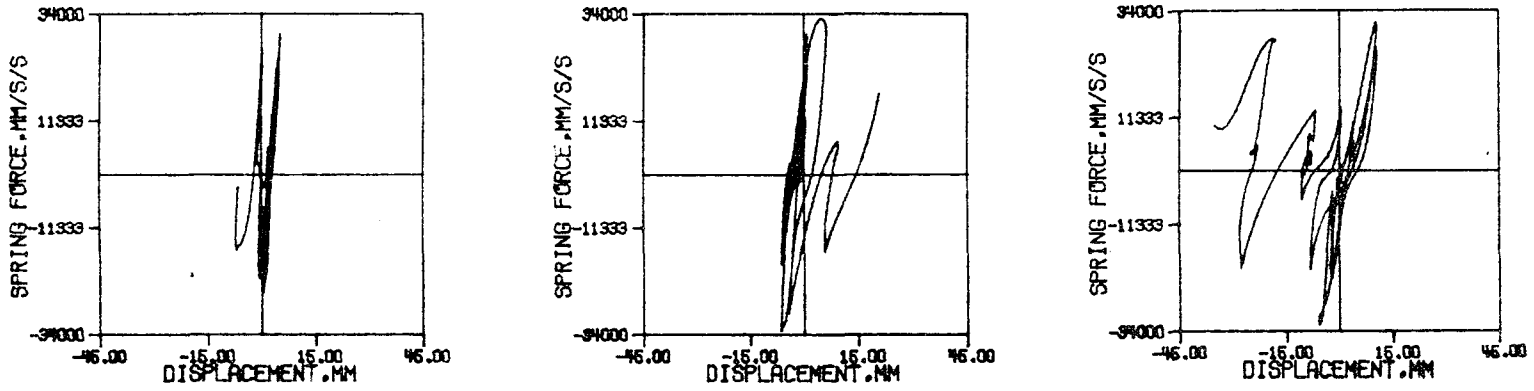

Figure 38: A Comparison of the Third-Floor Response Due to (a) Test Run 1, (b) Test Run 2, and (c) Test Run 3.

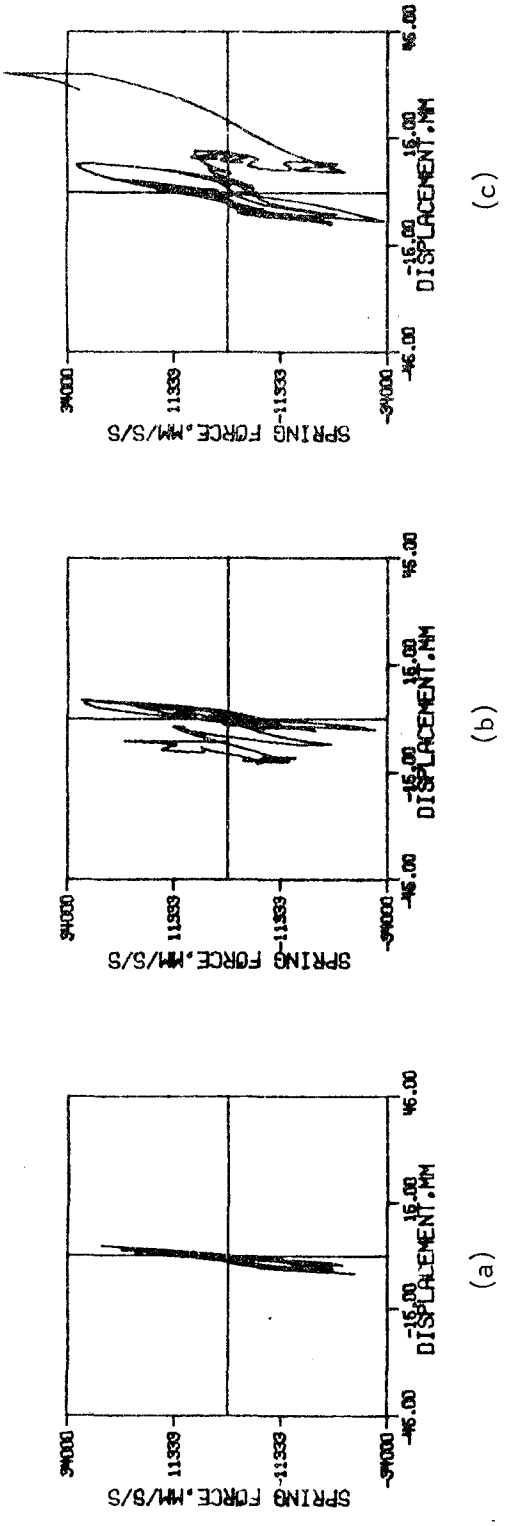

Figure 39: A Comparison of the Fourth-Floor Response Due to (a) Test Run 1, (b) Test Run 2, and (c) Test Run 3.

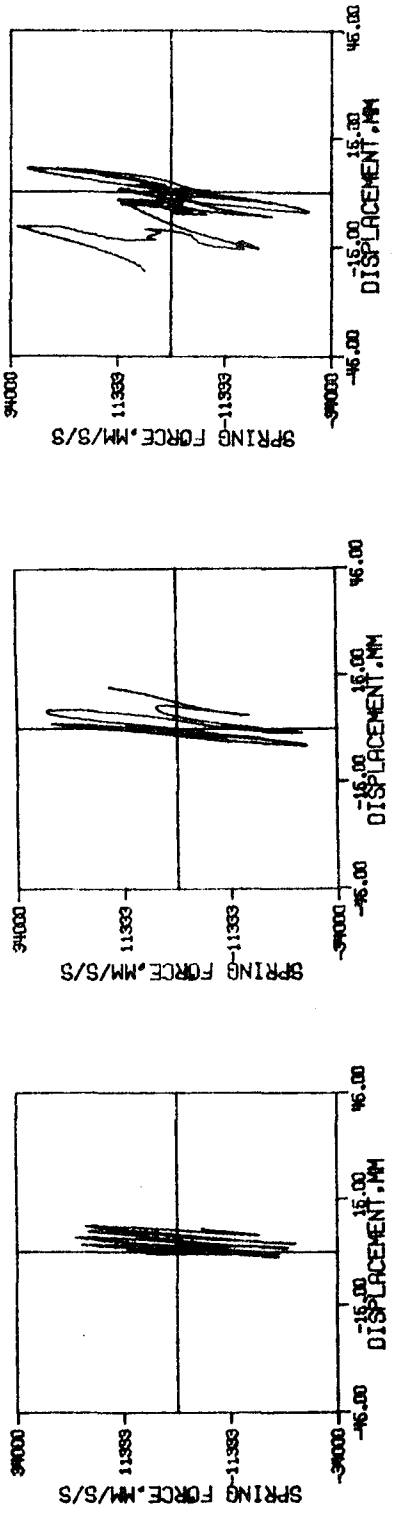

Figure 40: A Comparison of the Fifth-Floor Response Due to (a) Test Run 1, (b) Test Run 2, and (3) Test Run 3.

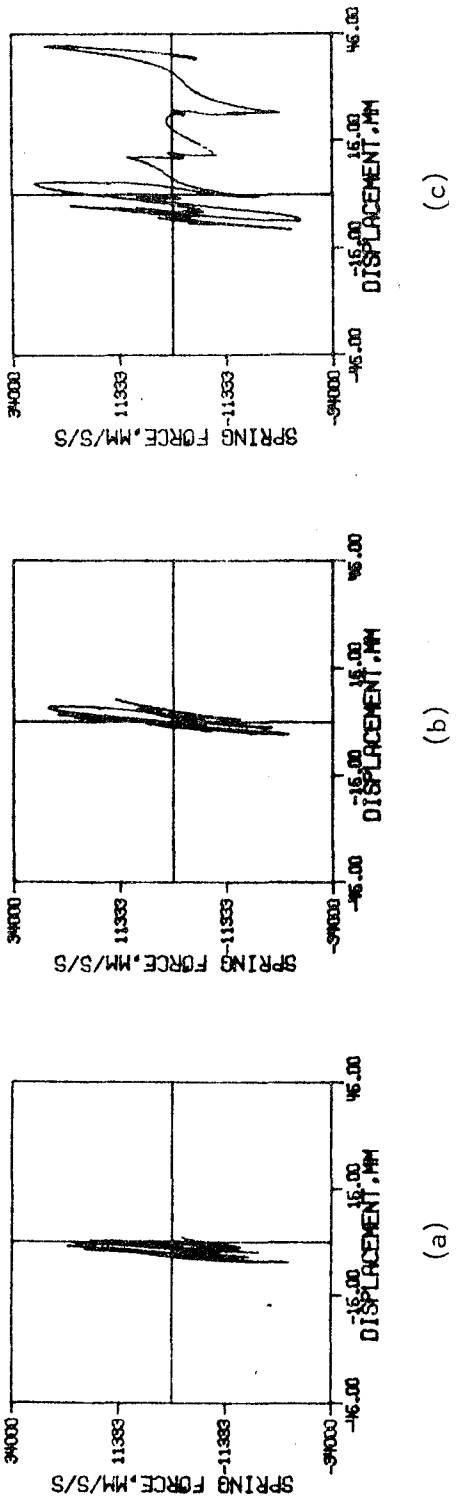

Figure 41: A Comparison of the Sixth-Floor Response Due to (a) Test Run 1, (b) Test Run 2, and (c) Test Run 3.

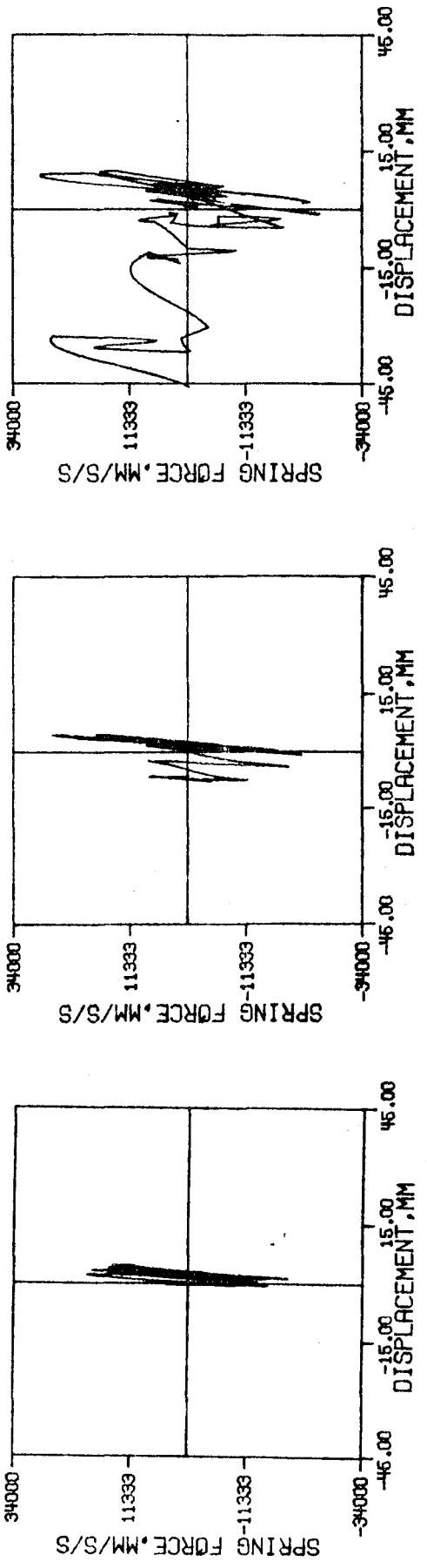

Figure 42: A Comparison of the Seventh-Floor Response Due to (a) Test Run 1, (b) Test Run 2, and (c) Test Run 3.

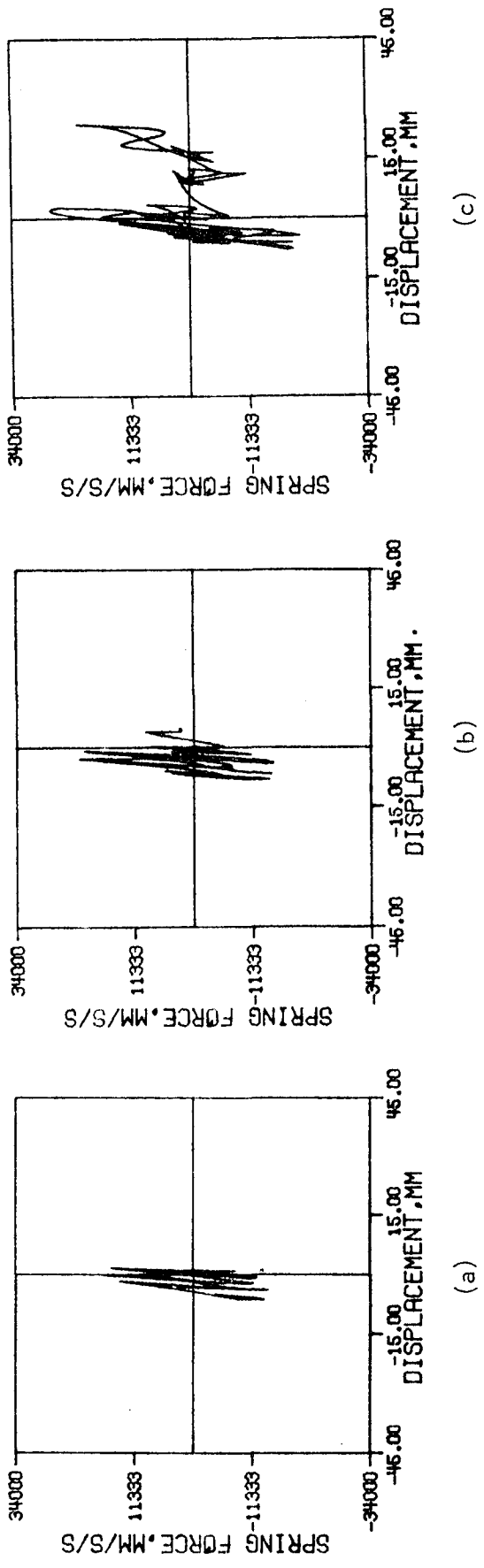

Figure 43: A Comparison of the Eighth-Floor Response Due to (a) Test Run 1, (b) Test Run 2, and (c) Test Run 3.

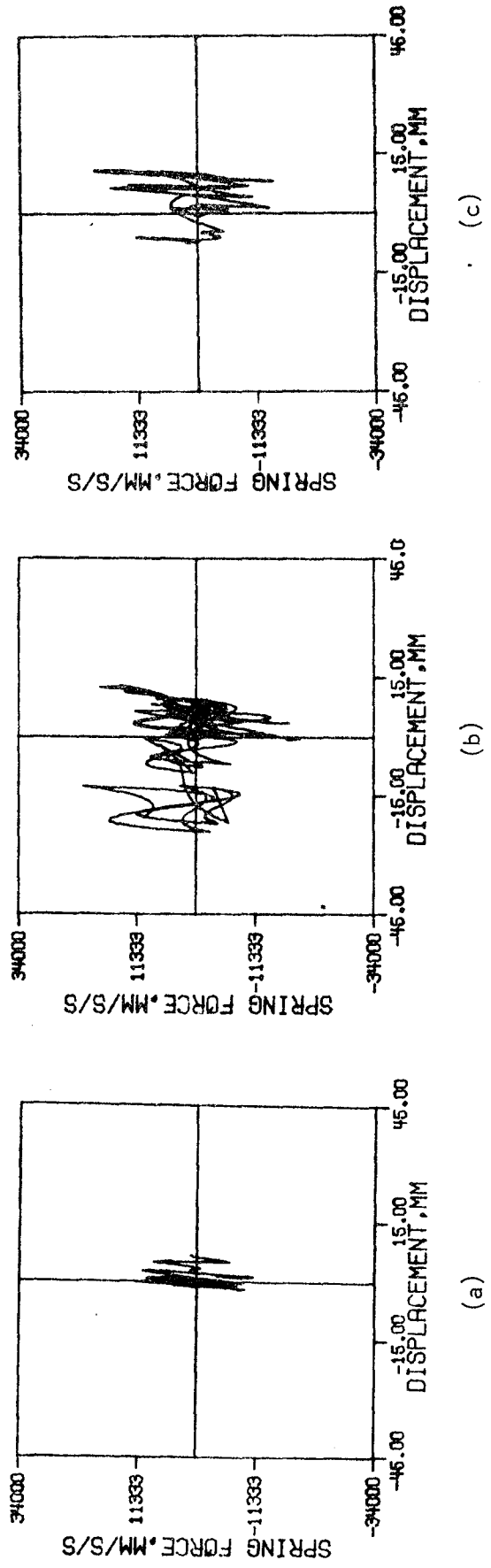

Figure 44: A Comparison of the Ninth-Floor Response Due to (a) Test Run 1, (b) Test Run 2, and (c) Test Run 3.

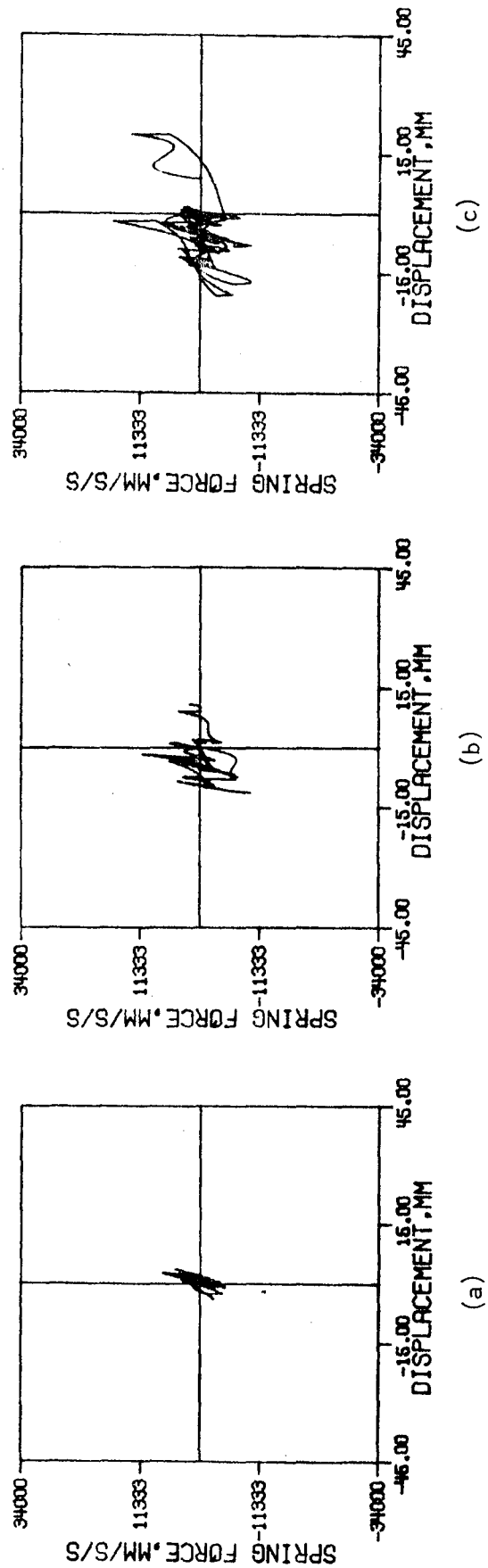

Figure 45: A Comparison of the Tenth-Floor Response Due to (a) Test Run 1, (b) Test Run 2, and (c) Test Run 3.

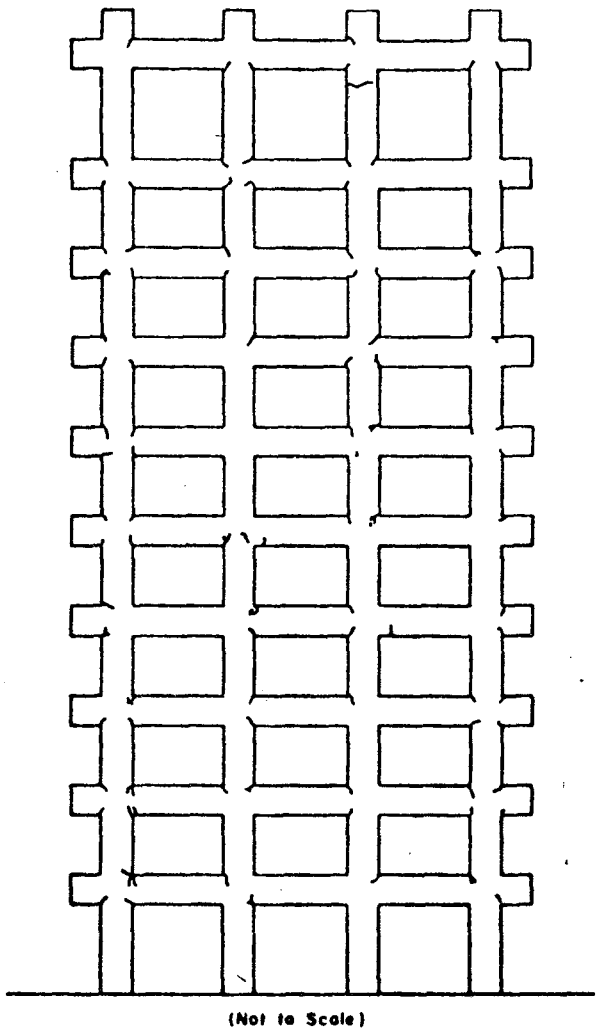

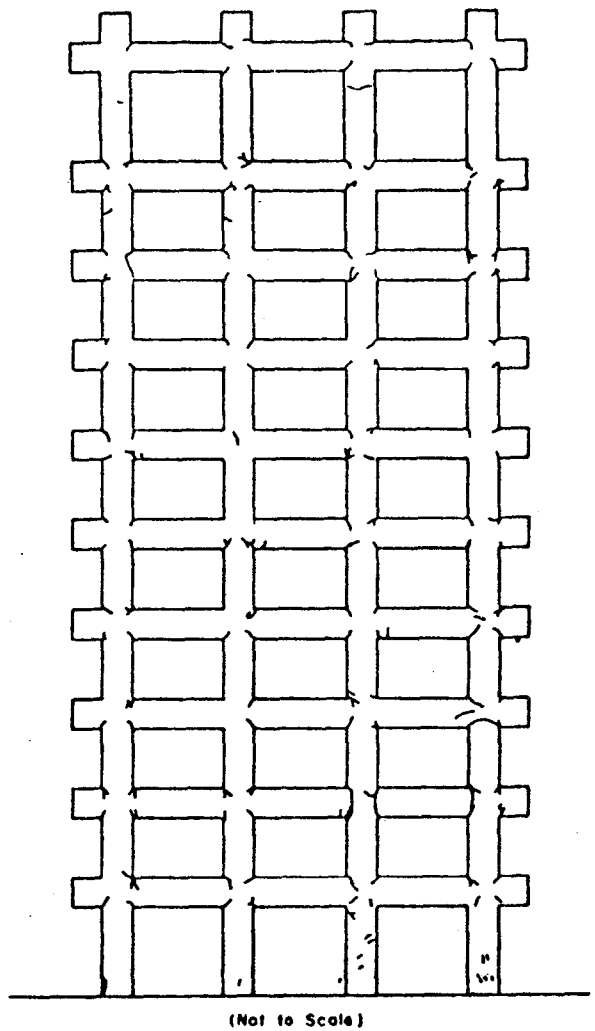

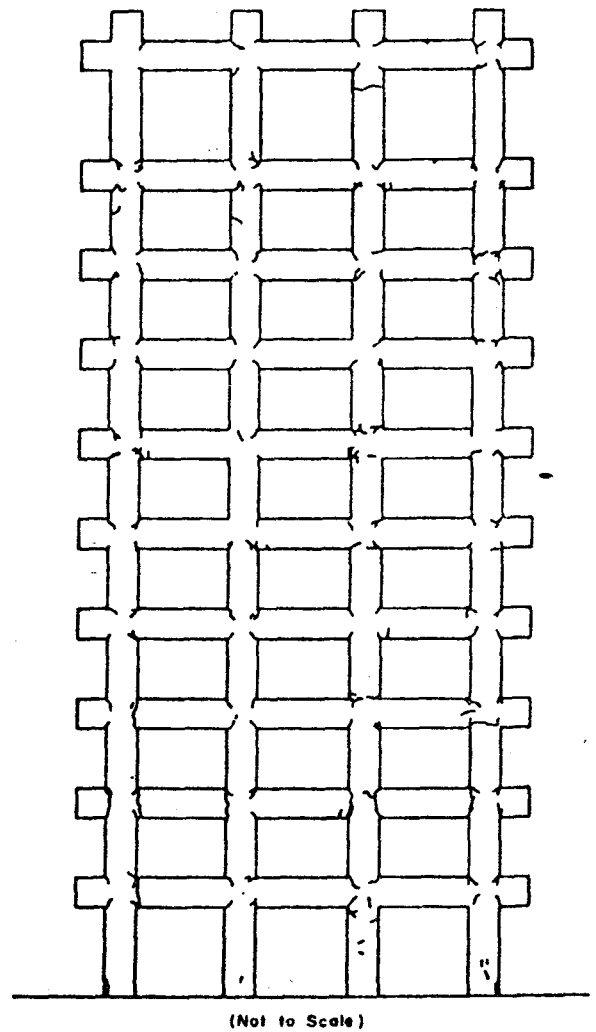

Figure 46: Observed Crack Patterns (Healey and Sozen [3]).

PUBLICATIONS
CREDIT RESEARCH CENTER

MONOGRAPH No. 1: An Empirical Analysis of Retail Revolving Credit
MONOGRAPH No. 2: Credit Policies and Store Locations in Arkansas Border Cities: Merchant Reactions to a Ten Percent Finance Charge Ceiling
MONOGRAPH No. 3: Research Topics in Mortgage Markets: Proceedings of a Seminar
MONOGRAPH No. 4: An Economic Report on Consumer Lending in Texas
MONOGRAPH No. 5: Mortgage Banking 1963 to 1972: A Financial Intermediary in Transition
MONOGRAPH No. 6: A Thesaurus of Terms in Mortgage and Consumer Credit
MONOGRAPH No. 7: A Bibliography of Consumer Financial Services and Regulation
MONOGRAPH No. 8: A Compilation of Federal and State Laws Regulating Consumer Financial Services
MONOGRAPH No. 10: The Impact of Regulation on the Provision of Consumer Financial Services by Depository Institutions: Research Backgrounds and Needs
MONOGRAPH No. 12: Cost/Benefit Analysis of Creditors' Remedies
MONOGRAPH No. 13: Consumer Perception of Credit Insurance on Retail Purchases
MONOGRAPH No. 14: An Economic Analysis of the "Due On Sale" Clause in the California Mortgage Market
MONOGRAPH No. 15: Credit Unions: CRC 1979 Creditors Survey
MONOGRAPH No. 16: Savings and Loan Associations: CRC 1979 Creditors Survey
MONOGRAPH No. 17: Commercial Banks: CRC 1979 Creditors Survey
MONOGRAPH No. 18: Consumer Finance Companies: CRC 1979 Creditors Survey
WORKING PAPER No. 1: The Use of Department Store Revolving Credit: Account Use Patterns, Customer Profitability, the Value of Revolving Credit, and the Probable Incidence of Credit Rationing
WORKING PAPER No. 2: EFTS and Consumer Credit (Revised)
WORKING PAPER No. 3: The Impact of General Credit Restraint on Consumer Instalment Credit Flows
WORKING PAPER No. 4: The Effect of Alternative Billing Methods Upon Retail Revolving Credit Yields
WORKING PAPER No. 5: Delinquency Rates on Consumer and Mortgage Debt: Their Determinants and Impact
WORKING PAPER No. 6: Determinants of Commercial Bank Automobile Loan Rates
WORKING PAPER No. 7: Personal Loan Cash Flows at Finance Companies
WORKING PAPER No. 8: Discrimination on the Basis of Sex Under the Equal Credit Opportunity Act
WORKING PAPER No. 9: Competition Between Banks and Finance Companies: A Cross Section Study of Personal Loan Debtors
WORKING PAPER No. 10: Regulatory Influences on Commercial Bank Personal Loan Rates
WORKING PAPER No. 11: Commercial Bank Consumer Loan Refinancings
WORKING PAPER No. 12: The Impact of Restricted Creditors' Remedies on Automobile Finance Companies in Wisconsin
WORKING PAPER No. 13: Changes in Finance Personal Loan Policies Following Enactment of the Wisconsin Consumer Act
WORKING PAPER No. 14: Creditor Remedy Restrictions and Interstate Differences in Personal Loan Rates and Availability: A Supplementary Analysis
WORKING PAPER No. 15: The Impact of Creditors' Remedies on Consumer Loan Charges
WORKING PAPER No. 16: Cost/Benefit Analysis of Minimum Charges on Revolving Credit Accounts
WORKING PAPER No. 17: Occupational and Employment Variations in Commercial Bank Consumer Credit Risk
WORKING PAPER No. 18: Problems in Applying Discriminant Analysis in Credit Scoring Models
WORKING PAPER No. 19: Testing for Sex Discrimination in Commercial Bank Consumer Lending
WORKING PAPER No. 20: Banks' Lending Response to Restricted Creditor Remedies
WORKING PAPER No. 21: Bank and Retail Credit Card Yields Under Alternative Assessment Methods
WORKING PAPER No. 22: An Economic Analysis of Electronic Funds Transfer System: The Theory of Credit Markets
WORKING PAPER No. 24: The Community Re-investment Act of 1977: Its Legislative History and Its Impact on Applications for Changes in Structure Made by Depository Institutions to the Four Federal Financial Supervisory Agencies
WORKING PAPER No. 25: Junior Mortgage Financing and Other Borrowing Against Inflated Housing Equity
WORKING PAPER No. 26: Consumer Perceptions of Credit Bureaus
WORKING PAPER No. 27: Mobile Home Demand and Sources of Financing
WORKING PAPER No. 28: An Investigation of Sex Discrimination of Commercial Banks' Direct Consumer Lending
WORKING PAPER No. 29: The Transfer Implications of Consumer Credit Regulation
WORKING PAPER No. 30: Accelerating Inflation and the Distribution of Household Savings Incentives
WORKING PAPER No. 31: Rates of Return on GNMA Securities: the Cost of Mortgage Funds
WORKING PAPER No. 32: The Response of Commercial Banks to Rate Ceilings and Restrictions on Remedies on Consumer Credit Contracts
WORKING PAPER No. 33: Second Mortgage Survey, 1979
WORKING PAPER No. 34: Value Pricing of Bank Card Services
WORKING PAPER No. 35: Restrictive Effects of Rate Ceilings on Consumer Choice: The Massachusetts Experience
WORKING PAPER No. 36: Evidence of the Effect of Restrictive Loan Rate Ceilings on Prices of Consumer Financial Services
WORKING PAPER No. 37: Household Financial Behavior: Implications For Consumer Spending
REPRINT No. 1: John J. McConnell, "Evaluation Model Can Maximize Single-Family Servicing Profits," *Mortgage Banker,* March 1975; and "Profit/Loss Evaluation Model Has Varied Applications," *Mortgage Banker,* May 1975 (Out-of-print)
REPRINT No. 2: Robert W. Johnson, "The Rationale For Acquisition of Finance Companies by Bank Holding Companies," *The Banking Law Journal,* April 1975 (Out-of-print)
REPRINT No. 3: William C. Dunkelberg and Robert H. Smiley, "Subsidies in the Use of Revolving Credit," *Money, Credit, and Banking,* November 1975
REPRINT No. 4: Michael S. Long, "Credit Screening System Selection," *Journal of Financial and Quantitative Analysis,* June 1975 (Out-of-print)
REPRINT No. 5: John J. McConnell, "Valuation of a Mortgage Company's Servicing Portfolio," *Journal of Financial and Quantitative Analysis,* September 1976
REPRINT No. 6: Richard L. Peterson, "The Impact of General Credit Restraint of the Supply of Commercial Bank Consumer Instalment Credit," *Money, Credit, and Banking,* November 1976
REPRINT No. 7: John J. McConnell, "Mortgage Company Bids on the GNMA Auction," *Journal of Bank Research,* winter 1977
REPRINT No. 8: Richard L. Peterson, "Factors Affecting the Growth of Bank Credit Card and Check Credit," *The Journal of Finance,* May 1977
REPRINT No. 9: John J. McConnell, "Price Distortions Induced by the Revenue Structure of Federally-Sponsored Mortgage Loan Programs," *Journal of Finance,* September 1977
REPRINT No. 10: James F. Smith, "The Equal Credit Opportunity Act of 1974: A Cost/Benefit Analysis," *The Journal of Finance,* May 1977
REPRINT No. 11: David S. Kidwell and Richard L. Peterson, "A Close Look at Credit Unions," *The Bankers Magazine,* January-February 1978
REPRINT No. 12: Robert W. Johnson, "Pricing of Bank Card Services," *The Journal of Retail Banking,* June 1979
REPRINT No. 13: Richard L. Peterson, "The Costs of Consumer Credit Regulation," *Issues in Bank Regulation,* Winter 1979
REPRINT No. 14: Robert W. Johnson, "Economic Effects of Graduated Rate Ceilings on Revolving Credit."